9-13-2016 12:00 AM

The Role of GABA Signalling in Lung Macrophage Immune Response

Jacob W. Poirier
The University of Western Ontario

Supervisor
Dr. Wei-Yang Lu
The University of Western Ontario

Graduate Program in Physiology and Pharmacology
A thesis submitted in partial fulfillment of the requirements for the degree in Master of Science

ABSTRACT

Lung macrophages (LMϕs) play a key role in pulmonary innate immunity. They polarize into different phenotypes adapting to the needs of the immediate pulmonary environment, and adjust their functional responses via autocrine signalling. Previous studies in our laboratory suggest that murine LMϕs are endowed with an autocrine gamma-aminobutyric acid (GABA) signaling system. My honors thesis study found that antagonizing the autocrine GABA signaling in alveolar macrophages (AMϕs) increased the secretion of the M1 cytokine tumor necrosis factor-alpha (TNF-α), suggesting a role for GABA signaling in immune response. This thesis project explored whether GABA signaling plays a role in LMϕ polarization. As previously reported, results from this study confirmed that bacterial toxin lipopolysaccharide (LPS) and the Th1 cytokine interferon gamma (IFNγ) shifted LMϕs to the pro-inflammatory M1 phenotype, marked by increased expression of inducible nitric oxide synthase (iNOS). On the other hand, the Th2 cytokines interleukin (IL)-4 and IL-13 shifted LMϕs toward the M2 phenotype marked by increased arginase-1. Importantly, in both RAW 264.7 cell line and primary LMϕs, LPS and IFNγ treatment increased iNOS expression while decreasing glutamic acid decarboxylase (GAD) and A-type GABA receptor α2-subunit (α2-$GABA_AR$). Conversely, treatment with IL4/13 induced an upregulation of arginase-1, GAD, and α2-$GABA_AR$. Moreover, treatment of primary LMϕs with IL4/13 and $GABA_AR$ antagonist picrotoxin decreased arginase-1 and GAD expression, and increased iNOS levels. These results suggest that the autocrine GABA signaling system in LMϕs dynamically changes along with their phenotypic polarization. This signaling system functions to limit the M1 response but facilitate M2 responses, and thus a change in the GABA signaling may alter the inflammatory responses of these cells.

KEYWORDS

Macrophage polarization

iNOS

Arginase-1

GABA signalling

Pulmonary inflammation

CO-AUTHORSHIP

Dr. Sean Gill graciously provided all $CD45^+$ lung macrophages used for immunocytochemistry and Luminex analysis. Cynthia Pape provided assistance in surgical removal of the lung as well as lung tissue digest procedures. Furthermore, my colleague Matthew Maksoud performed patch-clamp experiments on hippocampal neurons using media from my RAW 264.7 cell cultures.

Otherwise, Jacob Wilson Poirier performed all experiments conducted as part of this thesis under supervision of Dr. Wei-Yang Lu in the department of Physiology and Pharmacology at Western University.

ACKNOWLEDGEMENTS

Completing this thesis project over the past two years has been a challenging, yet rewarding experience. I would like to thank Dr. Wei-Yang Lu for pushing me to my limits as a young scientist, allowing me to grow and learn to my fullest potential. Without your many motivational talks I could not have made it this far. I would also like to thank Dr. Yun-Yan Xiang for her assistance in lab techniques, especially with troubleshooting my experiments. Thank you to my lab mates over the years, Allen, Allison, Amy, Matt, and Dong for providing a relaxed and friendly lab environment. Special thanks to Matt for performing patch clamping studies for my thesis.

I must also give thanks to my advisory committee, Drs. Gregory Dekaban, Sean Gill, and Sean Cregan. Your valuable input helped to shape my experiment and make me think more critically about the details of my experiments. Furthermore, I would like to thank Dr. Gill and Cynthia Pape for providing me with primary lung macrophages for my studies.

I must also give thanks to my family and friends. Thank you to Andre, Candace, Darci, and Don for your constant positivity and support. Thank you Ruth for being a great friend and TA buddy, your stories never fail to entertain. Thank you to my partners in the accelerated MSc program, Alvin and Mandy, I couldn't have picked better people to share this unique experience with. Finally, thank you Robyn for supporting me and being so understanding through this entire experience, and putting up with all my late nights at the lab.

Table of Contents

LIST OF FIGURES

LIST OF ABBREVIATIONS

AMϕ	alveolar macrophage
ANOVA	analysis of variance
BAL	bronchoalveolar lavage
CCR	C-C chemokine receptor
CD	cluster of differentiation
CRAC	calcium-release activated channels
CXCL	C-X-C ligand motif
Cy3	cyanine 3
DAPI	4’,6-diamidino-2-phenylndole
DNA	deoxyribonucleaic acid
EDTA	ethylenediaminetetraacetic acid
EMP	erythro-myeloid progenitors
FCγR	Fc gamma receptor
FITC	fluorescein isothiocyanate
FIZZ1	found in inflammatory zone/resistin-like molecule alpha
GABA	gamma-aminobutyric acid
$GABA_AR$	A-type GABA receptor
$GABA_BR$	B-type GABA receptor
$GABA_CR$	C-type GABA receptor
GABA-T	GABA transaminase
GAD	glutamic acid decarboxylase
GAT	GABA transporter

GPCR	G-protein coupled receptor
GR-1	granulocytic marker
HBSS	Hank's balanced salt solution
IFNγ	interferon gamma
IFNGR	interferon gamma receptor
IκB	nuclear factor of kappa light polypeptide gene enhancer in B-cells inhibitor
IKK	IκB kinase
IL	interleukin
IL-1ra	IL-1 receptor antagonist
IL-4Rα	interleukin 4 receptor alpha
IL-13Rα	interleukin 13 receptor alpha
IMϕ	interstitial macrophage
iNOS	inducible nitric oxide synthase
JAK	Janus kinase
KCC2	K^+-Cl^- co-transporter
KLF	Krüppel-like factor
LAMP	lysosomal associated membrane protein
LMϕ	lung macrophage
LPS	lipopolysaccharide
Lys-EGFP-ki	lysozyme M-enhanced green fluorescent protein-knock in
MD-2	lymphocyte antigen 96
MHC	major histocompatibility complex
Mrc1	mannose receptor

MyD88	myeloid differentiation primary response gene 88
NDS	normal donkey serum
NF-κB	nuclear factor kappa-light-chain-enhancer of activated B cells
NKCC	Na^+-K^+-Cl^- transporter
NO	nitric oxide
OVA	ovalbumin
PAMP	pathogen-associated molecular pattern
PBS	phosphate buffered saline
PCR	polymerase chain reaction
PRR	pattern recognition receptor
RNA	ribonucleic acid
RPMI	Roswell Park Memorial Institute Medium
SOCE	store-operated calcium entry
STAT	signal transducer and activator of transcription
TBS-T	tris-buffered saline and tween 20
TGF-β	transforming growth factor beta
Th	T helper cell
TIRAP	TIR domain-containing adaptor protein
TLR	toll-like receptor
TNF-α	tumor necrosis factor-alpha
TRAF	TNF receptor-associated factor
TRAM	TRIF-related adaptor molecule
TRIF	TIR domain-containing adaptor inducing IFN-β

1.0 INTRODUCTION

1.1 Preface

Macrophages are a primary mediator of the innate immune system, and exist in almost every tissue of the body. While all parts of the mammalian body require protection from pathogens, perhaps the most important loci for host defence are organs that are exposed to the external environment including the gastrointestinal tract and the lungs. In these tissues macrophages are the predominant type of immune cell. In order to adapt to the needs of the immediate pulmonary environment, alveolar macrophages (AMϕs) polarize in response to infectious pathogens as well as cytokines secreted from nearby T cells. For example, bacterial toxin lipopolysaccharide (LPS) and T helper (Th) 1 cytokines such as interferon gamma (IFNγ) stimulate AMϕs to shift to the pro-inflammatory M1 phenotype, marked by the upregulation of inducible nitric oxide synthase (iNOS). M2 polarization is typically characterized by upregulation of arginase-1 and can be prompted by parasite infection and/or Th2 cytokines such as interleukin-4 (IL-4) and IL-13. More detailed descriptions of M1/M2 polarization may be found in section 1.4.

Studies in my lab suggest that AMϕs are endowed with an autocrine gamma-aminobutyric acid (GABA) signalling system. More specifically, AMϕs express the GABA-synthesizing enzyme glutamic acid decarboxylase (GAD) and A-type GABA receptors ($GABA_ARs$). However, whether the autocrine GABA signalling plays a role in AMϕ polarization remains to be investigated. My thesis focuses on the role of GABA signalling in the regulation of AMϕ polarization.

1.2 Macrophage lineage

1.2.1 Macrophage hematopoiesis

Hematopoiesis is the process of generating blood cells from stem cell origins. The genesis of the blood cells is complex, with shifting sites of hematopoiesis occurring during development. There are two waves of macrophage hematopoiesis: primitive and definitive (McGrath et al., 2015). Primitive hematopoiesis occurs before birth in the ectoderm of the yolk sac and results in macrophages populating the tissues without the need of monocyte progenitors (Italiani and Boraschi, 2014). In the murine embryo, examination of embryonic macrophage and monocyte populations reveals that the first wave of macrophage hematopoiesis arises in the yolk sac (Gomez Perdiguero et al., 2015; Hoeffel et al., 2015). These macrophage progenitors are the source of early macrophages throughout the embryonic tissues including the brain, where macrophage progenitors develop into microglia (Ginhoux et al., 2010). These macrophages bypass the monocytic intermediate stage.

The second wave of hematopoiesis, also in the yolk sac, gives rise to multipotent erythro-myeloid progenitors (EMPs) that colonize the fetal liver, initiating myelopoiesis (McGrath et al., 2015). Macrophages generated from the second hematopoietic wave are distributed in most fetal tissues before the onset of fetal monocyte production by the fetal liver (Gomez Perdiguero et al., 2015; Frame et al., 2013). These primitive macrophages retain a high proliferative potential and participate in many fundamental processes during mid and late embryogenesis, including definitive macrophage hematopoiesis and in the clearance of dead cells during tissue maturation. Definitive hematopoiesis of myeloid progenitors takes place in the fetal liver during embryogenesis, and then in the bone marrow after birth. More precisely, EMPs in the fetal liver become the source circulating monocytes

during embryogenesis, and following birth and bone development, the definitive hematopoiesis process relocates to the bone marrow (Italiani and Boraschi, 2014). The hematopoietic systems in humans and mice are coordinated in a similar manner (Tavian & Péault, 2005).

1.2.2 Monocytes

Monocytes are circulating phagocytic white blood cells that are derived from EMPs during definitive hematopoiesis and spread to various organs where they differentiate into macrophages (Shi & Pamer, 2011; Goncalves et al., 2011). Circulating monocytes were thought to replace tissue-resident macrophages as the host matures (van Furth & Cohn, 1968). However new evidence suggests tissue-resident macrophages are largely derived during primitive hematopoiesis in the yolk sac, populate the tissue before birth, and are capable of self-renewal continuing into adulthood (Schulz et al., 2012; Sieweke & Allen, 2013, Epelman et al., 2014). For example, tissue macrophages are able to maintain population size in the absence of monocyte precursors in homeostatic conditions, as well as during monocytopenia (Schulz et al., 2012, Yona et al., 2013, Jakubzick et al., 2013). In addition, following lung macrophage depletion, repopulation occurred *in situ* rather than by infiltration of blood monocytes (Hashimoto et al., 2013). Therefore, it is believed that monocytes are not generally necessary for maintenance of tissue-resident macrophage populations during homeostatic conditions. Instead, monocyte activity appears to mainly provide additional macrophages to the tissue necessary for resolution of acute inflammation (Jenkins & Hume, 2014).

Monocytes only remain in the bloodstream for 1-2 days, during which time they must be recruited to tissue by an inflammatory response or they will perish and be replaced (Italiani and Boraschi, 2014). There are two specific subtypes of monocytes defined by chemokine receptor expression in mice. The GR-1^{high} $CCR2^{high}$ CX_3CR1^{low} monocytes are pro-inflammatory and migrate to infected sites to assist with pathogenic clearance (Herold et al., 2011). The GR-1^{low} $CCR2^{low}$ CX_3CR1^{high} monocytes populate both healthy and infected areas, and are involved in resolution of inflammation and tissue repair (Auffray et al., 2007; Geissmann et al., 2010). During inflammatory responses GR-1^{high} $CCR2^{high}$ CX_3CR1^{low} monocytes are recruited by chemokines, including monocyte chemoattractant protein-1 and Growth-related oncogene-α, released from pro-inflammatory tissue resident macrophages (Barnes 2004; Herold et al., 2011). Upon arrival to the tissue, recruited monocytes differentiate into monocyte-derived inflammatory macrophages, and assist the elimination of pathogens by phagocytosis, and nitric oxide (NO) production (Serbina et al., 2008). Monocyte-derived inflammatory macrophages also assist the inflammatory responses by secreting pro-inflammatory cytokines that induce T-cell polarization (Serbina et al., 2008; Evans et al., 2009)

1.3 Macrophages

1.3.1 Resident macrophages

Macrophages represent 10-15% of the total cell number during homeostasis and are the first line of defence of the innate immune system. (Murray & Wynn, 2011; Italiani and Boraschi, 2014). Generally, resident macrophages proliferate regularly to maintain their population at steady state, without the need for repopulation by monocyte progenitor cells

(Sieweke & Allen, 2013). Many types of resident macrophages exist, each of which express different transcription profiles based on the needs of the environment. Therefore, each type of tissue resident macrophage is unique and is assigned a specific name according to tissue location such as microglia in the central nervous system, Kupffer cells in the liver, and alveolar macrophages in pulmonary alveoli (Gautier et al., 2012). Despite differences at the transcriptional level, the roles of macrophages in each tissue are in general similar. They are an integral component of tissue development, tissue surveillance and initiation of inflammatory response to pathogen, and maintenance of tissue homeostasis by clearing cellular debris and repairing tissue (Maus et al., 2002; Italiani and Boraschi, 2014).

Macrophages express cytosolic and membrane bound pattern recognition receptors (PRRs), including Toll like-receptors (TLRs), which recognize pathogen-associated molecular patterns (PAMPs) (Akira et al., 2006). Within an hour of PAMP detection, macrophages initiate inflammation to attempt to sterilize the area of infection (Chen & Nunez, 2010). During the initial phase of inflammatory responses, it becomes necessary to increase the population of pro-inflammatory cytokine secreting cells in order to produce a complete inflammatory response. The local increase in inflammatory macrophages is generally accomplished by recruitment of neutrophils, a type of leukocyte. Neutrophils are an important component of the acute inflammatory response, both by bacterial killing and secretion of chemokines such as CCL2 which will ultimately aid in the recruitment of blood monocytes (Kolaczkowska & Kubes, 2013). Upon exposure to the pro-inflammatory environment, exudated monocytes become monocyte-derived inflammatory macrophages and further propagate the inflammatory response (Italiani and Boraschi, 2014).

1.3.2 Lung macrophages

Macrophages are the most abundant immune cell in the lung and are strategically positioned to play a pivotal role in airway defence (Byrne et al., 2015). Lung macrophages (LMϕ) have dual origins: an F4/80^{High} population derived from primitive yolk sac representing the majority of lung macrophages including AMϕs, along with a smaller population of F4/80^{Low} of definitive hematopoetic origin which are continually replaced (Yona et al., 2013). There are two primary subtypes of lung macrophages: alveolar macrophages, and interstitial macrophages (IMϕs). The two macrophage subtypes may be distinguished based on their expression patterns of integrins cluster of differentiation (CD) 11b and CD11c. AMϕs express high levels of CD11c and lack CD11b, whereas IMϕs and recruited monocytes possess the opposite expression pattern (Hussel & Bell, 2014).

Alveolar macrophages

AMϕs are the predominant immune effector cell in the alveolar space and the conducting airways. AMϕs exist in a unique environment which is directly exposed to the external environment, contains high partial pressure of oxygen, and high lipid concentrations. This environment setting differentiates AMϕs from other types of macrophages, and therefore AMϕs exhibit vastly different characteristics. For example, under homeostatic conditions AMϕs have an incredibly long life span with a half-life which exceeds 12 months, in stark contrast to peritoneal macrophages which exhibit a half-life of merely 15 days (Janssen et al., 2011). Another unique property of AMϕs is how the population changes over the course of inflammation and resolution phases. Tissue macrophages in general have been described as polarizing from M2 to M1 upon stimulation

with a pathogen, along with recruitment of monocytes to fight the infection and clear dead cells (Romo et al., 2011). Following pathogenic clearance, the M1 tissue macrophages were thought to perish due to their own NO production, and eventually the tissue would be repopulated by monocytes in the absence of pro-inflammatory signals (Mills 2012; Italiani and Boraschi, 2014). However, a study by Janssen *et. al* demonstrated that AMϕs follow a much different process, whereby the resident AMϕ population remained stable throughout the inflammatory response and recruited monocytes are wholly responsible for increase in macrophage numbers during the inflammatory response. Furthermore, during the resolution phase recruited monocytes/macrophages undergo *in situ* programmed cell death and are phagocytosed by neighboring tissue macrophages (Janssen et al., 2011).

Interstitial macrophages in the lung

Whereas AMϕs are found in the airways and are directly exposed to the external environment, IMϕs reside inside the lung tissue (Byrne et al., 2015). In the lung, as a whole, IMϕs are roughly two times less abundant than AMϕs. IMϕs have a low phagocytic potential relative to AMϕs but play a very important role regarding antigen presentation and express much higher levels of MHC class II molecules than AMϕs (Bedoret et al., 2009). Due to their antigen-presenting capability the primary focus of IMϕs is to interact with interstitial lymphocytes in order to initiate a specific immune response, which is distinct from AMϕs which are more effective as non-specific first line of defence (Franke-Ullmann et al., 1996; Prokhorova et al., 1994; Fathi et al., 2001). Although IMϕs are poorly characterized compared with AMϕs, it is clear the two macrophage populations are distinct and play different roles in pulmonary immune responses.

1.4 Macrophage polarization

Macrophages demonstrate remarkable plasticity as they can assume different functional phenotypic states in response to different environmental states. Typically, macrophages have been classified as being either M1 or M2, corresponding to the Th1 and Th2 paradigms seen in helper T cells (Mantovani et al., 2004; Hume 2015). The M1/M2 concept originates from the differences observed in macrophage polarization between C56BL/6 (M1) and BALB/c (M2) mice due to differences in their gene expression profiles (Heinz et al., 2013; Raza et al., 2014; Wells et al., 2003). These differences may be due to differences in expression of transcription factor binding sites and/or DNA methylation patterns (Heinz et al., 2013; Schilling et al., 2009). The M1 phenotype marked by CD38 produces pro-inflammatory cytokines including TNF-α to recruit other immune cells to the site of infection (Murugan & Peck, 2009; Jablonksi et al., 2015) Conversely, alternatively activated (M2) macrophages marked by mannose receptor (Mrc1) and CD83 secrete anti-inflammatory cytokines such as transforming growth factor beta (TGF-β), IL-4, and IL-10 to stimulate Th2 cytokine production and assist with the resolution of cell-mediated inflammation (Spellberg & Edwards, 2001; LaFlamme et al., 2012; Gao et al., 2015; Jablonski et al., 2015; Yamaguchi et al., 2015). In addition, Th2/M2 responses are found to be the dominant response in allergy, asthma, and parasite infections (Bønnelykke et al., 2015; Chung 2015, Chávez-Galán et al., 2015).

iNOS and arginase-1

The regulation of arginine metabolism is critical for macrophage polarization. iNOS is an enzyme which converts arginine to NO and citrulline, and is considered to be a marker

of M1 phenotype. Upregulation of iNOS is an important component of the M1 phenotype, as secreted NO is a critical microbicidal molecule and can also be further metabolized to other reactive oxygen species such as peroxynitrite (Ignarro 1990; Italiani and Boraschi, 2014). Furthermore, NO can nitrosylate proteins which may in turn alter protein function (Rath et al., 2014). Additionally, it has been found that arginine concentrations decline to undetectable levels at inflammatory sites, highlighting the importance of selective arginine metabolism in regulating the M1/M2 response (Mills 2012).

M2 polarization may be induced by cytokines secreted from Th2 cells including IL-4 and IL-13 (Gordon 2003; Van Dyken and Locksley, 2013). These cytokines cause a shift in the arginine metabolism such that there is an increase in arginase-1 activity leading to L-ornithine production which promotes proliferation and repair (Morris, 2007). L-ornithine may be decarboxylated to produce polyamines necessary for cell growth, protein translation, and differentiation, or it may be converted to proline increasing production of collagen which may be important for tissue remodelling (Hesse et al., 2001; Van Dyken & Locksley, 2013). Due to increased arginase-1 activity—and a relative decrease in iNOS activity—there are low levels of pro-inflammatory NO within the cell, and the macrophage will now release anti-inflammatory mediators including TGF-β and IL-10 (Lech & Anders, 2013). TGF-β appears to be important for maintenance of M2 phenotype within the system, as it may exert anti-inflammatory effects by further inhibiting NO production (Mills 2012).

The M1/M2 paradigm demonstrates a balanced cellular system wherein upregulation of arginase-1 activity due to M2 phenotype will break down the substrate which M1-associated iNOS requires to produce NO (**Figure 1.1**). However, the M1/M2 classification is a limited view of macrophage phenotypes. In reality macrophages alter their phenotype

along a continuum in order to produce typical M1/M2 responses, or anywhere between these two extremes (Stout et al., 2009). This ability for macrophages to adopt various phenotypes allows them to orchestrate the systemic immune response. Each phenotype has distinct cytokine secretion profile depending on their polarized state, which is influenced by signals in their microenvironment (Mosser and Edwards, 2008; Xue et al., 2014; Robbe et al., 2015).

1.5 M1 polarization

M1 polarization is the most prevalent monocyte and tissue macrophage type seen in classical inflammation (Robbe et al., 2015). The M1 polarization of macrophages can be initiated by pro-inflammatory cytokines released from Th lymphocytes, including IFNγ; or triggered by PAMPs from pathogens such as LPS.

1.5.1 IFNγ and IFNGR

The IFNγ receptor (IFNGR) is composed of two IFNGR1 chains responsible for ligand binding and signalling, and two IFNGR2 chains mainly associated with signal transduction (Schroder et al., 2004). While IFNGR1 expression is constitutively high, IFNGR2 limits the responsiveness of IFNγ as its expression is constitutively low and may be upregulated according to cellular activation state (Bernabei et al., 2001). IFNGR lack kinase activity, and therefore must associate with other proteins for receptor phosphorylation and consequent signal transduction. The intracellular domain of IFNGR1 expresses a Janus Kinase 1 (JAK1) binding site, as well as a signal transducer and activator of transcription 1 (STAT1) docking site which must be phosphorylated prior to association. IFNGR2 is associated with JAK2 (Bach et al., 1997). Typical IFNγ signalling occurs via the

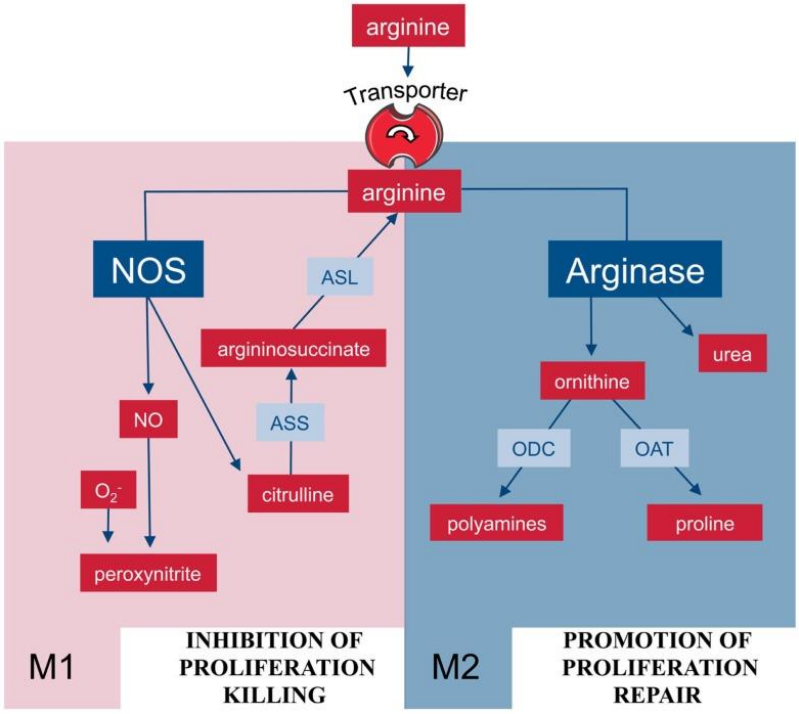

Figure 1.1. Arginine metabolism pathways. Adapted from Rath et al., 2014. iNOS and Arginase-1 are prominent markers of the M1 and M2 phenotype, respectively. iNOS metabolizes arginine to NO and citrulline. NO, as well as its metabolite peroxynitrite, possess microbicidal function, while citrulline may be converted back to arginine for further metabolism. Arginase-1 primarily converts arginine to ornithine. Ornithine is further converted to polyamines by ornithine decarboxylase (ODC) and proline by ornithine aminotransferase (OAC), important for promotion of proliferation and tissue repair.

JAK/STAT1 signalling pathway. Upon ligand binding to the IFNGR1, JAK1 and JAK2 are activated and can then phosphorylate INFGR1 (Stark, 2007). Following phosphorylation, unphosphorylated STAT1 dimers located in the cytoplasm may associate with the receptor. Once associated STAT1 is phosphorylated which allows for its translocation to the nucleus where it stimulates target genes (Hu & Ivashkiv, 2009). The IFNγ/STAT1 pathway is primarily responsible for the induction of iNOS expression, pro-inflammatory cytokine secretion, as well as chemokines including C-X-C ligand motif (CXCL) 9, CXCL10 and CXCL11 which attract natural killer and T cells to assist in the inflammatory response (Martinez et al., 2008; Trinchieri 2003; MacMicking et al., 1997).

Many immune cells have the capacity to produce and secrete IFNγ, including Th1 cells, natural killer cells, and professional antigen-presenting cells including macrophages (Young, 1996; Frucht et al., 2001). Macrophage release of IFNγ may be a key component of early inflammatory responses, likely involved in autocrine activation as well as paracrine activation of nearby immune cells (Gessani & Belardelli, 1998; Frucht et al., 2001). IFNγ has been shown to inhibit proliferation of Th2 cells without affecting Th1 cell proliferation. As a result, the T-lymphocyte population shifts towards the pro-inflammatory Th1 state (Bach et al., 1995). Furthermore, IFNγ causes increased cell surface expression of class I MHC on macrophages which effectively increases the likelihood for cytotoxic T cell recognition of non-self peptides and subsequent cell-mediated immunity (Boehm et al., 1997). Exposure to IFNγ has been shown to result in upregulation of iNOS and shift the cellular priorities away from proliferation and towards effector functions including the production and secretion of pro-inflammatory cytokines, and synthesis of NO and other

reactive oxygen species in order to kill invading microbes (Schroeder et al., 2004, van Dyken and Locksley, 2013; Fairfax et al., 2014; Hume & Freeman, 2014)

1.5.2 LPS and TLR4

LPS, a component of gram-negative bacterial cell wall, is a PAMP and thus its molecular structure and receptor are well studied. LPS consists of three parts: lipid A, an oligosaccharide core, and a highly variable O side chain (Raetz & Whitfield, 2002; Miller et al., 2005). The main PAMP of LPS is lipid A which has been highly conserved throughout evolution (Płóciennikowska et al., 2015). TLRs are a group of PRRs expressed by cells of the innate immune system, which respond to structural motifs known as PAMPs (Akira et al, 2006). Thirteen different types of TLRs have been identified in mammals, twelve of which are found in mice and ten in humans (Płóciennikowska et al., 2015). TLR4 is an essential PRR which recognizes LPS and begins a downstream cascade to initiate an inflammatory response (Kawai and Akira, 2010; West et al., 2006, Beutler, 2009). A sequence of molecular interactions must take place before LPS elicits a response from TLR4. First LPS must bind to LPS binding protein, a soluble shuttle protein which facilitates the association between LPS and CD14, a glycosylphosphatidylinositol-anchored glycoprotein found on the cell surface of macrophages (Wright et al., 1989; Simmons et al., 1989; Lu et al., 2008). The primary binding site for LPS is located in an N-terminal hydrophobic pocket of CD14 monomers (Kim et al., 2005; Kelley et al., 2013). Next CD14 transfers LPS to MD-2, a soluble protein which is associated with TLR4 (Nagai et al., 2002; Gioannini et al., 2004). By interacting with MD-2 and the adjacent TLR4 simultaneously, LPS promotes dimerization with a second MD-2/TLR4 receptor complex (Park et al., 2009). Following

oligomerization, four adapter proteins including myeloid differentiation primary response gene 88 (MyD88), Toll/interleukin-1 receptor domain-containing adaptor protein (TIRAP), TIR domain-containing adaptor inducing IFN-β (TRIF), and TRIF-related adaptor molecule (TRAM), are recruited through interactions with TIR domains (O'Neill & Bowie, 2007). LPS engagement of TLR4 can initiate signalling via both MyD88-dependent and MyD88-independent pathways.

MyD88-dependent signalling involves MyD88 and TIRAP. Following TLR4 activation, MyD88 recruits IL-1 receptor-associated kinase-4 and inducing a protein phosphorylation cascade ultimately resulting in activation of IκB kinase (IKK) (Motshwene et al., 2009; Lin et al., 2010b; Gay et al., 2014). IKK phosphorylates inhibitor of κ light chain gene enhancer in B cells (IκB), resulting in degradation of inhibitory IκB proteins and consequent translocation of nuclear factor kappa-light-chain-enhancer of activated B cells (NF-κB) to the nucleus (Lu et al., 2008). Mitogen-activated protein kinase pathways extracellular signal-regulated kinase, p38, and c-Jun N-terminal kinase are also activated downstream of TLR4, all of which also play a critical role in the secretion of pro-inflammatory cytokines (Sato et al., 2005; Peroval et al., 2013).

MyD88-independent signalling functions through adapter protein TRAM and signalling molecule TRIF. TRIF recruits another adapter protein (TRAF3) to activate interferon regulatory factor 3 resulting in induction of type I interferon genes as well as IFN inducible chemokines such as IL-10 (Oganesyan et al., 2006; Kawai & Akira, 2011). TRIF also recruits and activates IKK leading to NF-κB activation (Meylan et al., 2004; Ea et al., 2006). Macrophage interaction with various types of bacteria and viruses induces transcription of many pro-inflammatory genes associated with the M1 phenotype, including

TNF-α, IL-6, and iNOS (Benoit et al., 2008). This response consequently stimulates Th1 cell population expansion and release of IFNγ. However, some studies demonstrate that TLR signalling, when accompanied by ligation of Fc gamma receptor (FCγR) results in M2b phenotype that is characterized by arginase-1 upregulation along with TNF-α and IL-10 secretion (Anderson et al., 2002). These macrophages are considered to be inhibitors of the acute inflammatory response due to their large secretion of IL-10, which can stimulate Th2 cell proliferation and secretion of IL-4/IL-13 (Martinez et al. 2008). Macrophage phenotypic polarizations are not mutually exclusive. A recent study examining AMϕ response to influenza virus demonstrated the AMϕs polarize to the M1 phenotype by 4 hours post-infection, and shift to M2b phenotype by 8 hours post-infection (Zhao et al., 2014). These findings highlight the plasticity of macrophage populations, not only in response to different stimuli but also over time with the same stimuli.

1.6 M2 polarization

Macrophages also take part in inflammation resolution and tissue repair, a highly organized process which reverses the inflammatory response by induction of counter-regulatory mechanisms, including halting neutrophil recruitment, as well as removal of apoptotic neutrophils. In a model of LPS induced lung injury it has been demonstrated that exudate macrophages derived from GR-1^{high} $CCR2^{high}$ $CX3CR1^{low}$ monocytes release IL-1 receptor antagonist (IL-1ra), which may block activity of IL-1 receptor (IL-1R) on AMϕs and alveolar epithelial cells (Benoit et al., 2008; Hussel & Bell., 2014). As a result of IL-1R antagonism, the release of macrophage inflammatory protein 2 by AMϕs and alveolar epithelial cells decreases, effectively reducing neutrophil recruitment, but triggering

neutrophil apoptosis (Herold et al., 2011). It is proposed that upon recognition of apoptotic neutrophils the pro-inflammatory transcriptional profiles within the AMϕs are switched, wherein pro-inflammatory cytokine secretion decreases as a result of decreasing NF-κB stimulation (Cvetanovic and Ucker, 2004).

M2 phenotype AMϕs are heterogenous, and they may be further described by three specific and distinct phenotypes: M2a, M2b, and M2c. The M2a subtype is the phenotype which is traditionally referred to simply as M2 or alternatively activated macrophages. Macrophages polarize to the M2a phenotype in response to IL-4/IL-13 and exhibit upregulated arginase-1, Ym1, FIZZ1, and secrete IL-10, and TGF-β (Rőszer, 2015). These macrophages are important for anti-inflammatory properties including cell proliferation, growth factor release, and apoptotic cell removal (Gensel & Zhang, 2015). M2b macrophages are often referred to as type II macrophages and are activated by TLR ligands including LPS and may secrete pro-inflammatory cytokines IL-6 and TNF-α. Studies suggest that M2b is of particular importance in the proliferative phase of inflammation resolution in order to trigger tissue remodelling (Mosser and Edwards 2008; Lech and Anders, 2013). M2b macrophages also release IL-10 which may potentially play a role in activation of M2c macrophages, which are primarily activated by IL-10 and TGF-β (Mantovani et al., 2004; Novak and Koh, 2013; Rőszer 2015). M2c macrophages are highly immunosuppressive and are found in higher quantities during the remodeling phase of inflammation resolution, as indicated by high levels of TGF-β (Lech and Anders, 2013; Novak and Koh, 2013).

1.6.1 IL-4 and IL-13 receptors

IL-4 and IL-13 are both typical Th2 cytokines and can induce similar physiological effects. However, they are independently regulated and have distinct functions in a Th2/M2 response. In macrophages IL-4 and IL-13 can elicit a myriad of cellular responses by interacting with two types of heterodimeric transmembrane receptor complexes. The type I receptor is composed of an IL-4Rα chain paired with a common gamma (γC) chain, whereas the type II receptor results from the pairing of the IL4-Rα chain with an IL-13Rα1 chain (Munitz et al., 2008). Consequently, only IL-4 may activate the type I receptor, but both IL-4 and IL-13 are capable of binding type II receptors. Both receptor types mediate their signalling responses via JAK-STAT pathways: IL-4Rα is associated with JAK1, γC associates with JAK3, and IL-13Rα1 with JAK2 (Kelley-Welch et al., 2003; Heller et al., 2012). There is also a decoy receptor IL-13Rα2 for which IL-13 has four orders of magnitude greater binding affinity than IL-13Rα1, however this receptor does not interact with a JAK and is generally considered to be indirectly inhibitory (Lupardus et al., 2010; Madala et al., 2011; Heller et al., 2012). The shared IL4-Rα chain stimulates JAK1 which activates STAT6, a key component of IL-4/IL-13-mediated upregulation of arginase-1 and downregulation of NO production (Rutschman et al., 2001). In macrophages, the type I receptor also exhibits γC dependent tyrosine phosphorylation of insulin receptor substrate 2, which can recruit phosphoinositide 3-kinase and consequently lead to upregulated expression of several M2-related genes including arginase-1, and Ym1 (Heller et al., 2008).

1.6.2 IL-4/IL-13 downstream signalling

One established action of IL-4 in tissue resident macrophages is to increase proliferation (Jenkins et al., 2011). Activated STAT6 translocates to the nucleus where it upregulates/activates transcription of several target genes, one being stem cell-inducing factor Krüppel-like factor 4 (KLF4), an important factor in macrophage self-renewal and development (Aziz et al., 2009). KLF4 has also been noted to co-operate with STAT6 to upregulate arginase-1 along with Mrc1, and resistin-like molecule (Retnla/FIZZ1) alpha, all of which are hallmarks of the M2 phenotype (Liao et al., 2011). Simultaneously KLF4 has been shown to actively suppress M1-associated NF-κB activation (Liao et al., 2011; Pello et al., 2012). Both IL-4 and IL-13 appear to activate peroxisome proliferator-activated receptor gamma and delta via STAT6, leading to suppression of inflammation (Odegaard et al., 2007; Odegaard et al., 2008; Kang et al., 2008). Despite these discoveries made in various cell types, the specific role of IL-4/IL-13 and their respective receptors have not yet been fully elucidated in AMϕs.

1.7 GABA signalling in macrophages

1.7.1 GABA synthesis, release and uptake

Gamma-aminobutyric acid (GABA) is the primary inhibitory neurotransmitter in the central nervous system (Sieghart, 2006). Therefore, knowledge of GABA signalling is obtained mainly from studies of neuronal cells. GABA is produced by decarboxylation of L-glutamate through the enzymatic activity of glutamic acid decarboxylase (GAD), which has two different isoforms: GAD65 and GAD67 (Nasreen et al., 2011). In neurons GAD65 is localized to the nerve terminals and is involved with GABA synthesis for neurotransmission

(Soghomonian & Martin, 1998). Vesicular GABA transporter (GAT) transports GAD65-produced GABA into secretory vesicles until release (McIntire et al., 1997). GAD67 is distributed throughout the cell body and synthesizes GABA for development and normal cell function (Kanaani et al., 2010). Murine knockout studies have demonstrated the importance of GADs, specifically GAD67, in development. Fetuses lacking GAD_{67} may perish from respiratory failure, and possess abnormalities in axonal and synaptic morphogenesis making the organism unviable (Kuwana et al., 2003, Salazar et al., 2008). GABA transaminase (GABA-T) is an enzyme which functions to degrade GABA and convert it back into L-glutamate, balancing glutamate-GABA metabolism (Bhat et al., 2010, Liu et al., 2004).

After GABA has generated its signalling effects it must be removed from the extracellular environment by the GAT in order to limit signalling duration. There are four types of GATs (GAT1–4), and their activity is Na^+/Cl^- dependent (Salazar et al., 2008). GAT-1 is primarily responsible for GABA uptake in the adult central nervous system (Gadea & Lopez-Colome, 2001; Schousboe et al,. 2004), however GAT-3 is most prevalent during development (Evans et al., 1996; Minelli et al., 2003).

1.7.2 GABA receptors

GABA generates signals through ionotropic A-type and C-type receptors, as well as metabotropic B-type receptors (Möhler, 2006; Benarroch, 2007; Lujan, 2007). $GABA_AR$s are GABA-gated ion channels that are permeable to anions such as chloride. A functional $GABA_AR$ is composed of five subunits and each $GABA_AR$ subunit has four transmembrane domains (M1-M4), as well as a large extracellular N-terminal domain and a short intracellular C-terminal domain (Barnard et al., 1998; Sigel & Steinmann, 2012). Humans

express a myriad of genes which may code for the following GABA receptor subunits: α1–6, β1–3, γ1–3, δ, ε, θ, and π (Simon et al., 2004). While a variety of subunits may be used to form the GABA receptor, most physiologically relevant receptor compositions are formed by two α, two β, and one other subunit which is most frequently γ. (Sigel & Steinmann, 2012). As a result, $GABA_A$Rs may achieve functional diversity by variations in subunit combinations, affecting factors such as affinity for GABA, or ion channel kinetics, which will alter the result of GABA binding (Macdonald & Olsen, 1994; Benarroch, 2007). Subunit composition also has important pharmacological consequences; as different subunit compositions may affect the degree to which GABAergic drugs such as benzodiazepines open the receptor pore. For example, zolpidem shows preferential affinity for the α1 subunit and has hypnotic effects, while diazepam exerts its anxiolytic effects through $GABA_A$Rs which express α2 (Crestani et al., 2000; Crestani et al., 2001; Möhler, 2006). Gephyrin is a scaffolding protein for $GABA_A$Rs. In neurons, gephyrin interacts with $GABA_A$R subunits and helps to anchor and cluster receptors at inhibitory synapses (Choii & Ko, 2015).

$GABA_A$Rs are ligand gated ion channels, which upon activation by the endogenous ligand GABA results in Cl^- flow through the channel in the direction determined by electrochemical gradient (Sieghart, 2006). In typical neurons Cl^- flows inward resulting in hyperpolarization of the cell. However, in premature neurons it has been found by patch clamp recording that Cl^- flow is outward resulting in cellular depolarization (Bhat et al., 2010; Ben-Ari Y et al., 2007). The direction of Cl^- flow has been determined to be a result of variations in intracellular Cl^- concentration. Immature neurons have intracellular concentration of Cl^- of roughly 30mM, whereas the Cl^- concentration in mature neurons is closer to 10mM. As a result, $GABA_A$R binding causes efflux in neuroblasts, and influx in

mature neurons (Owens et al., 1996). Elevated Cl^- in premature neurons can be attributed to NKCC1, a $Na^+/K^+/2Cl^-$ active symporter, which results in intracellular accumulation of Cl^-. This effect is balanced in matured neurons by the K^+/Cl^- co-transporter KCC2, which pumps Cl^- out of the cell (Owens & Kriegstein, 2002). This process has also been hypothesized to occur in immune cells (Tian et al., 2004; Prud'homme et al., 2015).

$GABA_C$Rs are GABA-gated pentameric anionic channels that are composed of subunits ρ1–3. Similar to $GABA_A$Rs they can be inhibited by treatment with picrotoxin and activated by muscimol, however these receptors do not respond to bicuculline (Bormann & Feigenspan, 1995; Feigenspan & Bormann, 1998). Pharmacological differences between $GABA_A$R and $GABA_C$R are not fully understood, however, ρ1 subunit of $GABA_C$R is highly expressed in both the olfactory bulb and the retina, implicating a potential role for $GABA_C$ signalling in these systems (Cutting et al., 1991; Chen et al., 2007).

$GABA_B$R is a G-protein coupled receptor (GPCR), a large protein family which bind ligands outside the cell and activate signal transduction pathways by coupling with specific G proteins (Trzakowski et al., 2012). A functional $GABA_B$R is formed by two subunits, $GABA_{B1}$ and $GABA_{B2}$. In the brain the $GABA_B$R are most commonly linked via G proteins to open K^+ channels in order to hyperpolarize neurons (Chen et al., 2005). In addition, $GABA_B$R suppresses voltage-gated Ca^{2+} channels effectively decreasing Ca^{2+} entry (MacDermott et al., 1999).

1.7.3 $GABA_A$R signalling in neural development

GABA signalling has been hypothesized to play an important role during neurogenesis, affecting proliferation, differentiation, and migration (Owens & Kriegstein,

2002; Ben-Ari, 2002). During the developmental stages the GABA-mediated inhibitory effect is not present. Instead, activation of $GABA_A$Rs in developing neuroblasts results in a depolarizing effect due to Cl^- efflux. This depolarization has been shown to inhibit DNA synthesis and arrest the cell cycle, effectively preventing proliferation which may initiate a shift towards differentiation (LoTurco et al., 1995; Estefanía et. al, 2012). For example, a study by Tozuka et al., shows that treatment of brain slices with GABA increases expression of NeuroD, a transcription factor that contributes to neuronal differentiation (Tozuka et al., 2005). Since GABA signalling is critical for development and differentiation in the brain, it is possible that GABA signalling may also influence phenotypic shift in other cell types.

1.7.4 GABA signalling in immune cells

Recent research has demonstrated the presence and activity of GABA signalling within the peripheral system, including the pancreas and immune system (Bhat et al., 2010; Taneera et al., 2012). $GABA_A$R subunits α1, α2, β3 and δ have also been discovered in murine peritoneal macrophages (Reyes-García et al., 2007). Furthermore, recent research has demonstrated the presence of $GABA_A$R on human AMs (Sanders et al., 2015). There are several noted functions for $GABA_A$Rs in the immune system, including immunosuppression. Prud'homme et al., demonstrated GABA signalling in T cells and macrophages resulted in a decrease of pro-inflammatory cytokine secretion via NF-kB inhibition (Prud'homme et al., 2013). Peritoneal macrophages isolated from mice and treated with GABA-T inhibitor vigabatrin secreted significantly lower quantities of pro-inflammatory cytokine IL-1β following LPS stimulation (Bhat et al. 2010). GAT2 expression and consequently GABA uptake has been found to be upregulated following inflammatory activation (Dionisio et al.,

2011, Paul et al., 2014). Taken together, these findings illustrate the inflammation suppression due to GABA signalling, and the inflammatory response that occurs when the signalling is interrupted. GABA is also reported to contribute to increased proliferation in response to endogenous GABA or by treatment with $GABA_AR$ selective agonist muscimol (Takehara et al., 2007; Tamayama T et al., 2005).

1.8 GABA signalling in AMϕs – Preliminary data

Unpublished studies in my laboratory using lys-EGFP-ki mice (Faust et al., 2000) have demonstrated the presence of α2-$GABA_AR$ on AMϕs in murine lungs, of which the expression decreases when the animal is injected peritoneally with LPS (**Figure 1.2**). Conversely in an ovalbumin (OVA)-induced asthma model, the α2-$GABA_AR$ expression in AMϕs increases in comparison with controls (**Figure 1.3**). These findings suggest a link between GABA signalling and AMϕ polarization. Therefore, I began to explore whether $GABA_AR$-mediated signalling plays a role in AMϕ polarization when carrying out an honors thesis project. My studies demonstrated that under culture conditions AMϕs extracted from bronchoalveolar lavage (BAL) expressed high levels of α2- and β2/3-subunits of $GABA_AR$, as well as GAD65/67 (**Figure 1.4**).

When these AMϕs were treated with LPS, the expression of α2-$GABA_AR$ decreased drastically while the expression of F4/80, an immunoregulatory GPCR in mouse macrophages (Lin et al., 2010a), increased significantly (**Figure 1.5**). Treatment of the primary AMϕs with the $GABA_AR$ channel blocker picrotoxin increased TNF-α secretion suggesting that an autocrine GABA signalling in AMϕs critically regulates the cells' function Interestingly, following LPS treatment picrotoxin no longer affected TNF-α

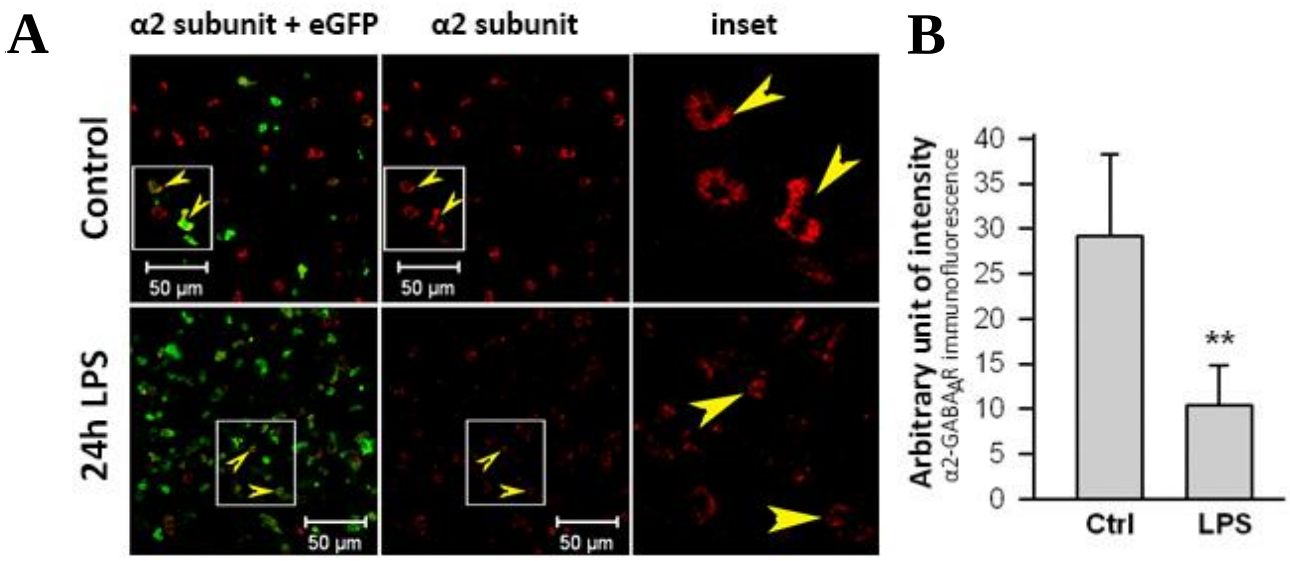

Figure 1.2. GABA$_A$R expression is decreased following LPS treatment. (A) Lung tissues prepared from naïve (Control) lys-EGFP-ki mice (Faust et al., 2000) and lys-EGFP-ki mice intraperitoneally injected with LPS (100 μg/kg) were immune-stained for α2-subunit of GABA$_A$R (red). Twenty-four hours after LPS treatment, a large number of macrophages infiltrated the lung, which express both GFP and α2-GABA$_A$R. (**B**) Plotting data from image analyses showed that the immunofluorescent intensity of α2-GABA$_A$R in AMϕs of LPS-treated mice significantly decreased, in comparison with control mice. Plotted data represent mean ± SEM. Significant difference (unpaired T-test), $p < 0.01$ (**).

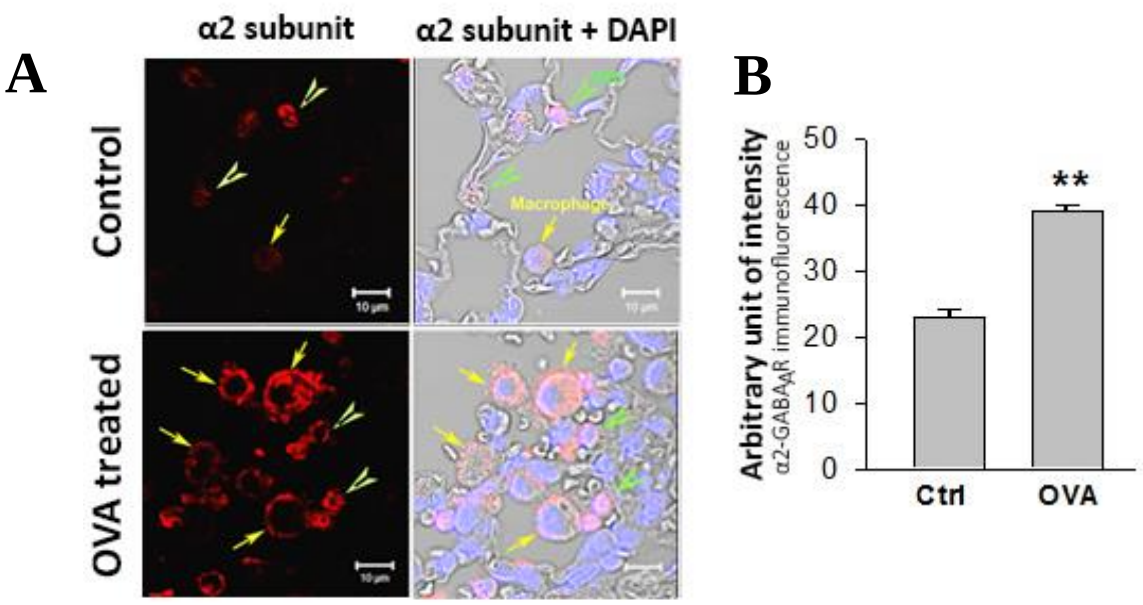

Figure 1.3. $GABA_AR$ expression is increased in OVA-treated mice. BALB/c mice were sensitized twice at day-1 and day-11 and then challenged at day-30 with ovalbumin (OVA) to induce allergic asthmatic reaction, an immune response characterized by Th2 inflammation (Singh et al., 2011). (**A**) Lung tissues of naive mice (control) and OVA-treated mice were double-strained for α2-subunit of $GABA_ARs$ (red) and DAPI (blue). AMϕs and alveolar type II epithelial cells were indicated with yellow arrows and green arrows, respectively. (**B**) The immunofluorescence intensity of α2-$GABA_AR$ increased significantly in AMϕs of OVA-treated mice, in comparison with control mice. Plotted data represent mean ± SEM. Significant difference (unpaired T-test), $p < 0.01$ (**).

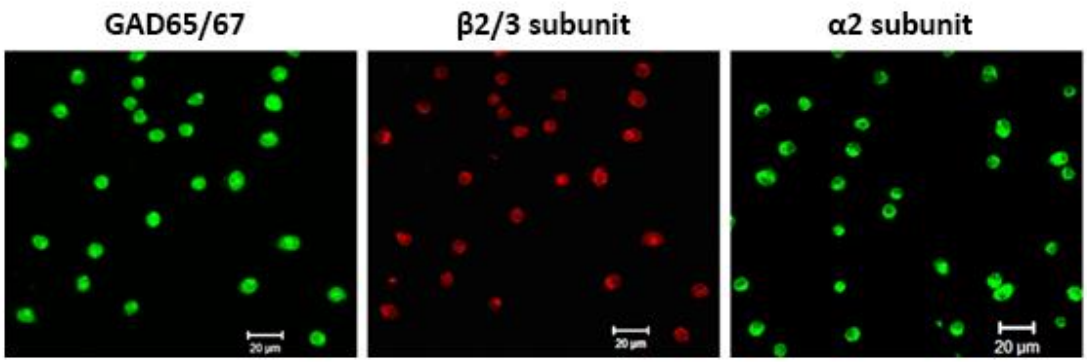

Figure 1.4. AMϕs express GABA signalling molecules. AMϕs were isolated by BAL of C57BL/6 mice. Immunocytochemical assays showed that AMϕs express GAD65/67, as well as the α2- and β2/3-subunits of $GABA_AR$.

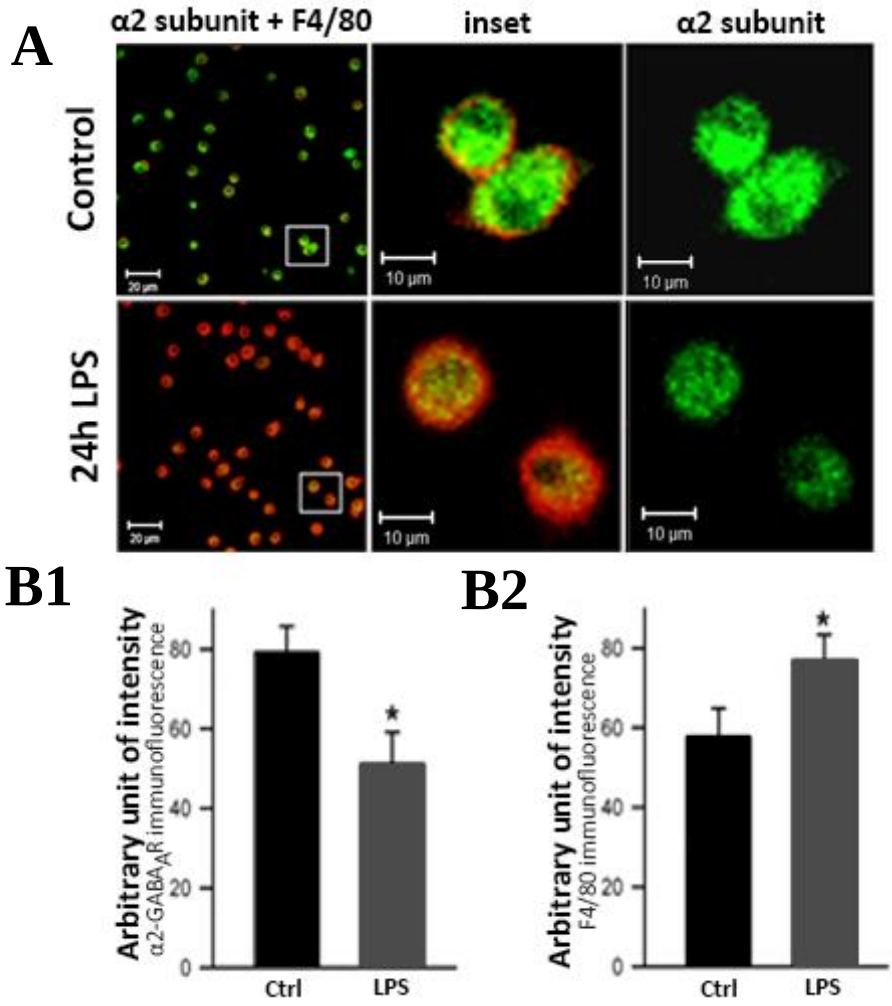

Figure 1.5. Activation of murine AMϕs with LPS reduces GABA$_A$R expression. (**A**) AMs extracted from BAL of C57BL/6 mice were treated with LPS (500ng/mL) for 16 hours. Naïve (control) and LPS-treated (+ LPS) cells were then double-stained for F4/80 (red) and α2-GABA$_A$R (green). (**B**) Plotted data showed that LPS treatment largely increased the immunofluorescence of F4/80 (**B2**), indicating an activation of AMϕs, but decreased the immunofluorescence of α2-GABA$_A$R (**B1**). Plotted data represent mean ± SEM. Significant difference (unpaired T-test), $p < 0.05$ (*), $n = 3$.

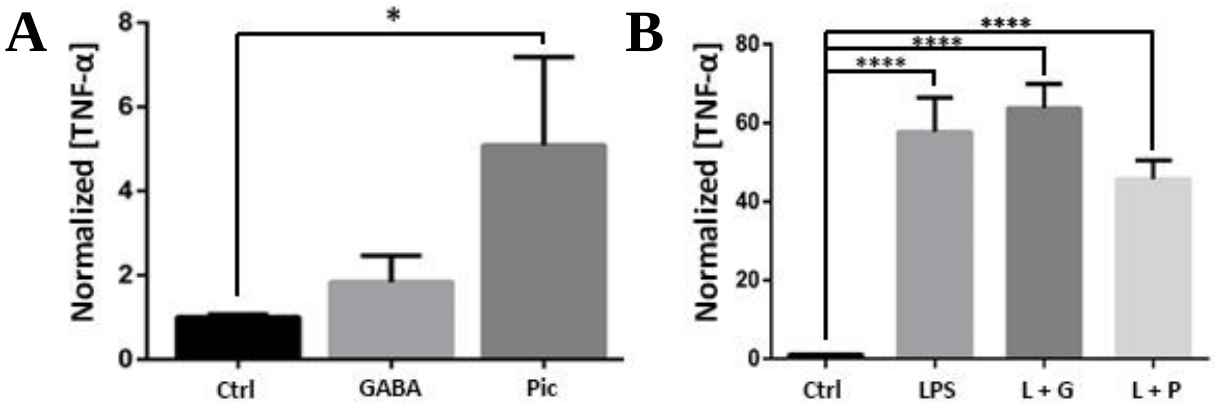

Figure 1.6. $GABA_AR$ blockade increased TNF-α secretion from control, but not LPS-treated AMϕs. (**A**). ELISA of culture media revealed that treating AMϕ with $GABA_AR$ antagonist picrotoxin (PIC, 50μM), but not GABA (100 μM), for 24 hours significantly increased TNF-α secretion, suggesting an autocrine GABA signalling of the cells. (**B**). Treating AMϕs with LPS (500ng/mL) for 24 hours greatly increased TNF-α secretion. However, treating the cells with LPS and GABA (L + G), or with LPS and picrotoxin (L + P) for 24 hours had no significant effect on TNF-α secretion. Plotted data represent mean ± SEM. Significant difference (ANOVA/Tukey's HSD), $p < 0.05$ (*), $p < 0.0001$, $n = 3$.

secretion, which may be related to the downregulation $GABA_A$Rs by LPS (**Figure 1.6**).

1.9 Rationale, hypothesis, and aims

1.9.1 Rationale

AMϕs are unique tissue resident macrophages due to their direct exposure to the atmosphere. Over the course of an immune challenge to the lung, LMϕs—including AMϕs—play a pivotal role in both the inflammatory process and resolving inflammation. More precisely, LMϕs respond to stimuli present in their environment by polarizing to different phenotypes in order to maintain the homeostasis of lung tissues. Therefore, a tight regulation of phenotypic populations of LMϕs within the lung is critical for pulmonary immunity. Like other tissue resident macrophages, LMϕs express higher levels of iNOS when exhibiting an M1 phenotype, but express high levels of arginase-1 when polarizing to M2 phenotypes.

Previous studies in my laboratory demonstrated expressions of GAD65/67 and $GABA_A$Rs in LMϕs. Interestingly the expression levels of $GABA_A$Rs in LMϕs, particularly in AMϕs, decreased in mice treated with LPS but increased in mice experiencing allergic asthmatic reaction. My 4^{th} year honors thesis studies confirmed the expression of GAD65/67 and $GABA_A$Rs in AMϕs under culture conditions, and the $GABA_A$R expression decreased in cultured AMϕs 24 hours after exposure to LPS. Importantly, blocking $GABA_A$R-mediated signalling in control AMϕs increased TNF-α secretion. Taken together, these combined results from previous studies suggested that an autocrine GABA signalling plays a role in phenotypic polarization of AMϕs. Although GABA signalling has been identified in other immune cells such as peritoneal macrophages, very little study on GABA signalling has been done in either AMϕs or IMϕs. In particular, whether GABA signalling regulates LMϕ

polarization remains to be addressed. **This thesis study sought to determine if GABA signalling in LMϕs regulates their phenotypic polarization as well as inflammatory response**.

1.9.2 Hypothesis

On the basis of available data, **I hypothesized that GABA signalling regulates phenotypic polarization and inflammatory activities of LMϕs**.

1.9.3 Aims

To test the above hypothesis, I carried out experiments focused on the following two aims:

The first aim was to determine if GABA signalling plays a role in LMϕ polarization. To this end, I first established specific markers for each phenotype of LMϕs. I expected to confirm that treating macrophages with LPS and Th1/Th2 cytokines alter their expression profiles of the conventional M1 and M2 markers iNOS and arginase-1, respectively. Along with specific markers, I also examined secretion of pro-inflammatory cytokine TNF-α and anti-inflammatory cytokines IL-4 and IL-10. I would then be able to examine the effects of $GABA_AR$ agonist and/or antagonist on the expression of these M1 and M2 markers and cytokines.

The second aim was to study whether the expression levels of GABA signalling proteins in LMϕs are modified with their phenotypic polarizations. More precisely, I determined whether the expression of GAD65/67 and α2-GABAAR in macrophages

changes during M1/M2 polarization, and if so, whether the phenotypic markers and cytokine profiles reflect the changes of GAD65/67 and α2-$GABA_AR$ expressions in the cells.

Considering that quantification of phenotypic marker proteins would requires a large amount of cells but the quantity of LMϕs extracted from lung tissues was limited, I decided to use both primary LMϕs derived from C57BL/6 mice, as well as RAW 264.7 cells in my studies. RAW 264.7 cells are a macrophage cell line derived from BALB/c mice. These cells are widely used for studies as they maintain many of the properties of macrophages including NO production, motility, phagocytosis, and extreme sensitivity to TLR agonists.

2.0 MATERIALS AND METHODS

Usage of animals in this study was approved by the UWO Animal Care and Veterinary Services through the Animal Use Protocols #2010-038 (Dr. Wei-Yang Lu) and #2016-010 (Drs. Sanjay Mehta and Sean Gill)

2.1 RAW 264.7 cell culture

RAW 264.7 cells (ATCC, Manassas VA) were cultured in Dulbecco's Modified Eagle Medium (Gibco by Life Technologies) high glucose media containing 5.0 g/L L-Glutamine, Fetal Bovine Serum (10%; Life Technologies) and Penicillin-Streptomycin (100U/100µg/mL; Life Technologies). Cells were incubated at 37°C; 5% CO_2 and 95% O_2. Cell were maintained and used before they reached 60-70% confluency.

2.2 AM isolation and culture

Primary AMϕs were obtained from male C57BL/6 mice (8-10 weeks; Charles River Laboratories) by collecting bronchial alveolar lavage (BAL), of which it is estimated that 98% of the cells retrieved are macrophages and only 0.2% will be IMϕs (Huang et al., 2005; Bedoret et al., 2009). Mice were anaesthetized using 1 – chloro – 2, 2, 2 – trifluoroethyl difluoromethyl ether (Isofluorane; Baxter Corporation), and euthanized by laceration of the inferior vena cava. A small incision was made in the trachea into which a catheter tube (BD Angiocath; Becton, Dickinson and Company) was inserted. One millilitre of lavage fluid—1x Hanks Balanced Salt Solution (HBSS; $CaCl_2$/$MgCl_2$/$MgSO_4$ free, Gibco by Life Technologies) containing 15mM ethylenediaminetetraacetic acid (EDTA; 0.5M, pH 8.0, Ambion by Life Technologies)—was pumped through the catheter into the lungs, and pulled

back out three times using a 1mL insulin syringe (0.45mm x 13mm; Becton, Dickinson and Company) in order to collect the cells. This process was repeated three times in order to maximize cell collection, yielding a total of 3mL of lavage fluid per mouse and roughly one million cells.

After collection the cells in HBSS + EDTA were placed on ice until lavage of all mice was completed. The total lavage fluid was centrifuged at 1500rpm for 10 minutes at 4°C. The cellular pellet was then washed two times in Dulbecco's Phosphate Buffered Saline (PBS; $CaCl_2$/$MgCl_2$ free, Sigma Life Science), and the cell solution was centrifuged at 1500rpm for 10 minutes at 4°C after each wash. The cells were re-suspended in AM Culture Media Roswell Park Memorial Institute Medium (RPMI; Gibco by Life Technologies) 1640 medium containing Fetal Bovine Serum (10%; Life Technologies), L-glutamine (2mM; GlutaMAX 100x, Gibco by Life Technologies), and Penicillin-Streptomycin (100U/100µg/mL; Life Technologies). Cells were plated in 12-well plates on glass coverslips primed with Poly-D-Lysine and placed in a 37°C incubator containing 5% CO_2 and 95% O_2.

2.3 LMϕ isolation and culture

LMϕs were obtained courtesy of Dr. Sean Gill and with the assistance of Cynthia Pape. Male C57BL/6 mice 12-14 weeks of age were euthanized and lungs were removed. The lungs were then perfused via the right ventricle with 10 mL PBS in order to remove red blood cells, and immediately placed in digest buffer (1X 'S' buffer + Enzyme D & Enzyme A; components of Lung Dissociation Kit, Miltenyi Biotec, Bergisch Gladbach, Germany). Tissue was then disrupted using Miltenyi's gentleMACS dissociator, followed by a 30-

minute incubation period. During this time the sample was subjected to continuous rotation using MACSmix Tube Rotator in order to allow for maximal enzymatic dissociation. The sample was disrupted once more, then passed subsequently through 100 and 70 µm cell strainers. Cells were then centrifuged at 1500 rpm for 10 minutes at 4°C and resuspended in RPMI 1640 + 0.5% bovine serum albumin + 2mM EDTA. Next, the sample was incubated at 4°C with Milentyi $CD45^+$ microbeads for 15 minutes, which magnetically label the desired $CD45^+$ cells. The solution containing cells and microbeads were added to LS columns attached to magnetic MidiMACS Separator. The column was then washed out with 3mL media, which eluted all cells except for $CD45^+$ cells which were stuck to the magnetic microbeads. The column was removed from the magnetic separator and eluted resulting in the collection of only $CD45^+$ cells, which were then used in immunocytochemical studies. The CD45 microbeads have been demonstrated to have high specificity as determined by flow cytometry, such that cells negative for $CD45^+$ that are present in the original suspension do not flow through the column (Schiedlmeier et al., 2000).

2.4 Cell treatments

Treatments used for both RAW 264.7 murine cell line and primary cells include: LPS (500 ng/mL; Sigma-Aldrich, St. Louis, MO), Th1 cytokine IFNγ (100ng/mL;Cedarlane, Burlington ON), Th2 cytokines IL-4 (25ng/mL; R&D Systems Inc., Minneapolis, MN) and IL-13 (25ng/mL; R&D Systems Inc.), $GABA_AR$ agonist muscimol **(**20µM; Sigma-Aldrich**),** $GABA_AR$ channel blocker picrotoxin (50µM; Sigma-Aldrich), iNOS inhibitor 1400W dihydrochloride (20µM; R&D Systems**),** and IKK inhibitor BAY 11-7082 (25µM;Santa Cruz Biotechnology Inc., Dallas, TX). Cells were treated with LPS, IFNγ, IL-4, and IL-13

for 16 hours, while inhibitors picrotoxin, 1400W dihydrochloride, and BAY 11-7082 were given 90 minutes prior to LPS or IL-4/IL-13 treatments.

2.5 Western blot

Following treatment, cells were lysed and the protein concertation in lysate was determined using BioPhotometer Plus UV/Vis Photometer (Eppendorf, Hamburg, Germany). Western blotting was performed using an Owl^{TM} dual-gel vertical electrophoresis system (Thermo Fisher Scientific, Waltham, MA). Resolving gels were selected for each protein of interest based on molecular weight. For detection of α2-$GABA_AR$ (50kD), and arginase-1 (38 kD) 10% acrylamide gels were run, while iNOS (131kD) was run on an 8% gel. GAD (65/67kD) was run on an 8% gel despite small protein size in order to allow for sufficient separation of the two proteins. A 4% stacking gel was used for all experiments. Through trial and error, appropriate loading protein concentrations were determined for each protein of interest: 80µg for GAD, 120µg for $GABA_AR$, 70µg for arginase-1, and 60µg for iNOS. Samples were diluted in 2X sample buffer and electrophoresed in 192mM glycine/25mM Trizma base/0.1% SDS running buffer for 30 minutes at 60V, followed by one hour at 100V. Proteins were then transferred for two hours at 80V onto a 0.45µM nitrocellulose membrane (Bio-Rad laboratories, Mississauga, ON) using Mini Trans-Blot Cell (BioRad) containing 192mM glycine/25mM Trizma base/20% methanol transfer buffer. The membrane was then blocked for one hour in 5% skim milk in 10mM Tris-HCl/150mM NaCl/0.1% Tween-20 (TBS-T). Following the block, the membrane was probed overnight at 4°C with primary antibody against: α2-$GABA_AR$ (Rabbit; Alomone Labs Ltd., Jerusalem,

Israel), GAD 65/67 (Rabbit; Sigma-Aldrich), iNOS (Mouse, Santa Cruz Biotechnology), Arinase-1 (Chicken; Merck Millipore, Billerica, MA).

The following day, the membrane was washed three times in TBS-T for 10 minutes followed by secondary antibody application for 1.5 hours. Secondary antibodies used were horseradish peroxidase-conjugated goat anti-rabbit immunoglobulin G (BioRad), goat anti-mouse (Jackson ImmunoResearch Labs, West Grove, PA), and donkey anti-chicken (Jackson ImmunoResearch Labs). The membrane was washed three times for 10 minutes each. Clarity^{TM} Western enhanced chemiluminesence Blotting Substrate (BioRad) was applied to the membrane for 5 minutes to allow for chemiluminescent imaging. Images were taken using Molecular Imager VersaDoc^{TM} MP 5000 System (BioRad, #1708650) in conjunction with Quantity One 1-D Analysis Software. Anti-β-actin (Mouse; Sigma-Aldrich) antibody along with goat anti-mouse horseradish peroxidase (Jackson ImmunoResearch Labs) was used to detect β-actin as a loading control protein for all experiments. Image-J was used for densitometry analysis of Western blot images. Each experiment was repeated three times.

2.6 Immunocytochemistry

Collected cells were seeded onto poly-D-Lysine coated glass coverslips in 12-well plates, then treated as outlined in Section 2.4. Once the media was removed, cells were fixed to the coverslip using a 4% paraformaldehyde (Electron Microscopy Science) solution diluted in PBS. Coverslips were then washed once with PBS containing 0.1M glycine, and twice more with PBS. At this point cells were permeabilized with 0.1% Triton X-100 (Sigma-Aldrich), with the exception of studies examining α2- and β2/3-$GABA_AR$

expression. Coverslips were then blocked with 5% Normal Donkey Serum (NDS; Jackson ImmunoResearch) diluted in PBS for 1 hour. The cells were treated overnight at 4°C using the following primary antibodies in 1% NDS solution: α2-$GABA_AR$ (Rabbit; Alomone Labs Ltd.), Arinase-1 (Chicken; Merck Millipore), F4/80 (Rat; Abcam, Cambridge, United Kingdom), GAD65/67 (Rabbit; Sigma-Aldrich), gephyrin (Mouse; Synaptic Systems, Göttingen, Germany) iNOS (Rabbit; Abcam), iNOS conjugated to Alexa Fluor 488 (Mouse, Santa Cruz Biotechnology Inc.), LAMP1 (Rat; R&D Systems), GAT-1 (Mouse; Synaptic Systems).

The next day coverslips were washed three times, then secondary antibody in 1% NDS was applied for one hour. The following secondary antibodies were purchased from Jackson ImmunoResearch for these studies: Alexa Fluor 488 Donkey Anti-Chicken, FITC Donkey Anti-Rabbit, FITC Donkey Anti-Rat, Cy3 Donkey Anti-Rat, Cy3 Donkey Anti-Mouse, Cy3 Donkey Anti-Rabbit. Coverslips were washed three times, and 4′,6-Diamidino-2-phenylindole dihydrochloride (DAPI; Sigma-Aldrich) was applied for 10 minutes in order to stain the nuclei. Finally, coverslips were mounted using Fluromount G (Electron Microscopy Sciences; Hatfield PA) and preserved until imaging.

Cells were examined and photographed using the Zeiss LSM 510 Meta Confocal Microscope at the Confocal Microscopy Core Facility located at the Robarts Research Institute. Ten randomly selected cells were imaged from each treatment group, and each experiment was repeated three times. Image-J software was used for quantification of fluorescence intensity amongst test groups. For each cell in which staining intensity was to trace the perimeter of the cell was using Image-J, and the average staining intensity within

the enclosed area was calculated (**Figure 2.1**). After measurements of each cell were completed, the mean values were calculated for comparison between groups.

2.7 Luminex assay

Following treatment, the supernatant was removed and combined with Halt Protease Inhibitor Cocktail (Thermo Fisher Scientific) at a ratio of 1µL:100µL media, then centrifuged at 2000rpm for 10 minutes at 4°C. The cellular pellet was discarded and the supernatant was preserved at –80°C for Luminex multiplex assay. Cytokine analysis was carried out by Shannon Seney at the Screening Lab for Immune Disorders, Canadian Centre for Human Microbiome and Probiotic Research located at Lawson Health Research Institute in London, Ontario. Cell supernatants were tested via Luminex multiplex assay for TNF-α, IL-4, and IL-10. Luminex assays were carried out as follows: colour-coded beads were conjugated to protein-specific capture antibodies and added along with cell supernatant samples into a microplate and incubated for two hours. After washing the beads, protein-specific, biotinylated detector antibodies were added and incubated with the beads for one hour. Excess biotinylated antibody was washed away, and phycoerythrin conjugated streptavidin was added to bind to biotinylated antibodies. After 30 minutes, the wells were washed to remove unbound streptavidin and the beads are analyzed with a dual-laser Luminex detection system. One laser analyzed which protein was being detected, while the other measured the intensity of the phycoerythrin signal, which is proportional to the protein concentration in the sample.

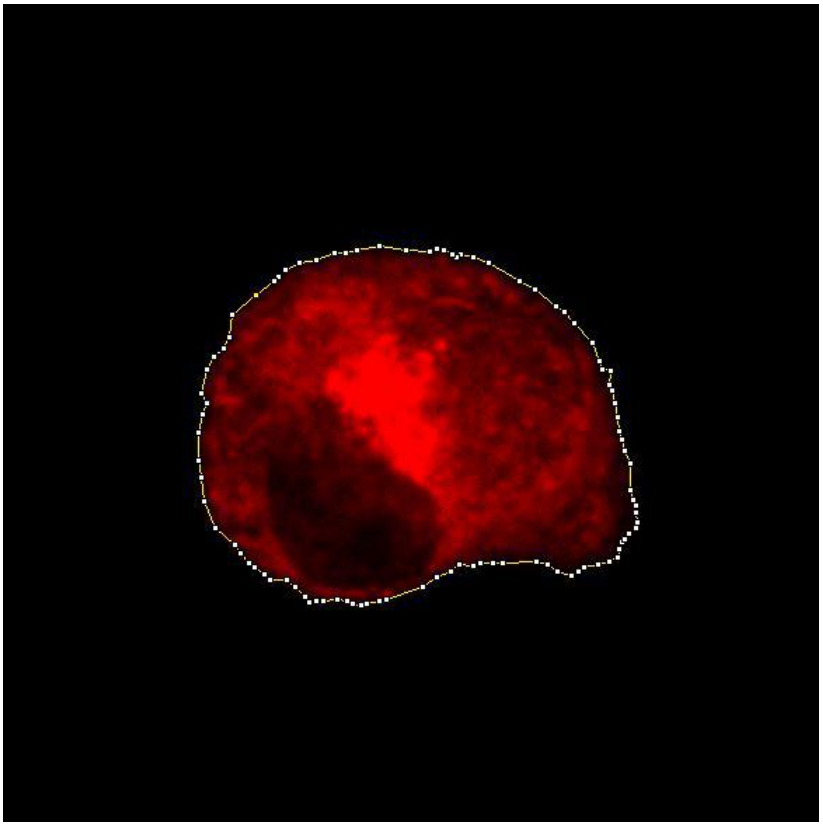

Figure 2.1. Illustration of delineating stained cells for immunofluorescence analysis. Images of immuno-stained macrophages were taken by confocal microscopy. Using ImageJ, the perimeter of an individual cell in each image file was delineated allowing for analysis of the average intensity of immuno-stained protein in each cell. More than ten cells were measured from each treatment group. The calculated mean value of fluorescence intensity was plotted and compared between treatment groups.

2.8 Patch-clamp recording

To test whether RAW264.7 cells produce and release GABA, we measured transmembrane current in cultured hippocampal neurons when exposing them to conditioned media from RAW264.7 cell cultures. Specifically, the conditioned media were collected from untreated RAW264.7 cells 24 hours after culture. Medium from the same bottle was incubated for 24 hours and then was used as controls.

As described previously (Fortin et al., 2001), cortical neurons were cultured from dissociated cortices of E14.5 mice. Briefly, cortices from C57BL/6 mouse embryos were dissected and incubated for 25 min at 37°C in Hank's balanced salt solution (GIBCO, BRL) containing 0.50 mg/ml trypsin. Trypsinization was stopped by incubating with 0.2 mg/ml trypsin inhibitor and 0.2 mg/ml DNase I for 2 min at 25°C. Cells were triturated in Neurobasal medium (GIBCO) and the cell suspension was centrifuged, and then the pellet was re-suspended in Neurobasal medium containing B-27 supplement, N-2 supplement, 0.5 mM glutamine, and 0.05 U/ml 0.05 mg/ml penicillin-streptomycin (GIBCO). Cortical cells were plated in Nunc 35 mm dishes coated with poly-D-lysine (Sigma-Aldrich). The cultured neurons were used for patch-clamp recordings 16 days after culture and they were bathed in the extracellular solution (ECS), which was composed of the following (in mM): 145 NaCl, 1.3 CaCl2, 5.4 KCl, 25 HEPES, and 33 glucose, pH 7.4 (osmolarity, 315 mOsm).

The procedures for whole-cell voltage-clamp recording were performed as previously described (Dong et al., 2004). Briefly, at room temperature (22°C) recordings were performed under voltage clamp (at -60 mV) mode with a MultiClamp 700 amplifier (Axon / Molecular Devices, San Francisco, CA). Electrodes (3-4 MΩ) were constructed from thin-walled glass (1.5 mm diameter; World Precision Instruments, Sarasota, FL). The

recording electrode was filled with an intracellular solution consisting of the following (in mM): 140 KCl, 35 KOH, 10 HEPES, 2 MgCl2, 1 CaCl2, 2 tetraethylammonium, and 4 ATP, pH 7.35 (osmolarity, 315 mOsm). Three to five minutes after a stable baseline recording was achieved, the control medium, conditioned medium, or medium containing 50 μM bicuculline was focally perfused to the test neuron, by means of a multibarrel perfusion system (SF-77B; Warner Instruments, Hamden, CT). The transmembrane conductance was continuously recorded, and the electrical signal was digitized, filtered (1 kHz), and acquired on-line using the program pClamp (Axon / Molecular Devices).

2.9 Statistical analysis

All graphs and statistics were produced using GraphPad Prism 6 software. Data are presented as mean values ± standard error of the mean. Statistical tests performed include non-parametric unpaired Student's t-test, along with one-way ANOVA followed by either Dunnett's or Tukey's multiple comparisons test using a significance level of at least $p < 0.05$.

3.0 RESULTS

3.1 Determining if GABA signalling plays a role in LMϕ polarization

3.1.1 Blockade, but not stimulation, of $GABA_AR$ caused an opposite change in the expression of iNOS and arginase-1 in macrophages

Typically, the M1 phenotype of macrophage is associated with elevated iNOS expression. My Western blotting assays determined that iNOS was undetectable in RAW 264.7 cells under control culture. However, sixteen to twenty-four hours after treatment with IFNγ or LPS, a high level expression of iNOS was detected (**Figures 3.1A** and **3.1B)**, indicating the inducible expression nature of this enzyme as previously demonstrated (MacMicking et al., 1997; Italiani & Boraschi, 2014). Interestingly, treating RAW 264.7 cells with LPS and the $GABA_AR$ antagonist picrotoxin further increased the expression level of iNOS by 2-fold (**Figure 3.1B**).

Immunocytochemistry, in combination with confocal microscopy, revealed a low level of iNOS immunofluorescence in control LMϕs. Exposure of LMϕs to IFNγ, however, induced roughly a five-fold increase in fluorescent intensity of iNOS (**Figure 3.1C**). Treating the cells with IL-4 + IL-13, or IL-4 + IL-13 together with the $GABA_AR$ agonist muscimol did not affect the level of iNOS fluorescence. In contrast, treatment with IL-4 + IL-13 together with picrotoxin yielded a significant 1.55-fold increase of iNOS-specific immunofluorescence (**Figure 3.2**).

Western blot analysis showed that arginase-1 expression in RAW 264.7 cells at an unstimulated state was too low to detect (**Figure 3.3**). Commonly, macrophages polarizing to M2 phenotypes display an increased expression of arginase-1. Indeed, upon stimulation

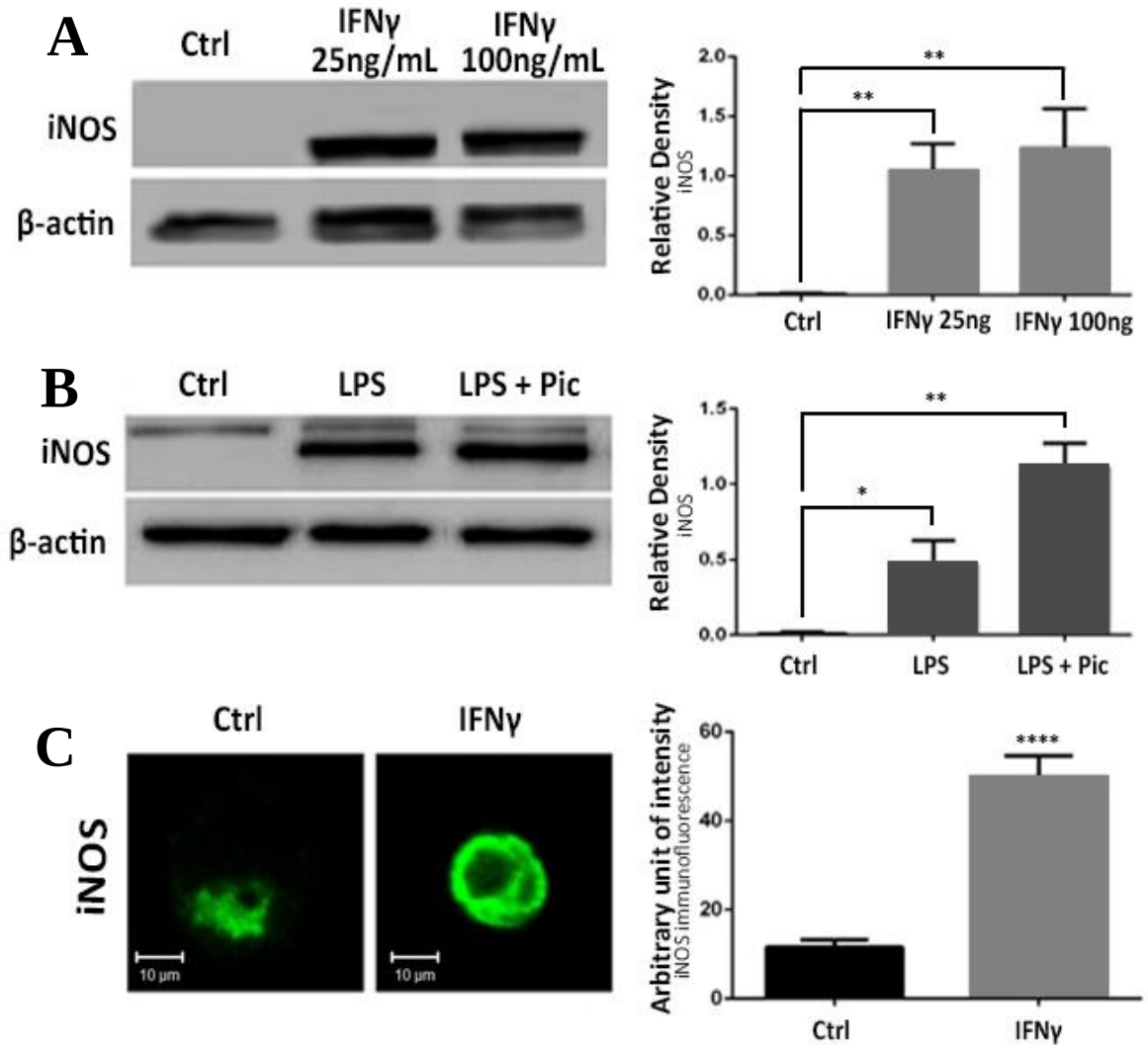

Figure 3.1. Inducible expression of iNOS is increased by picrotoxin. RAW 264.7 cells were treated with IFNγ, LPS (500ng/mL), and picrotoxin (50µM). Both IFNγ (**A**) and LPS (**B**) induced iNOS expression following 16-hour treatment as determined by Western blot. Treatment with picrotoxin 90 minutes prior to LPS treatment further increased iNOS expression. (**C**) In primary LMϕs examined by immunocytochemistry and confocal microscopy, IFNγ (100ng/mL) strongly increased iNOS. Plotted data represent mean ± SEM Significant difference (ANOVA/Tukey's HSD) $p < 0.05$ (*), $p < 0.01$ (**), $n = 3$.

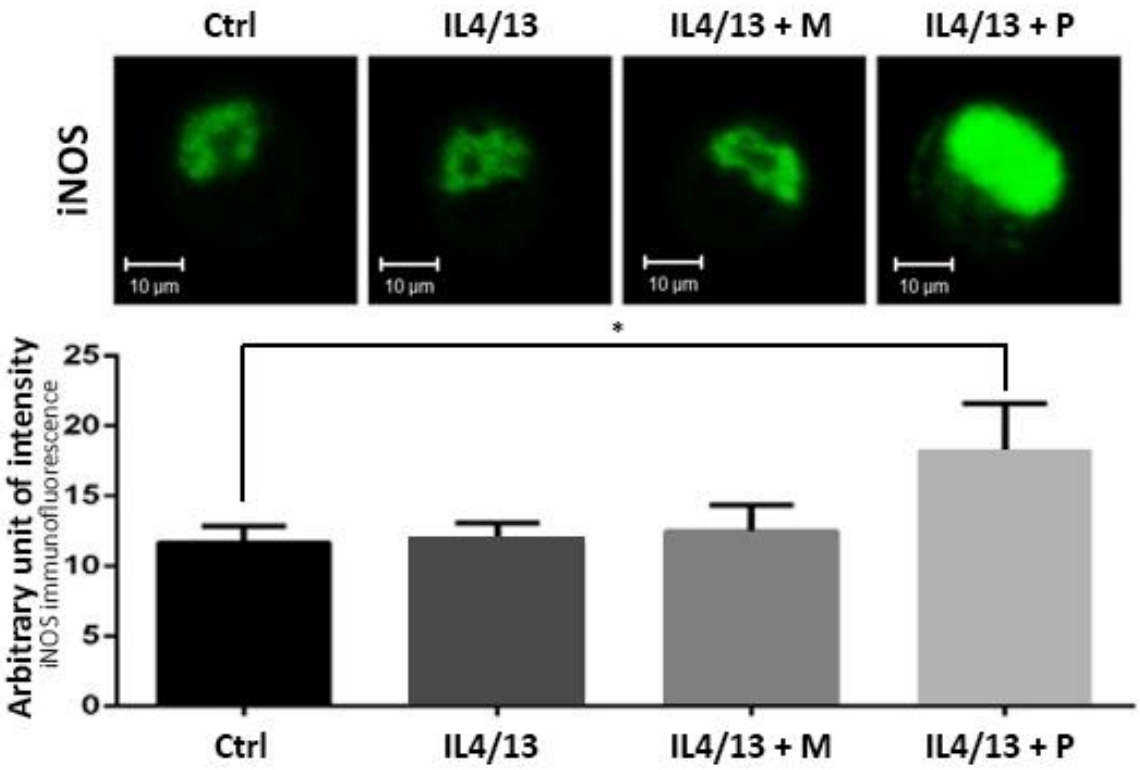

Figure 3.2. Picrotoxin increases iNOS expression in LMϕs treated with Th2 cytokines. Primary LMs were treated with IL-4 (25ng/mL) + IL-13 (25ng/mL) for 16 hours. Neither IL-4 + IL-13 nor IL-4 + IL-13 + muscimol (20µM) had an effect on the immunofluorescent intensity of iNOS. Treatment with picrotoxin (50µM), however, resulted in a significant increase of iNOS intensity in IL-4 + IL-13 treated LMϕs. Plotted data represent mean ± SEM. Significant difference (ANOVA/Dunnett's test) $p < 0.05$ (*), $n = 3$.

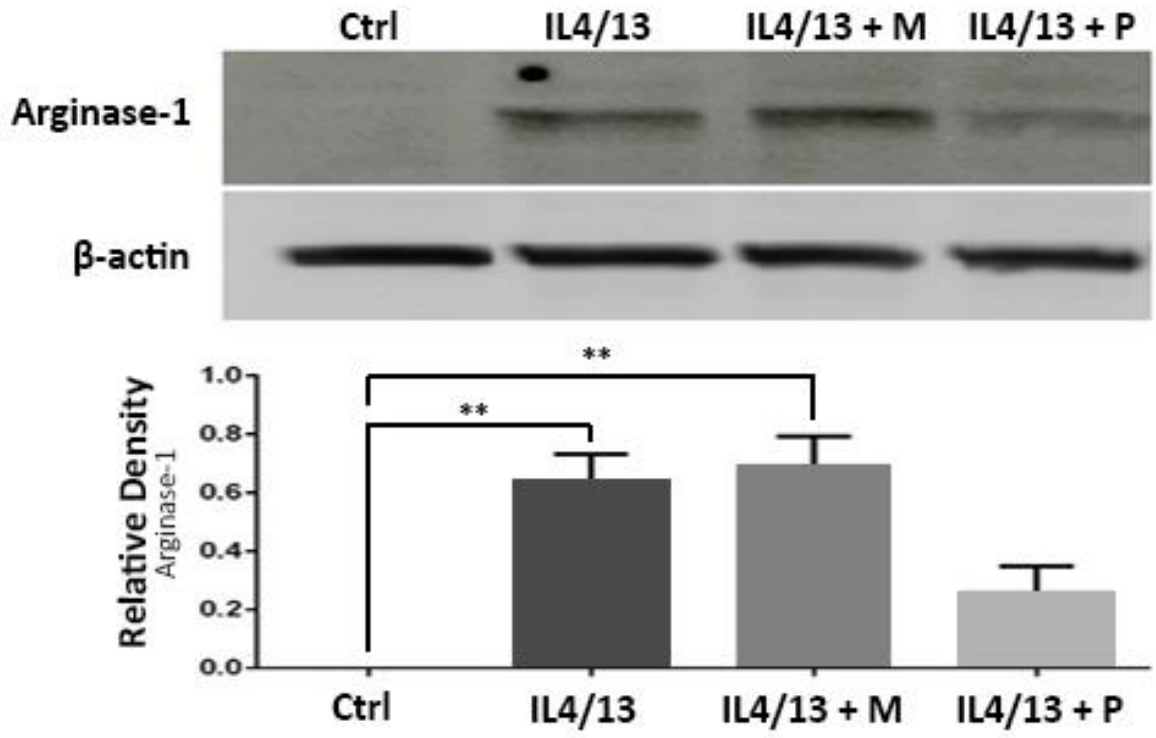

Figure 3.3. Picrotoxin decreases arginase-1 expression in RAW 264.7 cells. Treating RAW 264.7 cells with IL-4 (25ng/mL) + IL-13 (25ng/mL) increased arginase-1 expression significantly. Adding the $GABA_AR$ agonist muscimol (20μM) to the culture had no effect on arginase-1 expression. In contrast, the addition of $GABA_AR$ channel blocker picrotoxin (50μM) to the culture significantly decreased arginase-1 expression. Plotted data represent mean ± SEM. Significant difference (ANOVA/Dunnett's test) $p < 0.01$ (**), $n = 3$.

with Th2 cytokines IL-4 and IL-13, the protein level of arginase-1 was increased from relative density of 0 to 0.6. RAW 264.7 cells with the $GABA_AR$ agonist muscimol along with IL-4 and IL-13 did not appear to have an effect on arginase-1 expression. However, antagonizing $GABA_AR$ signalling with picrotoxin 90 minutes before IL-4 and IL-13 treatment significantly hindered the extent to which these Th2 cytokines upregulated arginase-1, lowering relative density to 0.2 (**Figure 3.3**). In LMϕs, a low-level baseline-expression of arginase-1 was detected by immunocytochemistry and confocal microscopy. Exposure of LMϕs to IFNγ effectively reduced the immunofluorescence intensity of arginase-1 (**Figure 3.4**). On the contrary, treating LMϕs with IL-4 and IL-13 increased the fluorescence intensity of arginase-1 by 1.35 fold. Notably, treating the cells with IL-4 and IL-13 and the $GABA_AR$ antagonist picrotoxin decreased arginase-1 levels, however in this instance arginase-1 was decreased below control expression levels (**Figure 3.5**).

3.1.2 Blockade, but not stimulation, of $GABA_AR$ distinctively altered cytokine secretion from macrophages depending on their phenotypic polarizations

In order to further classify phenotypic polarizations induced by LPS, IFNγ, and IL-4/IL-13 in the test macrophages, I employed the Luminex assay to analyze the concentrations of TNF-α, IL-10, and IL-4 in the media of RAW 264.7 cell and primary LMs. In addition, I applied muscimol and picrotoxin to examine the role of $GABA_AR$-mediated signalling in regulation of macrophage cytokine secretion.

TNF-α Secretion: Analyses showed that treating RAW 264.7 cells with IFNγ or with LPS significantly increased TNF-α secretion in comparison with control by 1.7 and 2.25 fold, respectively (**Figure 3.6A**).

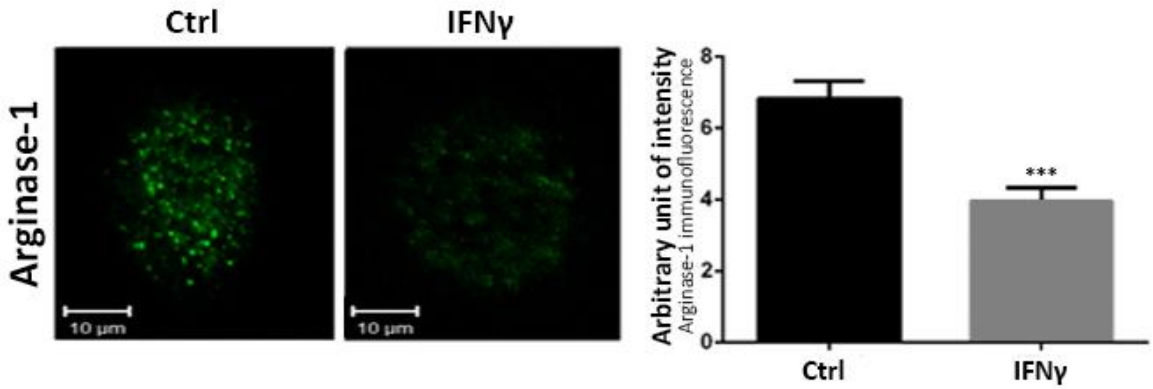

Figure 3.4. IFNγ decreases arginase-1 in primary LMϕs. Primary LMϕs were treated with IFNγ (100ng/mL) resulting in a decrease in arginase-1 expression. Plotted data represent mean ± SEM. Significant difference (unpaired T-test) $p < 0.001$ (***), $n = 3$.

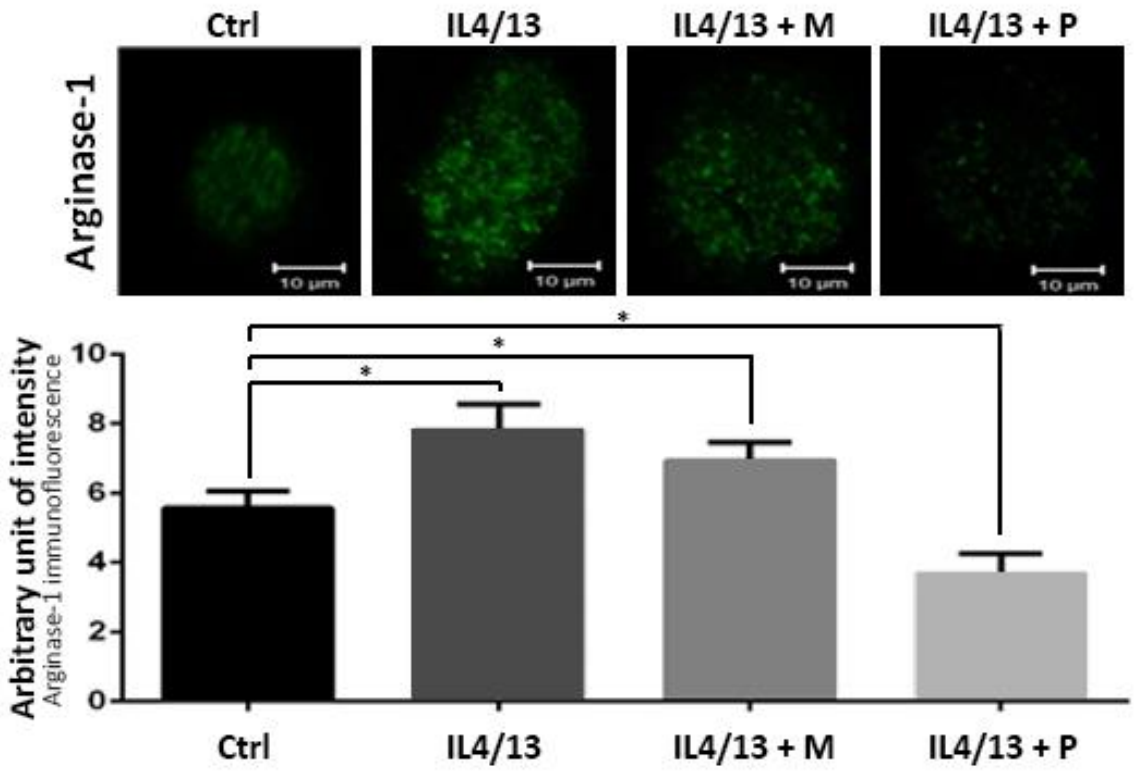

Figure 3.5. Picrotoxin decreases arginase-1 expression in primary LMϕs. Primary LMϕs were treated with IL-4 (25ng/mL) + IL-13 (25ng/mL) resulting in increased arginase-1 intensity. Adding muscimol (20µM) led to a slight decrease in arginase-1 expression compared with IL-4/IL-13 alone. Picrotoxin (50µM) pre-treatment decreased arginase-1 staining intensity below control level. Plotted data represent mean ± SEM. Significant difference (ANOVA/Dunnett's test) $p < 0.05$ (*), $n = 3$.

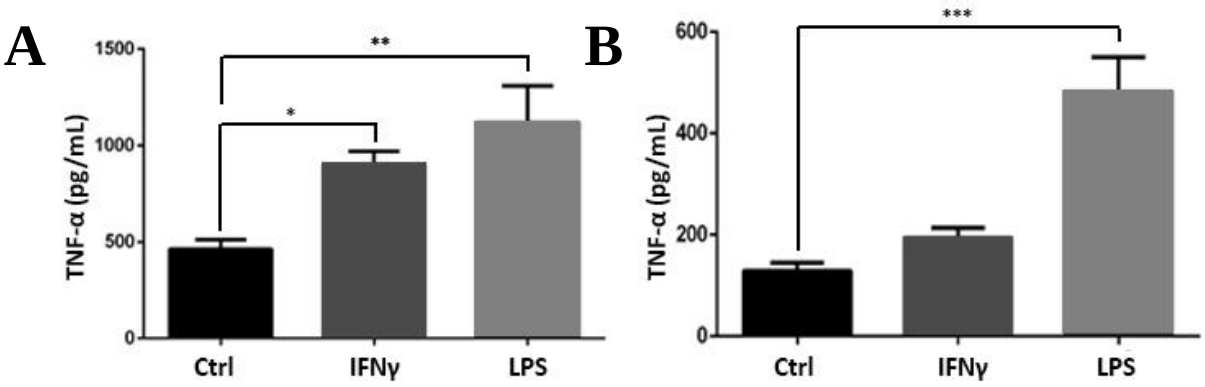

Figure 3.6. LPS and IFNγ increase TNF-α secretion. (**A**) In RAW 264.7 cells, IFNγ (100ng/mL) and LPS (500ng/mL) both increase TNF-α secretion. (**B**) In primary LMϕs, IFNγ (100ng/mL) did not increase TNF-α secretion. LPS (500ng/mL) however, resulted in a large increase in TNF-α release. Plotted data represent mean ± SEM. Significant difference (ANOVA/Tukeys's test), $p < 0.05$ (*), $p < 0.01$ (**), $p < 0.001$ (***), $n = 3$.

However, in primary LMϕs, only LPS treatment yielded a nearly 3 fold increase in TNF-α (**Figure 3.6B**). On the other hand, treating RAW264.7 cells with IL-4 + IL-13 reduced TNF-α secretion below control levels (**Figure 3.7A**). Addition of muscimol or picrotoxin did not have any impact on TNF-α secretion. In primary LMϕs IL-4 + IL-13 also reduced TNF-α secretion, however this effect was non-significant (**Figure 3.7B)**. Once again, addition muscimol and picrotoxin did not affect secretion of TNF-α.

IL-4 Secretion: Treatment with IFNγ and LPS induced a non-significant decrease of IL-4 secretion from RAW 264.7 cells (**Figure 3.8A**). However, both IFNγ and LPS resulted in a significant reduction of IL-4 secretion from LMϕs, with a more dramatic reduction following IFNγ treatment (**Figure 3.8B**). In contrast, treatment with IL-4/IL-13 greatly increased the detection of IL-4 in the media collected from both RAW 264.7 cells (**Figure 3.9A**) and primary LMϕs (**Figure 3.9B**). Treating RAW 264.7 cells or LMϕs with muscimol did not change the IL-4/IL-13-induced increase of IL-4 secretion. Treating the LMϕs with IL-4/IL-13 and picrotoxin also had no significant effect on IL-4 detection (**Figure 3.9B**), however, this might have resulted from mistaken medium collection. Remarkably, treating RAW 264.7 cells with IL-4/IL-13 and picrotoxin significantly reduced the increase in IL-4 secretion, in comparison with IL-4/IL-13 treatment alone.

IL-10 Secretion: IFNγ did not increase IL-10 secretion in RAW 264.7 cells or LMϕs. Contrary to our expectations, however, IL-10 secretion was largely increased by LPS treatment in both RAW 264.7 cells and LMϕs (**Figure 3.10A and 3.10B**), suggesting that LPS treatment may have induced a non-M1 phenotype. More surprisingly, IL-4/IL-13 significantly decreased IL-10 secretion from both RAW 264.7 cells (**Figure 3.11A**) and primary LMϕs (**Figure 3.11B**). IL-4/IL-13 + muscimol and/or picrotoxin had no effect.

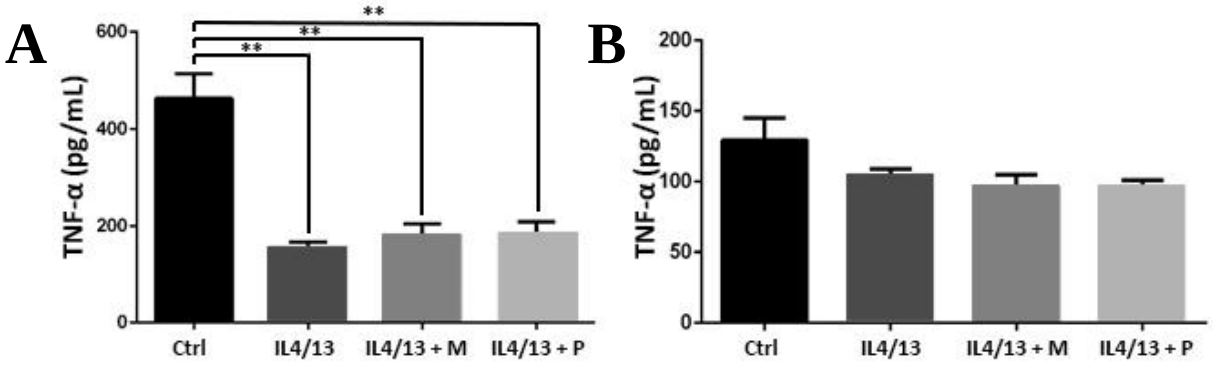

Figure 3.7. IL-4 + IL-13 decrease TNF-α secretion. (**A**) In RAW 264.7 cells, IL-4 (25ng/mL) + IL-13 (25ng/mL) caused a decrease in TNF-α release. Further addition of muscimol (20μM) or picrotoxin (50μM) did not further affect TNF-α secretion. (**B**) In primary LMϕs, IL-4 (25ng/mL) + IL-13 (25ng/mL) caused a slight but non-significant decrease in TNF-α secretion. Muscimol (20μM) or picrotoxin (50μM) did not have any effect. Plotted data represent mean ± SEM. Significant difference (ANOVA/Dunnett's test) $p < 0.01$ (**), $n = 3$.

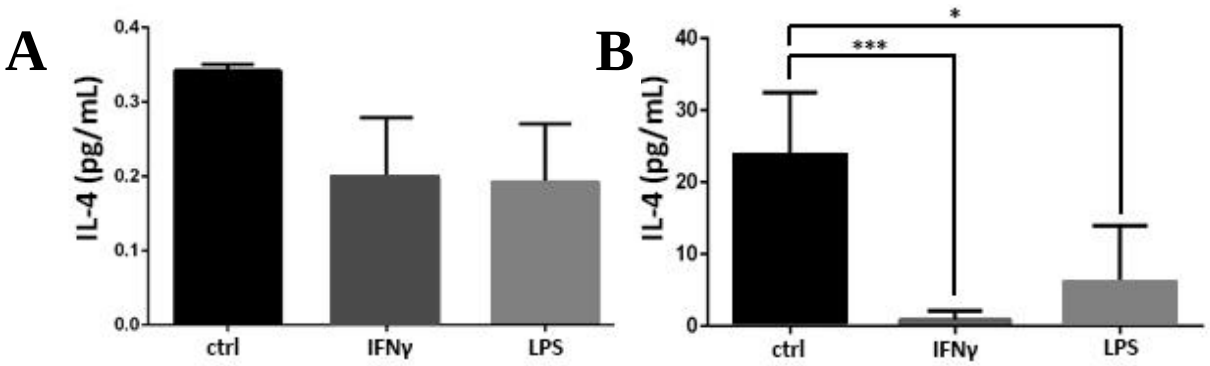

Figure 3.8. LPS and IFNγ decrease IL-4 secretion. (**A**) In RAW 264.7 cells, IFNγ (100ng/mL) and LPS (500ng/mL) both decrease TNF-α secretion, though this change is not significant. (**B**) In primary LMϕs, LPS (500ng/mL) caused a modest decrease in IL-4 secretion, while IFNγ (100ng/mL) nearly completely eliminated IL-4 secretion. Plotted data represent mean ± SEM. Significant difference (ANOVA/Dunnett's test) $p < 0.05$ (*), $p < 0.001$ (***), $n = 3$.

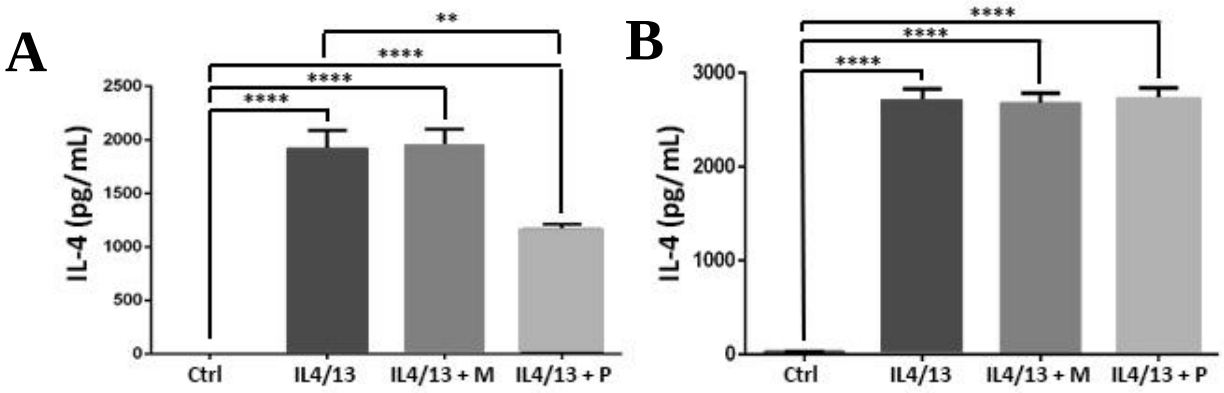

Figure 3.9. IL-4 + IL-13 increase IL-4 secretion, which is inhibited by picrotoxin (**A**) In RAW 264.7 cells, IL-4 (25ng/mL) + IL-13 (25ng/mL) cause an increase in IL-4 secretion. Further addition of muscimol (20μM) did not affect IL-4 secretion, however pre-treatment with picrotoxin (50μM) inhibited IL-4 secretion. (**B**) In primary LMϕs, IL-4 (25ng/mL) + IL-13 (25ng/mL) caused a large increase of IL-4 release. Further addition of muscimol (20μM) or picrotoxin (50μM) had no effect. Plotted data represent mean ± SEM. Significant difference (ANOVA/Tukey's HSD) $p < 0.01$ (**), $p < 0.001$ (****), $n = 3$.

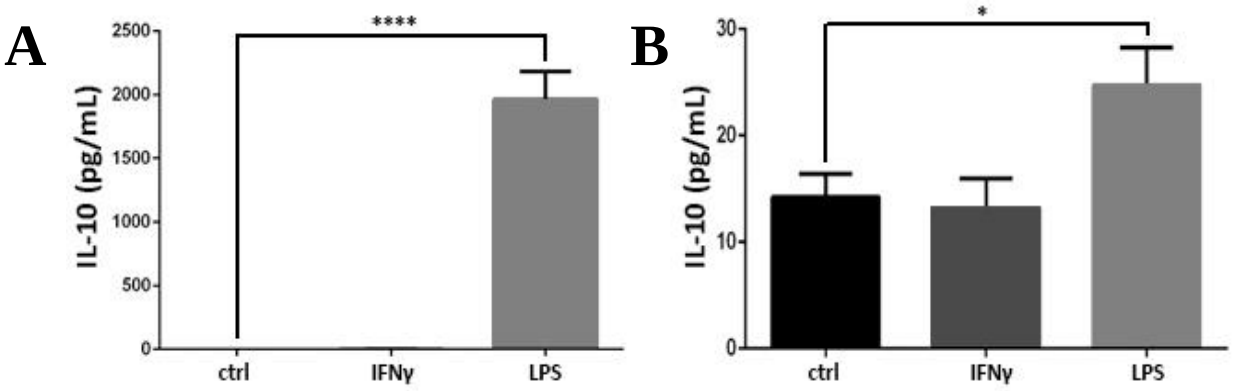

Figure 3.10. LPS increases IL-10 secretion. (**A**) Baseline secretion of IL-10 was minimal in RAW 264.7 cells, which was unaffected by treatment with IFNγ (100ng/mL). LPS (500ng/mL) induced a very large increase in IL-10 secretion, suggestive of M2b polarization. (**B**) In primary LMϕs, IFNγ (100ng/mL) treatment did not have an effect. However, LPS (500ng/mL) increased secretion of IL-10. Plotted data represent mean ± SEM. Significant difference (ANOVA/Dunnett's test) $p < 0.05$ (*), $p < 0.0001$ (****), $n = 3$.

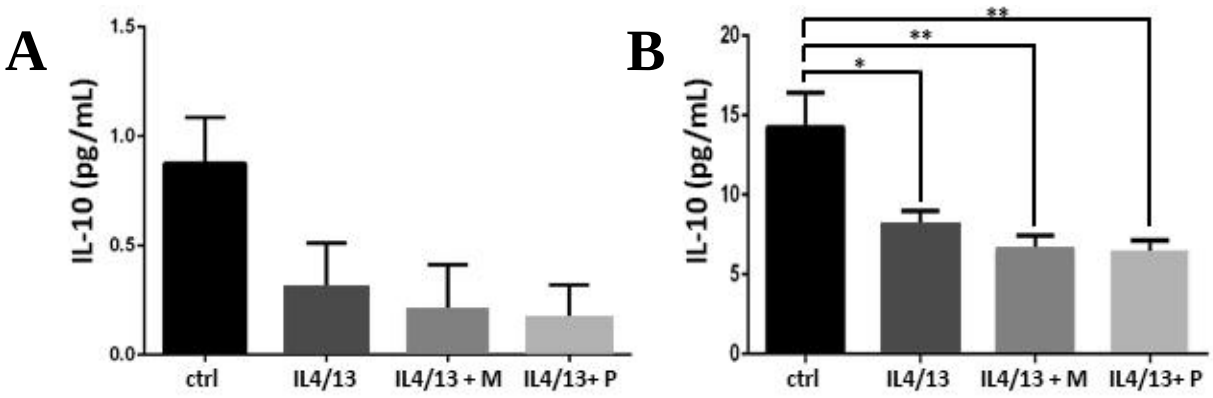

Figure 3.11. IL-4 + IL-13 decrease secretion of IL-10 (**A**) In RAW 264.7 cells, IL-4 (25ng/mL) + IL-13 (25ng/mL), IL-4 + IL-13 + muscimol (20μM), and IL-4 + IL-13 + picrotoxin (50μM) lowered IL-10 secretion, although these changes were not significant. (**B**) In primary LMϕs, IL-4 (25ng/mL) + IL-13 (25ng/mL) decreased secretion of IL-10, which decreased slightly further when muscimol (50μM) or picrotoxin (20μM) were added. Plotted data represent mean ± SEM. Significant difference (ANOVA/Dunnett's test) $p < 0.05$ (*), $p < 0.01$ (**), $n = 3$.

3.1.3 RAW 264.7 cells secrete GABA

The results described above showed that blockade, but not stimulation, of $GABA_AR$ affected the expression levels of iNOS and arginase-1, as well as IL-4 production by macrophages under specific conditions. Since both cell types express GABA-synthesizing enzyme GAD, I decided to examine whether these cells produce and secrete GABA. In collaboration with Matthew Maksoud, whole-cell voltage-clamp recordings were performed on cultured hippocampal neurons, which express $GABA_ARs$ that contains subunits with high affinity to GABA (Caraiscos et al., 2004). It is known that $GABA_ARs$ containing α5 subunit(s) has high affinity to GABA. Exposure of hippocampal neurons to the conditioned media collected from untreated RAW264.7 cell cultures, but not the control (blank) media, resulted in a transmembrane current in 4 out of 6 test cells. The amplitude of the media-induced current varied from 26-128 pA. Notably the current induced by the conditioned medium was blocked by the competitive $GABA_AR$ antagonist bicuculline (**Figure 3.12**). These results indicated that under normal conditions RAW 264.7 cells produce and secrete GABA.

3.2 Studying whether LMϕ polarization alters GABA signalling components

3.2.1 IFNγ and LPS lowered expression of GABA signalling proteins

Next I investigated whether macrophage polarization was associated with changes in protein expressions of GAD65/67 and α2-$GABA_AR$. Western blot assays showed that both α2-$GABA_AR$ (**Figure 3.13A**) and GAD65/67 (**Figure 3.13B**) were expressed in RAW 264.7 cells. Sixteen hours after treatment with IFNγ and LPS, the expression levels of α2-$GABA_AR$

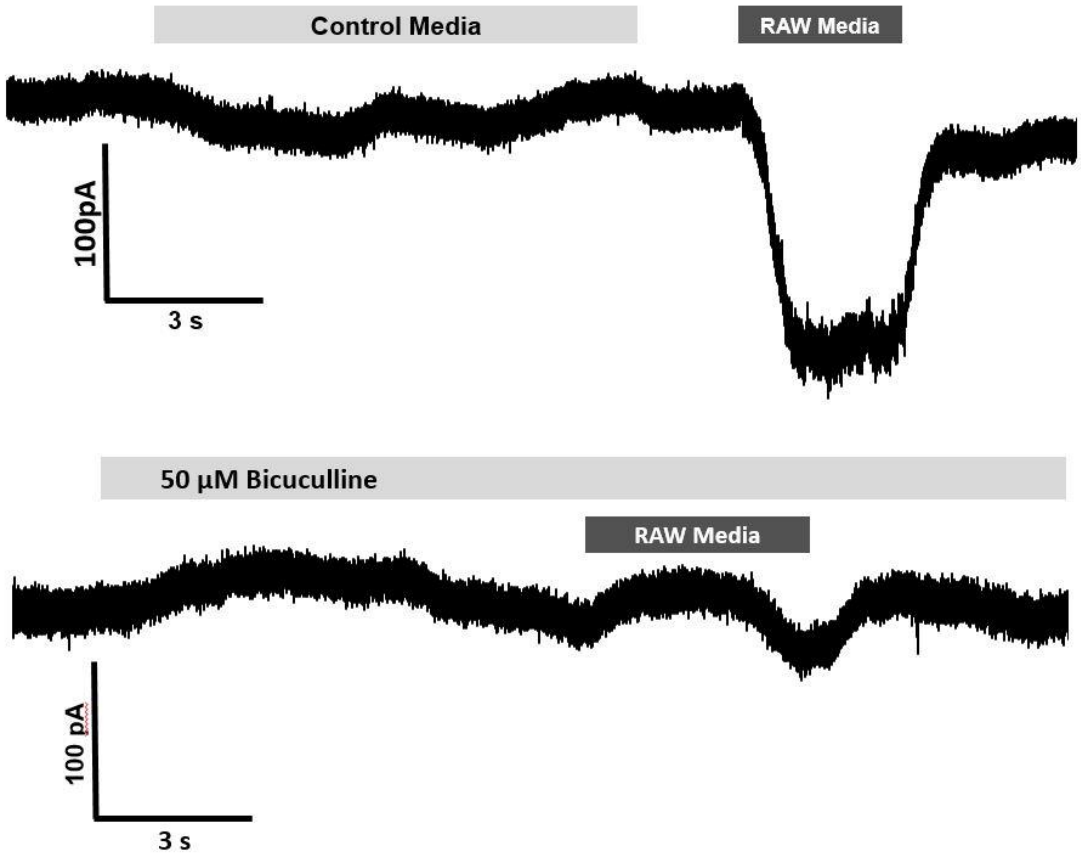

Figure 3.12. RAW 264.7 cell media induced bicuculline-sensitive transmembrane current in cultured hippocampal neurons. Shown are voltage-clamp recording traces in the same hippocampal neurons. *Upper trace*: exposing the cultured hippocampal neuron to conditioned media (RAW media), but not control (blank) media, induced a large transmembrane current. *Lower trace:* In the presence of 50µM bicuculline, a selective $GABA_AR$ antagonist, the conditioned media failed to induce current in the neuron. Note: Patch-clamp recording experiments were graciously performed by Matthew Maksoud, an MSc candidate in my lab.

and GAD65/67 in RAW 264.7 cells decreased significantly by a factor of 3.14 or 2.75 respectively (**Figures 3.13**). Immunocytochemistry and confocal microscopy revealed LMϕs were immunopositive for both α2-$GABA_AR$ (**Figure 3.14A**) and GAD65/67 (**Figure 3.14B**) in LMϕs. Similar to effects observed in RAW264.7 cells, treatment with IFNγ significantly decreased the immunofluorescence intensity of GAD65/67 and α2-$GABA_AR$ in LMϕs by 2.8 and 1.8 fold, respectively (**Figure 3.14**).

A previous study demonstrated that neuronal NOS (nNOS) induces S-nitrosylation of gephyrin, a $GABA_AR$ scaffolding protein, decreasing synaptic $GABA_ARs$ (Dejanovic & Schwarz, 2014). Thus, I examined whether LPS down-regulated $GABA_AR$ expression in RAW 264.7 macrophages through iNOS/NO signalling. My immunocytochemical analyses revealed positive immunofluorescence for both α2-$GABA_AR$ and gephyrin with low levels of co-localization in the plasma membrane and cytosol of RAW 264.7 cells (**Figure 3.15**, upper row). Interestingly, LPS treatment not only decreased the immunofluorescence of α2-$GABA_AR$ and gephyrin in the cells, but also caused internalization of both proteins to intracellular structures, which were co-localized in structures visualized as fluorescent clusters (**Figure 3.15**, mid row). Notably, treating the cells with the iNOS inhibitor 1400W dihydrochloride largely eliminated the effect of LPS on the fluorescence intensity and cellular location of α2-$GABA_AR$ and gephyrin (**Figure 3.15**, lower row). These results suggested that activation of TLR4 by LPS regulates $GABA_AR$ expression and localization in macrophages likely through upregulation of iNOS activity. Next, I performed double-staining for α2-$GABA_AR$ and *lysosomal-associated membrane protein* 1 (*LAMP*-1) in control and LPS-treated RAW264.7 cells.

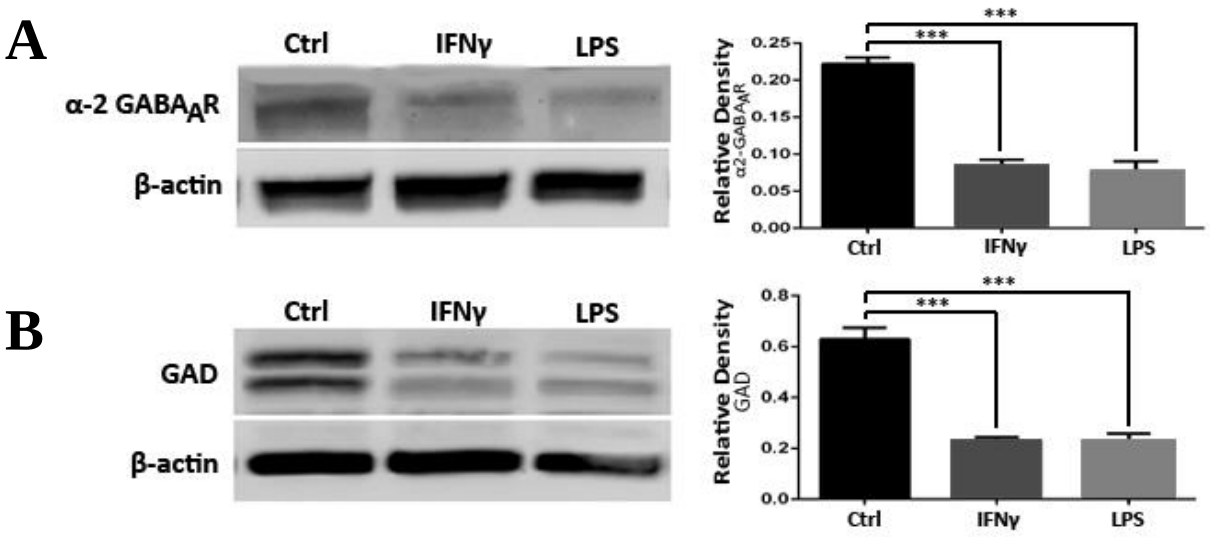

Figure 3.13. RAW 264.7 cells exhibit lower protein levels of α2-GABA$_A$R and GAD65/67 in response to LPS and IFNγ. RAW 264.7 cells were treated with LPS (500ng/mL) or IFNγ (100ng/mL) for 16 hours. Western blots showed that such treatments significantly decreased the expression of α2-GABA$_A$R (**A**) and GAD65/67 (**B**). Plotted data represent mean ± SEM. Significant difference (ANOVA/Dunnett's test) $p < 0.001$ (***), $n = 3$.

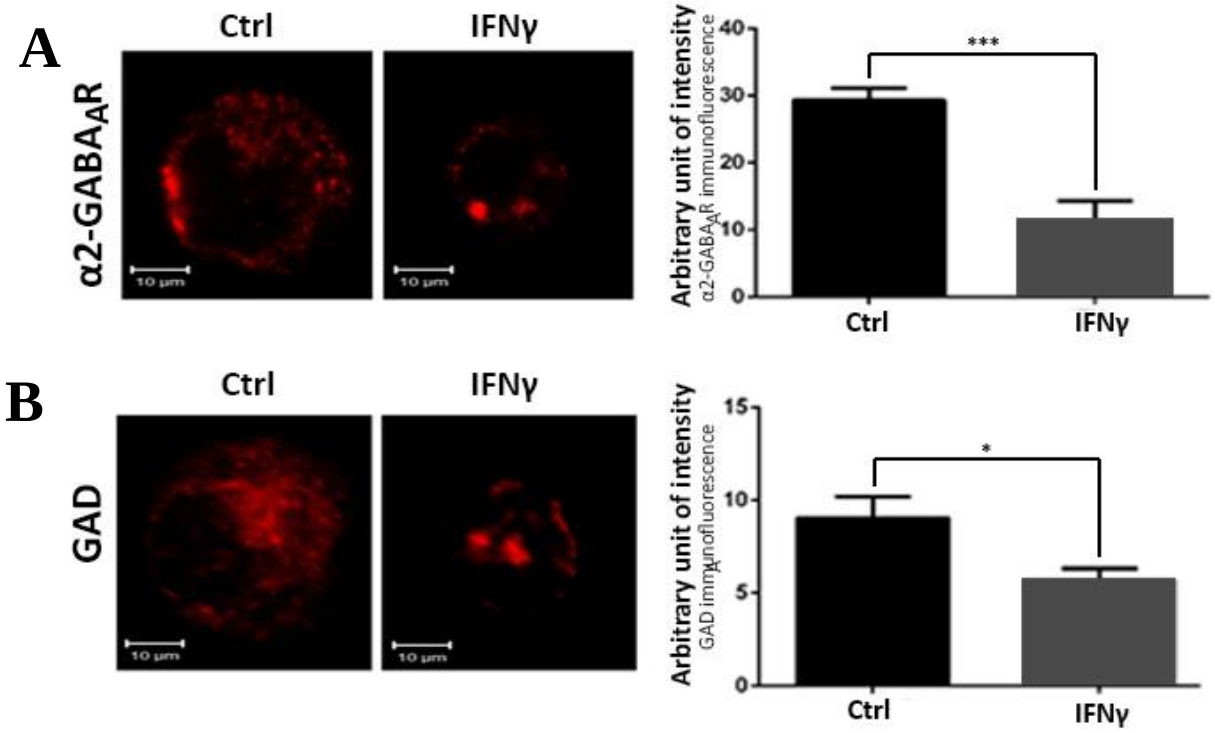

Figure 3.14. M1 polarization reduces expression of α2-GABA$_A$R and GAD65/67 in Primary LMϕs. Cultured LMs were treated with IFNγ (100ng/mL) for 16 hours to induce M1 polarization. The immunofluorescent intensity of α2-GABA$_A$R (**A**) and GAD65/67 (**B**) significantly decreased in IFNγ-treated LMϕs. Plotted data represent mean ± SEM. Significant difference (unpaired T-test) $p < 0.05$ (*), $p < 0.001$ (***), $n = 3$.

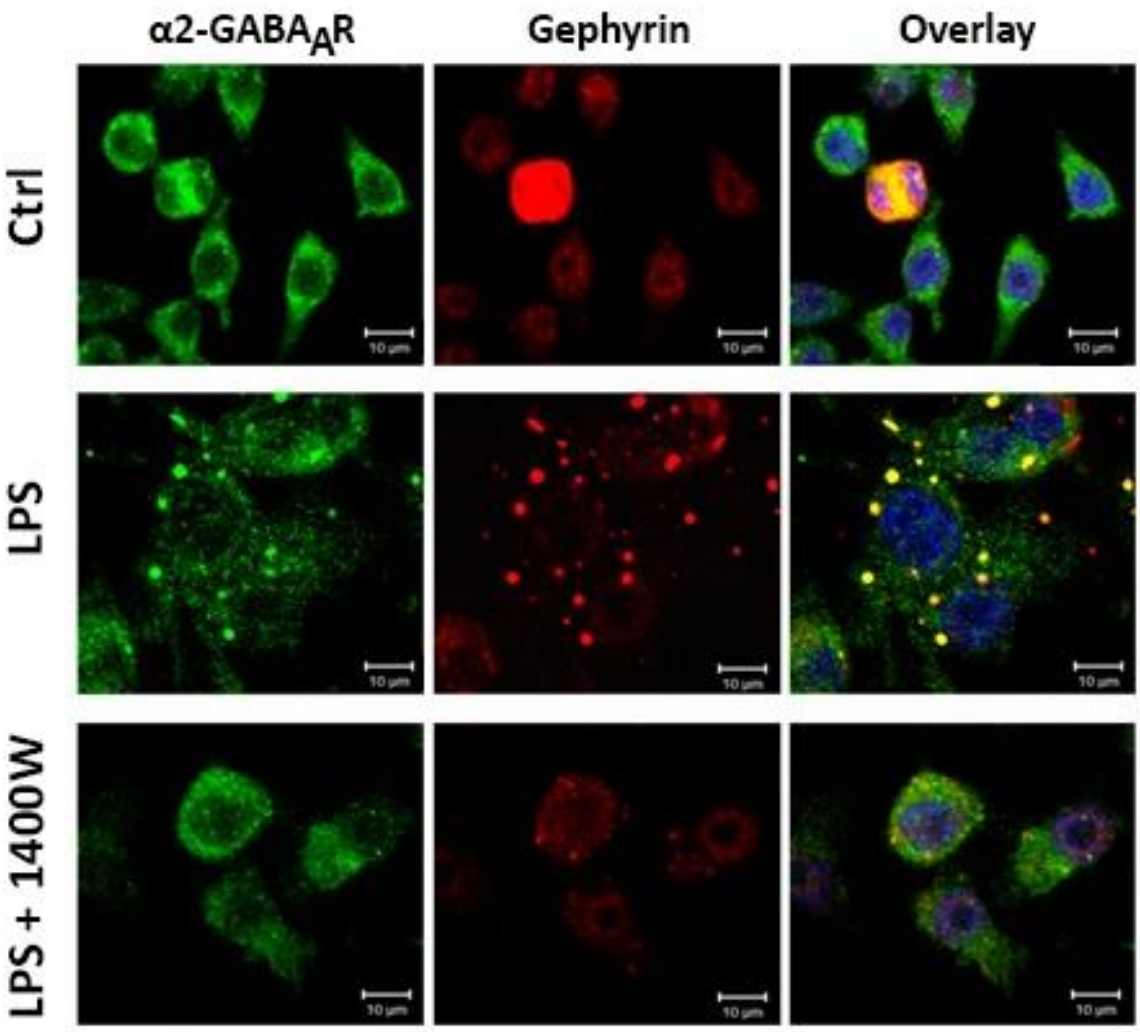

Figure 3.15. LPS induced reduction and relocation of α2-GABA$_A$R and gephyrin were reversed by inhibition of iNOS. Triple staining for α2-GABA$_A$R (red), gephyrin (green) and DAPI (blue) was made in control RAW 264.7 cell (upper row), as well as cells treated with LPS (500ng/mL, mid row) or with LPS together with an iNOS inhibitor 1400W dihydrochloride (20μM, lower row) for 16 hours. Note that LPS treatment not only lowered the expression levels of α2-GABA$_A$R and gephyrin, but also caused relocation of the two proteins to an intracellular structure. Treatment with 1400W dihydrochloride largely reversed the effect of LPS.

As shown in **Figure 3.16**, the immunofluorescence of α2-$GABA_AR$ and *LAMP*-1 were partially co- localized. After LPS treatment, the intracellular α2-$GABA_AR$ clusters were associated with LAMP-1 clusters.

I also explored whether the lowered level of α2-$GABA_AR$ and GAD65/67 proteins in LPS-treated macrophages was a result of activation of NF-κB pathway. To this end, RAW264.7 cells were treated with LPS, and LPS + BAY 11-7082, an inhibitor of IKK, a critical protein involved in NF-κB activation (Rauert-Wunderlich et al., 2013). Western blot assays revealed that the LPS induced an increase in the expression of both arginase-1 (**Figure 3.17A**) and iNOS (**Figure 3.17B**) which was significantly decreased by the co-treatment with BAY 11-7082. BAY 11-7082 also significantly blocked the LPS-induced down-regulation of GAD65/67 and α2-$GABA_AR$ in RAW264.7 cells (**Figure 3.18**). Furthermore, the increases in TNF-α (**Figure 3.19A**) and IL-10 (**Figure 3.19B**) secretion following LPS treatment were largely downregulated by BAY 11-7082. These results implicate that modulation of GAD65/67 and α2-$GABA_AR$, as well as secreted cytokines TNF-α and IL-10 occurs through the TLR4/NF-κB pathway.

3.2.2 IL-4 + IL-13 increased expression of GABA signalling proteins

I also investigated whether M2a polarization altered the levels of GABA signalling proteins. For this purpose, RAW 264.7 cells were treated with IL-4 and IL-13 for 16 hours. Western blot analysis revealed that these Th2 cytokines significantly increased protein level of both GAD65/67 by 1.36 fold and α2-$GABA_AR$ by 1.69 fold (**Figure 3.20**). Treating cultured LMϕs with IL-4 + IL-13 for 16 hours also greatly increased the immunofluorescent

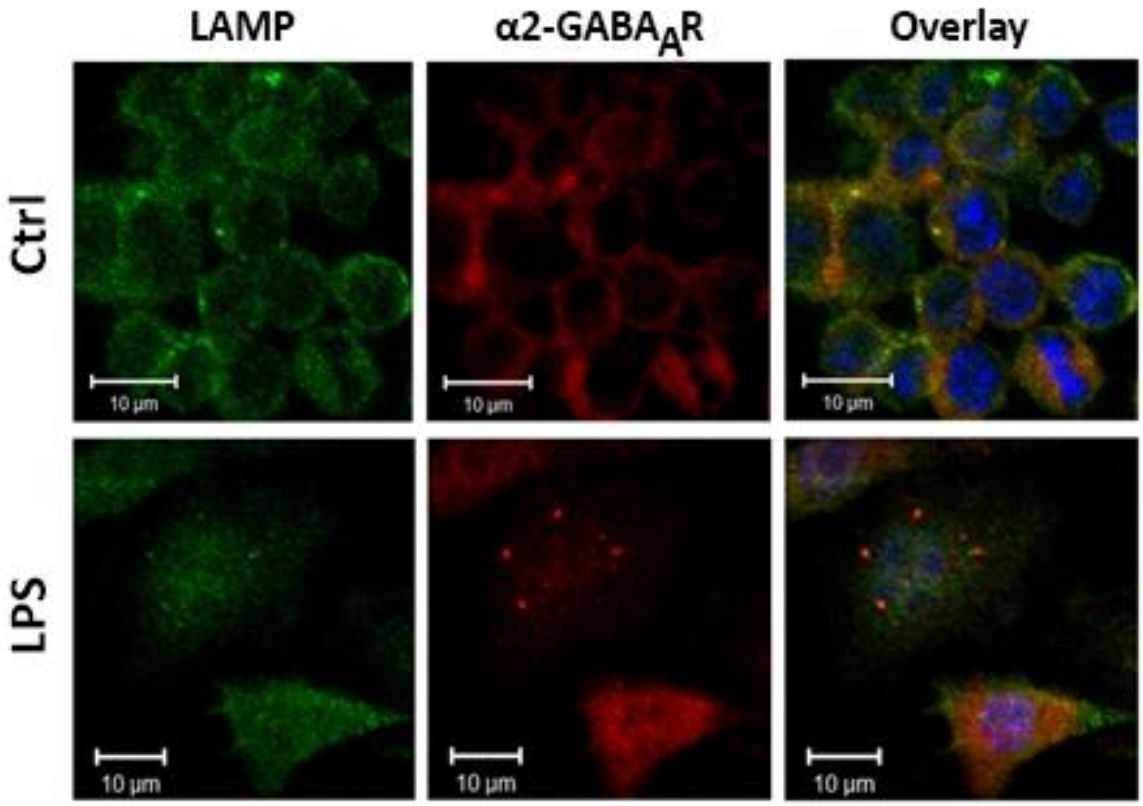

Figure 3.16. LPS treatment relocated LAMP-1 together with α2-GABA$_A$R in RAW 264.7 cells. LAMP-1 and α2-GABA$_A$R were immunostained in both control and LPS (500ng/mL) treated RAW264.7 cells. Sixteen hours after LPS treatment, immunofluorescence of LAMP-1 redistributed in RAW264.7 cells, becoming more uniform across the cell but with some large clusters. Interestingly, the large immunofluorescent clusters of α2-GABA$_A$R were co-localized with the large immunofluorescent clusters of LAMP-1.

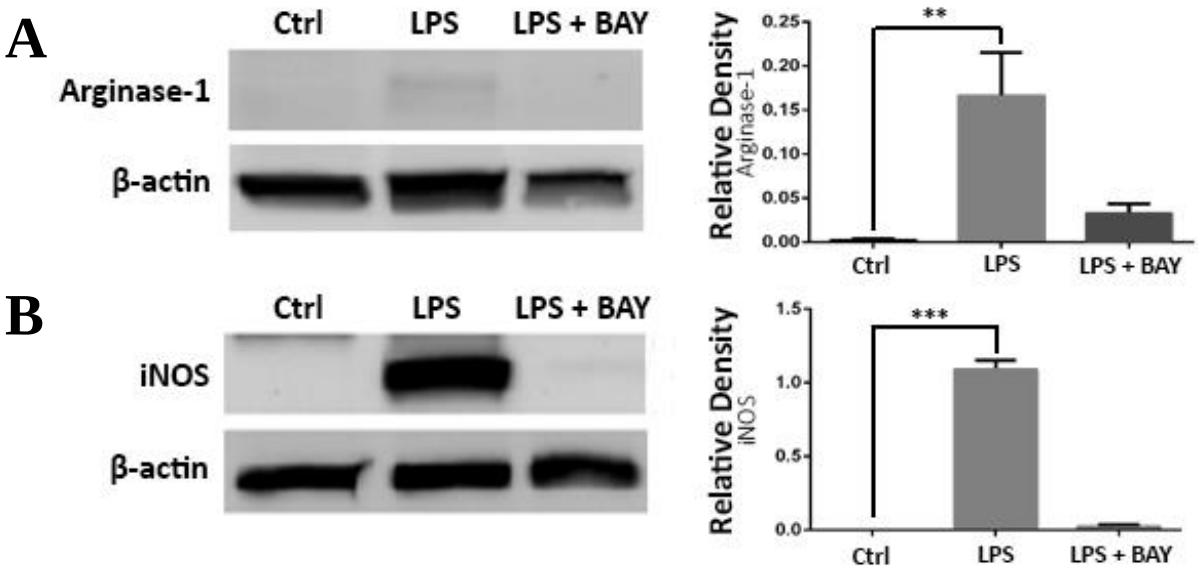

Figure 3.17. NF-κB inhibition reverses effects of LPS on arginase-1 and iNOS expression in RAW 264.7 cells. Western blots of control RAW 264.7 cells, and cells treated with LPS (500ng/mL) or with LPS + BAY 11-7082 (20μM) for 16 hours, were performed to assay arginase-1 (**A**) and iNOS (**B**) expression. Note that LPS upregulated the expression level of both arginase-1 and iNOS; and that the effects of LPS were reversed by the IKK inhibitor BAY 11-7082. Plotted data represent mean ± SEM. Significant difference (ANOVA/Tukey's HSD) $p < 0.01$ (**), $p < 0.001$ (***), $n = 3$.

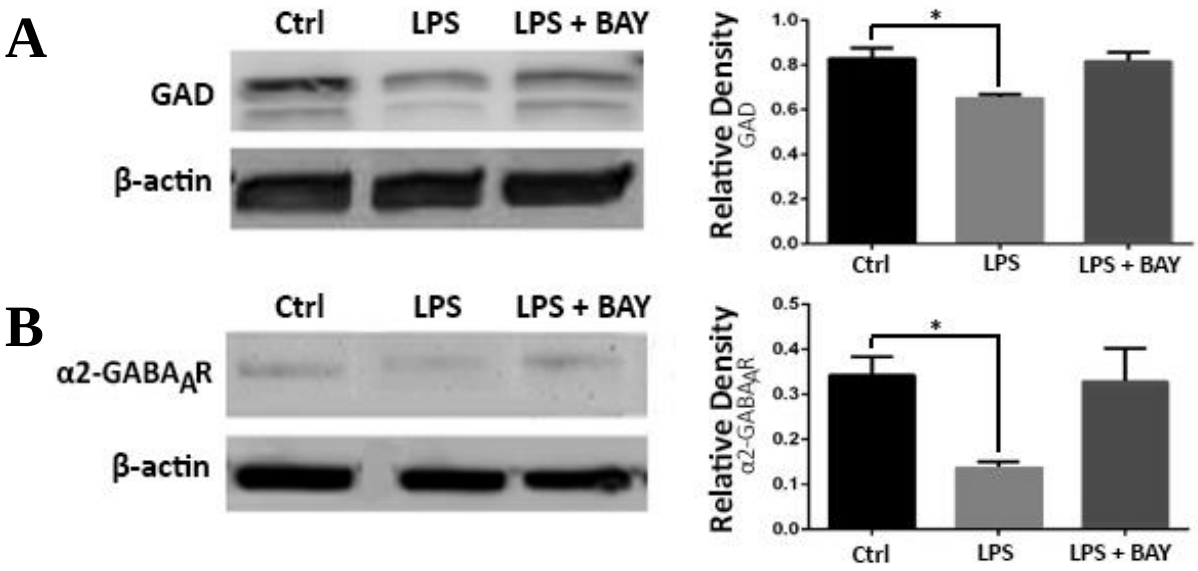

Figure 3.18. NF-κB inhibition reverses LPS-mediated GAD65/67 and α2-GABA$_A$R downregulation in RAW 264.7 cells. Western blots of lysates of control RAW 264.7 cells, and cells treated with LPS (500ng/mL) or with LPS + BAY 11-7082 (20μM) for 16 hours, were performed to assay GAD65/67 (**A**) and α2-GABA$_A$R (**B**). LPS treatment down-regulated the level of GAD65/67 and α2-GABA$_A$R. This effect of LPS were reversed by the IKK inhibitor BAY 11-7082. Plotted data represent mean ± SEM. Significant difference (ANOVA/Tukey's HSD) $p < 0.05$ (*), $n = 3$.

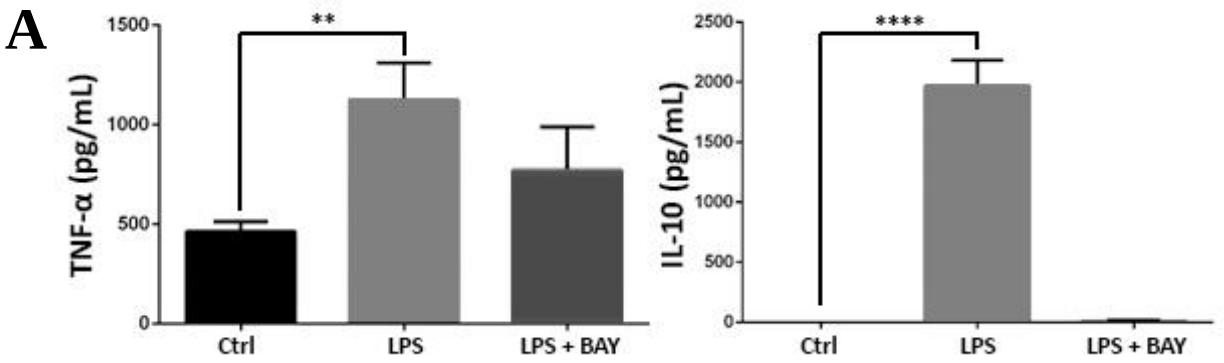

Figure 3.19. NF-κB inhibition reverses LPS-induced TNF-α and IL-10 secretion in RAW 264.7 cells. (**A**) LPS (500ng/mL) causes an increase in TNF-α secretion. Pre-treatment with IKK inhibitor BAY 11-7092 reverses LPS-induced increase in cytokine secretion. (**B**) LPS (500ng/mL) greatly induced IL-10 secretion, however BAY 11-7092 completely reverses this effect. Plotted data represent mean ± SEM. Significant difference (ANOVA/Tukey's HSD) $p < 0.01$ (**), $p < 0.0001$ (****), $n = 3$.

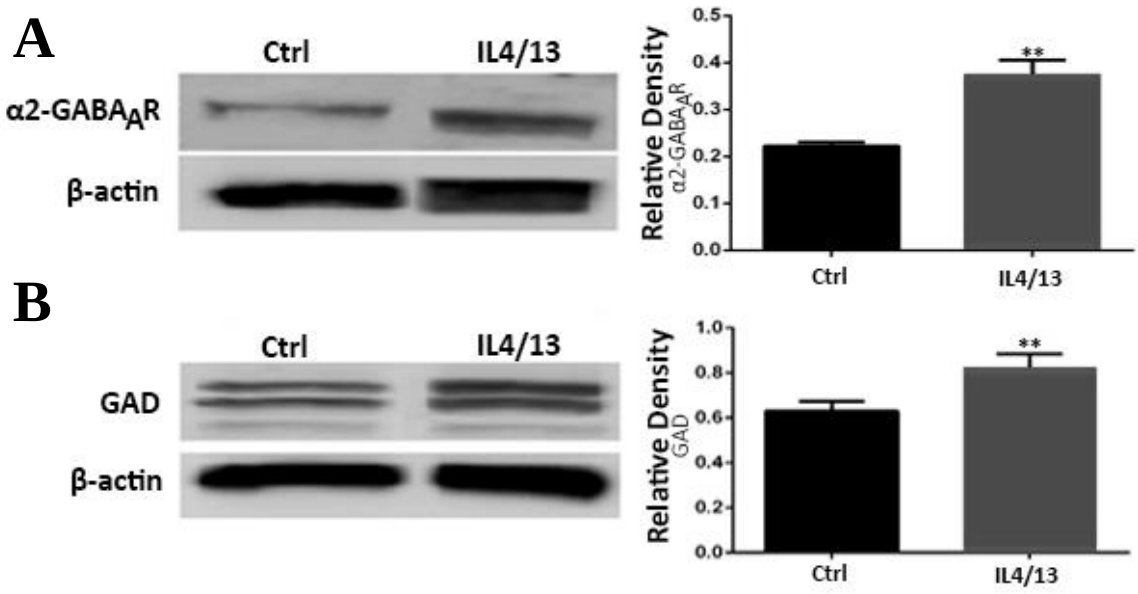

Figure 3.20. Th2 cytokines increase expression of α2-GABA$_A$R and GAD65/67 in RAW 264.7 cells. Western blots of the lysates of control RAW 264.7 cells and cells treated with IL-4 (25ng/mL) + Il-13 (25ng/mL) for 16 hours were performed to assay the protein levels of α2-GABA$_A$R (**A**) and GAD65/67 (**B**). Expression of α2-GABA$_A$R and GAD65/67 were increased in RAW264.7 cells after IL-4 + IL-13 treatment. Plotted data represent mean ± SEM. Significant difference (unpaired T-test) $p < 0.01$ (**), $n = 3$.

intensity of α2-$GABA_AR$ by 1.76 fold and GAD65/67 by 1.53 fold (**Figures 3.21** and **3.22**). Although addition of muscimol had no effect on the immunofluorescence intensity of α2-$GABA_AR$ and GAD65/67, picrotoxin significantly decreased the immunofluorescence intensity of GAD65/67 in cultured LMϕs (**Figure 3.22**). Treating cultured LMϕs with IL-4 + IL-13 for 16 hours also greatly increased the immunofluorescence intensity of α2-$GABA_AR$ by 1.76 fold and GAD65/67 by 1.53 fold (**Figures 3.21** and **3.22**). Although addition of muscimol had no effect on the immunofluorescence intensity of GAD65/67 and α2-$GABA_AR$, picrotoxin significantly decreased the immunofluorescence intensity of GAD65/67 in cultured LMϕs (**Figure 3.22**).

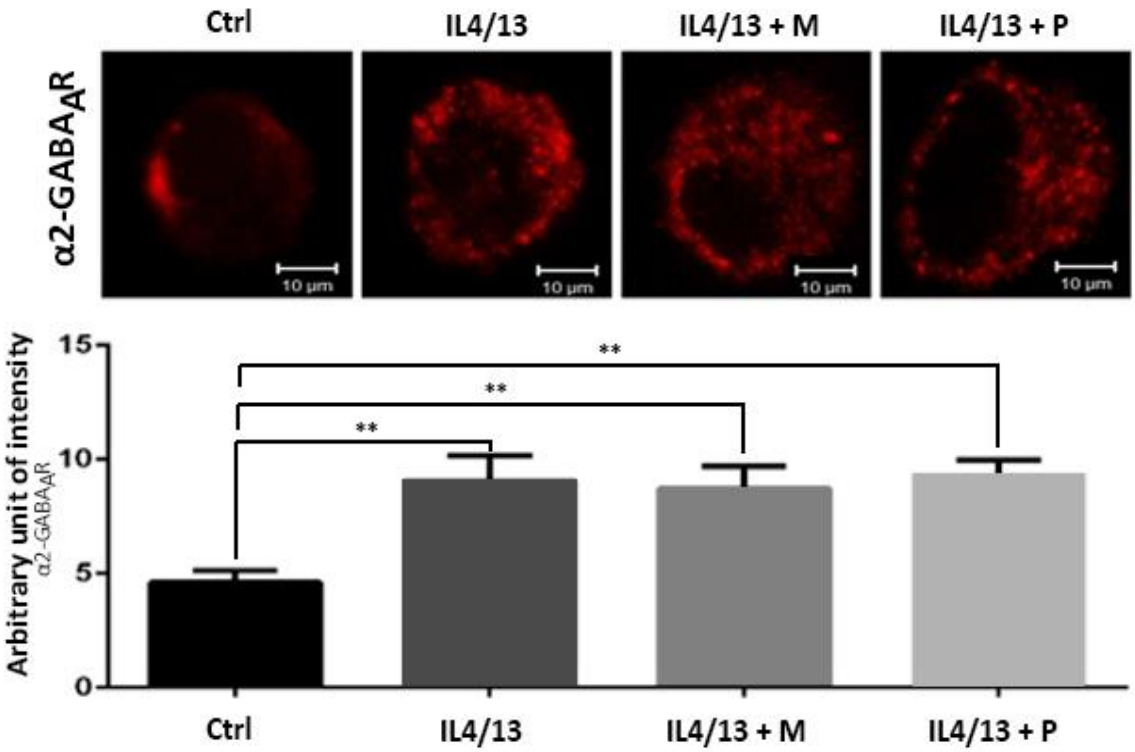

Figure 3.21. IL-4 + IL-13 increases expression of α2-GABA$_A$R in primary LMϕs. Primary LMϕs were treated with IL-4 (25ng/mL) + Il-13 (25ng/mL), or with IL-4 and IL-13 + muscimol (20µM) or picrotoxin (50µM). IL-4 + IL-13 treatment increased expression of α2-GABA$_A$R (**A**). The addition of muscimol or picrotoxin to IL-4 + IL-13 had no effect. Plotted data represent mean ± SEM. Significant difference (ANOVA/Dunnett's test) $p < 0.01$ (**), n = 3.

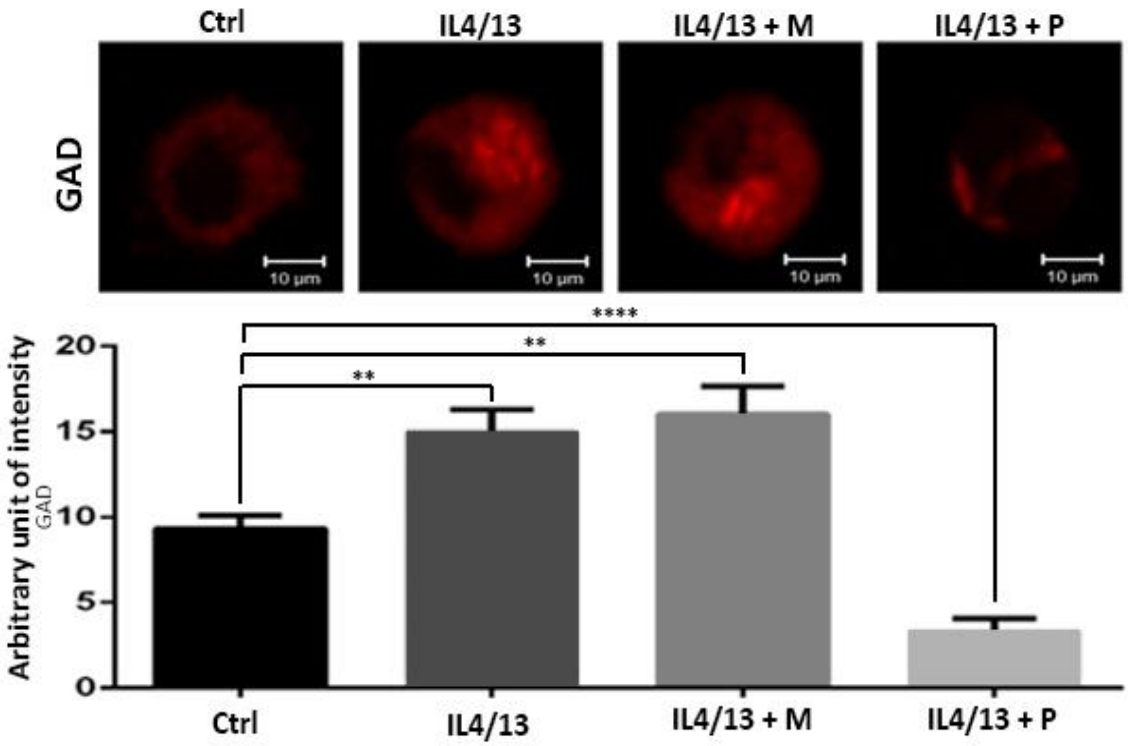

Figure 3.22. IL-4 + IL-13 increases expression of GAD65/67 in primary LMϕs. Primary LMs were treated with IL-4 (25ng/mL) + Il-13 (25ng/mL), with IL-4 and IL-13 + muscimol (20µM) or picrotoxin (50µM). IL-4 + IL-13 treatment increased expression of GAD65/67. The addition of muscimol to IL-4 + IL-13 had no effect, however picrotoxin reduced GAD65/67 expression below control levels. Plotted data represent mean ± SEM. Significant difference (ANOVA/Dunnett's test) $p < 0.01$ (**), $p < 0.0001$ (****), $n = 3$.

4.0 DISCUSSION

Previous studies in my laboratory demonstrated that AMϕs express both GAD and $GABA_AR$ subunits indicating an autocrine GABA signalling mechanism exists in these cells. In addition, my honors thesis study found that blockade of $GABA_ARs$ significantly increased secretion of the M1 cytokine TNF-α from AMϕs. The primary goal of this research project was to explore whether GABA signalling plays a role in phenotypic polarization of AMϕs. Specifically, I first determined if GABA signalling plays a role in LMϕ polarization, and then I studied whether the expression levels of GABA signalling proteins in LMϕs were modified with their phenotypic polarizations. The main results from this study showed that 1) LMϕs displayed multifaceted polarizations under different microenvironments; 2) the expression levels of GABA signalling proteins in macrophages were up- or down-regulated depending on which agents were used to induce the phenotypic polarization; and 3) LMϕs are endowed with an autocrine GABA signalling mechanism that modulates phenotypic polarization of the cells.

4.1 Multifaceted Macrophage Polarizations

Data from converging studies indicate that macrophages are functionally polarized to M1 and M2 phenotypes in response to microorganisms and host mediators such as cytokines secreted from Th1/2 cells. Gene expression profiling of macrophages show that different Gram-negative and Gram-positive bacteria often induce the transcription of genes belonging to the M1 program. However, some bacterial pathogens provoke specific M2 programs in macrophages (Benoit et al., 2008). Moreover, M2 macrophages cover a continuum of cell phenotypes, including M2a, M2b, and M2c subtypes with different

phenotypic and functional properties, depending on specific microenvironments. In order to understand the role of GABA signalling in M1/M2 polarization, one must first understand the complexities of macrophage polarization.

4.1.1 M1 phenotype

IFNγ is a typical Th1 cytokine. In agreement with previous findings demonstrating that IFNγ increases iNOS expression in murine macrophages (Stout et al., 2005, Staitieh et al., 2015), my results confirmed that IFNγ upregulates the M1 marker iNOS in both cell models (**Figure 3.1**). In contrast, IFNγ decreased the M2 marker arginase-1 in primary LMϕs (**Figure 3.4**).

Increased secretion of TNF-α is often associated with M1 macrophages. My analyses demonstrated that IFNγ upregulates secretion of TNF-α in RAW264.7 cells (**Figure 3.6**), which agrees with a previous study performed in the same cell line. (Vila-del Sol et al., 2008). IL-4 is a Th2 cytokine, and it is also secreted by macrophages (Gao et al., 2015). My assays showed that IL-4 secretion from control RAW264.7 cells was extremely low at baseline. Treatment of RAW 264.7 cells with IFNγ induced a slight decrease in IL-4 following treatment, however this change was too small to be considered statistically significant. Baseline secretion of IL-4 from LMϕs was slightly higher than in RAW 264.7 cells, and treating them with IFNγ significantly decreased the baseline secretion of IL-4 (**Figure 3.8)**.

Taken together, my results showed that treating macrophages with IFNγ not only increased the M1 marker iNOS and the M1 cytokine TNF-α but also decreased the M2 marker arginase-1 and the M2 cytokine IL-4, inducing a shift towards the M1 phenotype.

4.1.2 M2a phenotype

Both IL-4 and IL-13 are secreted by Th2 cells and they use the IL-4Rα chain as a component of their receptors. Thus, these two cytokines are often used together to stimulate their receptors (Hershey, 2003). Several previous studies showed that IL-4 and/or IL-13 increases arginase-1 expression via STAT6 signalling, and arginase-1 is cited as a marker for M2a phenotype in murine macrophages and cell lines (Müller et al., 2007; Sheldon et al., 2013). My results showed the combination of IL-4 and IL-13 increased expression of arginase-1 in both RAW 264.7 cells and primary LMϕs (**Figures 3.3** and **3.5**).

Past studies have demonstrated that IL-4 inhibits TNF-α secretion from human monocytes, and that IL-4 and IL-13 decrease TNF-α translation in RAW 264.7 cells (te Velde et al., 1990; Mijatovic et al., 1997). In agreement with these previous studies, my results revealed that IL-4 + IL-13 significantly reduced TNF-α secretions from RAW 264.7 cells, though only slightly reduced TNF-α secretions from primary LMϕs (**Figure 3.7**).

It was interesting to observe that 16 hours after IL-4/IL-13 treatment the IL-4 secretion largely increased in both RAW 264.7 cells and primary LMϕs (**Figure 3.9**). This finding is consistent with literature which reports that IL-4 is released from M2a macrophages (La Flamme et al., 2012; Murray et al., 2014, Gao et al., 2015). High levels of IL-10 secretion are associated with the M2 phenotype (Spellberg & Edwards, 2001; Lech & Anders, 2013; Yamaguchi et al., 2015). I therefore analyzed IL-10 as an example of an M2 anti-inflammatory cytokine. Surprisingly, IL-4 + IL-13 treatment decreased IL-10 secretion from both RAW 264.7 cells and primary LMϕs (**Figure 3.11**). It is reported that IL-4 may act to suppress IL-10 secretion in human monocytes (Bonder et al., 1999), suggesting increased IL-10 secretion may not be associated with all M2 phenotypes. Nonetheless,

combined results from my experiments showed that IL-4 + IL-13 treatment induces M2a polarization of LMϕs.

4.1.3 M2b phenotype

M2b phenotype is a unique subtype of macrophages that often mediate inflammatory responses. Although arginase-1 expression has typically been used as a marker for M2 polarization, some studies have suggested M2b and M2c phenotypes may be better characterized by high IL-10 and TGF-β secretion, respectively (Martinez et al., 2008; Saclier et al., 2013). For example, several studies have noted an increase in IL-10 release as a consequence of LPS stimulation, including in RAW 264.7 cells and human AMϕs (Chanteux et al., 2007, Van den Bosch et al., 2014). It is reported that M2b activation can be elicited by IL-1 receptor ligands, immune complexes, and LPS. Indeed, my assays showed that LPS treatment induced a great increase in IL-10 secretion (**Figure 3.10**) in RAW 264.7 cells and primary LMϕs, and an elevation of arginase-1 and expression (**Figure 3.17**) in RAW 264.7 cells. These combined results may suggest that under these experimental conditions, LPS treatment induces M2b phenotype. However, the LPS-treated cells also displayed high levels of iNOS, which reflects the complicity of macrophage phenotypical development. Given that M1 macrophages are not associated with high levels of IL-10 secretion (Murray et al., 2014) and that a mixed M1/M2b phenotype has been identified in the population of microglia (Lisi et. al., 2014), a type of macrophage in the brain, it is plausible to propose that LMϕs share the same capability.

4.2 Macrophage polarization alters autocrine GABA signalling

4.2.1 Decreased GABA signalling is associated with M1 and M2b phenotype

My immunoblot assays showed that when cultured RAW 264.7 and LMϕs polarized to M1 phenotype by IFNγ treatment or to M2b by LPS treatment, the expression level of both GAD and α2-$GABA_AR$ decreased (**Figure 3.13 and 3.14**). This result is in line with the earlier studies in our lab, in which significant decrease in immunofluorescence of GAD and α2-$GABA_AR$ occurred in AMϕs of mice that were systemically treated with LPS. Considering that iNOS expression is largely increased in these cells and NO down-regulates $GABA_AR$ expression in neurons by S-nitrosylation of the $GABA_AR$ anchoring protein gephyrin (Dejanovic & Schwarz, 2014), I investigated the role of iNOS/NO in the regulation of $GABA_ARs$ in RAW 264.7 cells. In RAW 264.7 cells, LPS treatment caused co-localization and clustering of both gephyrin and α2-$GABA_AR$ inside of the cells, which was largely blocked by the iNOS inhibitor 1400W, suggesting iNOS/NO may be responsible for internalization of $GABA_ARs$ (**Figure 3.15**). Furthermore, my studies demonstrated an association between α2-$GABA_AR$ and the lysosome marker LAMP-1 following LPS treatment (**Figure 3.16**), suggesting that the internalized $GABA_ARs$ might be degraded within lysosomes.

My results also showed that inhibition of the NF-κB signalling pathway in RAW264.7 cells by BAY 11-7082 not only significantly lowered the LPS-induced iNOS expression but also reduced the decrease in the expression of both GAD and α2-$GABA_AR$ (**Figures 3.17 and 3.18**). This finding was in line with a previous study, which reported that iNOS expression occurs through activation the NF-κB pathway (Aktan F, 2004). However, IFNγ treatment also yielded GAD and α2-$GABA_AR$ downregulation. The most well

understood downstream signalling of IFNγ is activation of STAT1, which has been suggested to be an important mediator of iNOS expression in epithelial cells (Stempelj et al., 2007). More study could be done on STAT1 to fully elucidate the mechanisms involved in GAD and $GABA_AR$ downregulation, however our results highlight the importance of NF-κB signalling.

4.2.2 M2a polarization is associated with increased GABA signalling

My results showed that in response to IL-4 + IL-13 both RAW 264.7 cells and primary LMϕs displayed a significant upregulation of both GAD and α2-$GABA_AR$ (**Figure 3.20 and 3.21**), although the signalling pathway through which Th2 cytokine upregulates the expression of GAD and $GABA_AR$ awaits further studies. Taken together my results demonstrated that M1/M2b polarization is linked to an overall decrease in GABA signalling, while M2a polarization is associated with an increase in GABA signalling (**Figure 4.1**).

4.3 Autocrine GABA signalling regulates macrophage polarization

4.3.1 Blockade of endogenous autocrine GABA signalling alters the phenotypic markers and cytokines

Results showed that at resting stage (M0), macrophages secreted GABA as evidenced by the occurrence of bicuclline-sensitive current in neurons when exposed to conditioned medium from RAW264.7 cells (**Figure 3.12**). To examine whether a $GABA_AR$ mediated autocrine signalling regulates macrophage phenotypical polarization, I treated RAW 264.7

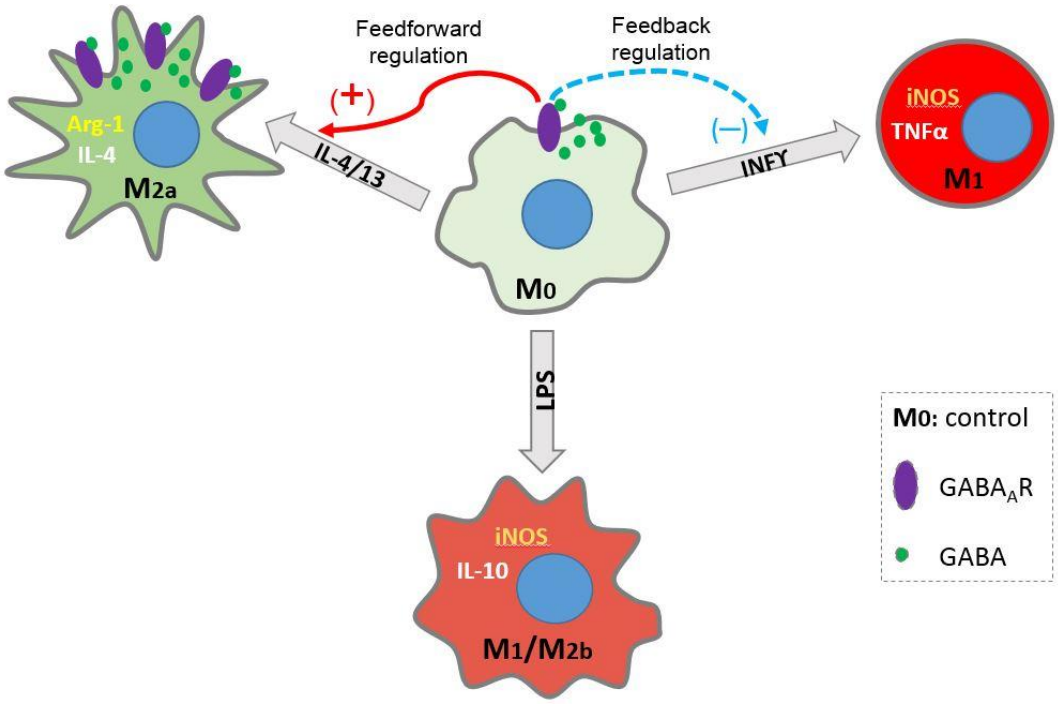

Figure 4.1. Changes in GABA$_A$R-mediated autocrine signalling and its role in macrophage polarization. Autocrine GABA signalling maintains the macrophage at a resting state (M0). Increased autocrine GABA signalling occurs in M2a phenotype while decreased GABA signalling is associated with M1 or M1/M2b phenotype.

cells and LMs with the $GABA_AR$ agonist muscimol and the $GABA_AR$ channel blocker picrotoxin. Results showed that muscimol did not affect the expression of iNOS, arginase-1, GAD65/67 and α2-$GABA_AR$, or the secreted cytokines. On the other hand, treating "naïve" AMϕs with picrotoxin significantly increased TNF-α secretion (**Figure 1.7**), while treating the IL-4/13 primed LMϕs with picrotoxin decreased IL-4 secretion along with arginase-1 and GAD expression (**Figures 3.3, 3.5, 3.9, and 3.21**). Notably, picrotoxin had no effect on TNF-α secretion from LPS-treated AMϕs (**Figure 1.7**), in which the expression of both $GABA_AR$s and GAD was greatly down-regulated (**Figures 1.6 and 3.13**). These results indicate that in M0 and M2a macrophages an active autocrine GABA signalling persistently regulates the function of the cells, whereas the autocrine GABA signalling is terminated when the cells shift to M1/M2b phenotypes.

4.3.2 Potential mechanism by which autocrine GABA signalling regulates macrophage polarization

$GABA_AR$ is a channel permeable for Cl^- and activation of this receptor leads to changes of membrane potential. My thesis study did not investigate the underlying mechanisms by which $GABA_AR$ regulates macrophage polarization. However, unpublished studies in my lab showed that activation of $GABA_AR$ can change intracellular Ca^{2+} concentrations. The enormous concentration difference between the extra- and intracellular compartments make Ca^{2+} entry to the cell a sensitive signal (Demaurex & Nunes, 2016). As a second messenger, intracellular Ca^{2+} plays a key role in the regulation of gene expression and cell differentiation (LoTurco et al., 1995, Johnson et al., 1997; van Haasteren et al., 1999; Barbado et al., 2009). In excitable cells, membrane depolarization will result in the

opening of voltage-gated Ca^{2+} channels allowing for a large influx of Ca^{2+} due to the concentration gradient (Bers, 2008; Atlas, 2013). However, there has been no substantial evidence to support the expression of voltage-gated Ca^{2+} channels in immune cells. Instead, Ca^{2+} entry in non-excitable cells including macrophages is largely mediated by store-operated Ca^{2+} entry (SOCE) through of the calcium-release activated channels (CRAC) on the plasma membrane allowing for Ca^{2+} entry (Putney et al., 2001).

How can a $GABA_AR$-mediated membrane potential change affect SOCE in macrophage? A study performed in peritoneal macrophages has demonstrated the resting potential of these macrophages is -75 mV, while the reversal potential for Cl^- is -35.3 mV (Randriamampita & Trautmann, 1987). In essence, this means $GABA_AR$ stimulation at rest will result in an efflux of Cl^- ions in peritoneal macrophages, although the resting and reversal potentials in LMs need to be determined. Due to the efflux of Cl^- through the $GABA_AR$ channels and hence the more positive membrane potential, less Ca^{2+} enters the cell. Results from my study showed that LPS downregulates $GABA_AR$ expression, which would result in a more negative membrane potential, and hence a larger Ca^{2+} influx to the cells.

My results showed that M2a polarization results in a feedforward GABA signalling marked by increased GAD and α2-$GABA_AR$, leading to upregulation of IL-4 secretion. M2a polarization might reduce Cl^- influx channel NKCC expression but increase Cl^- efflux channel KCC expression causing a lowered intracellular Cl^- concentration. Consequently, upon $GABA_AR$ activation there will be Cl^- influx causing membrane hyperpolarization, more Ca^{2+} entry and activated M2 gene expression. (**Figure 4.2**).

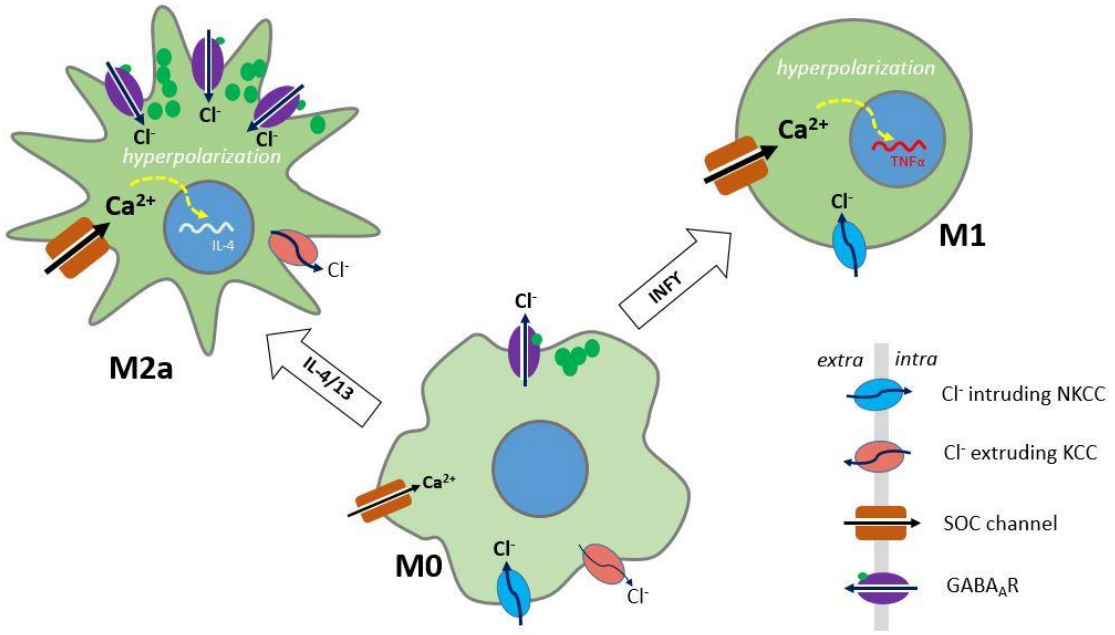

Figure 4.2. Proposed mechanisms by which the $GABA_AR$ mediated autocrine signalling regulates phenotypic polarization and function of macrophages. In "resting macrophages (M0), the higher expression and activity levels of the Cl^- intruding NKCC and the lower expression and activity levels of the Cl^- extruding KCC results in a higher intracellular Cl^- concentration. Therefore, autocrine GABA activates $GABA_ARs$ mediating Cl^- efflux, which consequently maintain the transmembrane membrane potential depolarized (less negative) and minimum Ca^{2+} entry through store-operated calcium (SOC) channels. M1 polarization results in a decreased expression of $GABA_ARs$ and GAD, causing membrane hyperpolarization and more Ca^{2+} entry through SOC channels, consequently M1 gene expression. In contrast, M2 polarization results in an increased expression of $GABA_ARs$ and GAD. However, M2 polarization might reduce NKCC expression but increase KCC expression and thus shift the reversal potential of Cl^-, consequently resulting in Cl^- influx through $GABA_ARs$, hence membrane hyperpolarization, more Ca^{2+} entry and activated M2 gene expression.

As previously mentioned, changes in Ca^{2+} signalling may also play a role in macrophage polarization by modification of gene transcription. Although exact mechanisms are still under investigation, several factors have been suggested to play important roles in Ca^{2+} mediated alterations in gene expression, including, nuclear factor of activated T-cells, and NF-Kb. Changes in Ca^{2+} signalling related to changes in Cl^- flow before and after neuronal maturation may be an indicator that differential gene expression may be related to phenotype change, and in LMϕs GABA/Ca^{2+} signalling may play an important role in phenotypic shifts seen in this study (Nachtomy et al., 2007).

4.4 Future studies

Several measures could be taken to strengthen already existing findings. Treatments and time points used in these experiments were based on treatments established in the literature. However, in the future dose-response curves should be established for each drug. Multiple time points should also be examined, which may be particularly important for examining how LMϕs/RAW 264.7 cells change phenotype and/or cytokine secretion over time. Along the same vein many studies could be repeated using bicuculline in the place of picrotoxin, since bicuculline is selective antagonist for $GABA_A$Rs rather than a channel blocker. Several additional experimental methods could also be applied to strengthen the current studies, including proteomics to further examine cytokine production, and real-time PCR to examine RNA expression of GAD and α2-$GABA_A$Rs at various time points following treatments with IFNγ, LPS, and IL-4 + IL-13. Furthermore, fluorescence-activated cell sorting should be done following LMϕ extraction from lung tissue based on differential expression of CD11, allowing for separation and independent study of IMϕ and AMϕ

populations. Finally, although it has been demonstrated that RAW 264.7 cell media contained secreted GABA, the same has not yet been confirmed in LM media. Therefore, the same patch clamping study we performed using cultured hippocampal neurons should be carried out once again. Patch clamping studies should also be performed using primary LMϕs to determine the resting membrane potential, and direction of Cl^- flow following GABAergic stimulation.

There are also areas which could be expanded upon in future study. Given that this study did not fully establish a mechanism for $GABA_AR$ downregulation, it is possible other unexplored mechanisms may be responsible. In neurons it has been suggested that $GABA_AR$ reduction may be attributed to degradation of receptor proteins followed by a decrease in de novo synthesis (Barnes EM Jr, 1996). One method that could be used to further investigate the fate of decreased $GABA_AR$ expression is by a biotin degradation assay. Biotinylation techniques may also be useful for investigating receptor endocytosis, which would confirm $GABA_ARs$ are being internalized into lysosomes as suspected. In this instance $GABA_ARs$ may be pretreated prior to biotinylation with a lysosomal inhibitor such as leupeptin to prevent proteolysis. A Western blot may then be run wherein the higher expression of biotin represents $GABA_AR$ internalization. (Mammen et al., 1997; Arancibia-Cárcamo et al., 2006). Biotin may also be useful for further examining whether upregulated iNOS is related to gephyrin nitrosylation in LMϕs/RAW 264.7 cells. One particular study known as the biotin-switch technique can effectively replace S-nitrosylated cysteine residues with biotin for relatively easy detection (Forrester et al., 2009). Receptor upregulation in M2a polarization should also be further examined. It is known that IL-4/IL-13 function primarily through the transcription factor STAT6, therefore one study that could be done involves

treatment with IL-4/IL-13 while inhibiting STAT6. Changes in GAD and α2-$GABA_AR$ could then be observed via Western blot, confocal microscopy, and/or PCR.

My results suggested a potential mechanism for changes in intracellular Cl^- concentration related to macrophage phenotypes. These changes are proposed to be due to differential expression of NKCC and KCC channels during polarization. In order to investigate the proposed mechanism, Western blots may be performed for KCC and NKCC in IFNγ and IL-4 + IL-13 treated cells.

The ultimate goal for studying GABA signalling in LMϕs should involve in vivo studies. Although in vitro studies allow for examination of isolated populations of single cell types, this is not necessarily realistic. Other cells including Type II epithelial cells and T cells reside in the environment and are constantly secreting factors which affect macrophage polarization. Furthermore, studies have shown T cells secrete GABA and studies in our laboratory have found that Type II epithelial cells also possess GABA signalling systems (Bhat et al., 2010; Prud'Homme et al., 2013, Xiang et al., 2013). Therefore, GABA signalling interactions between these cell types may also affect inflammatory responses within the pulmonary immune system.

4.5 Limitations

Although the findings outlined in the present study suggest an important role for GABA signalling as a regulator of LMϕ inflammatory response, there are several limitations to be considered. Due to the low number of primary LMϕs that could be obtained via lung digest, immunofluorescence techniques were utilized to measure changes in markers involved in cellular polarization, as well as GABA signalling proteins. Immunofluorescent

techniques have inherent limitations, including a potential for non-specific protein binding with fluorescent antibodies, and photo-bleaching. In addition, the results of fluorescence intensity are qualitative in nature. Regarding the selected experimental treatment groups, controls were not run for muscimol or picrotoxin, therefore it is unknown how these drugs would affect the cell on their own. Furthermore, only one type of agonist/antagonist were used at fixed concentrations, therefore it is difficult to ensure all results are induced by the intended purpose of the drug or an unanticipated side effect. Finally, all experiments in this study focussed on either the RAW 264.7 cell line or LMϕs in isolation. While these studies are good for investigating the role of GABA signalling within this specific cell type, it is likely the case that the cells would function differently *in vivo* when surrounded by neighboring immune cells.

4.6 Conclusion and significance

This study is the first to link GABA signalling in AMϕs to phenotypic polarization. First, it was found that blockade of $GABA_AR$ with picrotoxin shifts the cell towards M1 phenotype, while muscimol had no effect. This finding led to the discovery that RAW 264.7 cells possess an autocrine GABA signalling system, as they express GAD, produce GABA, and express α2-$GABA_ARs$. My study established a link between LMϕ polarization and GABA signalling. Increased GABA signalling is associated with M2a polarization, while a decrease in GABA signalling is related to M1 and M2b phenotypes. These findings provide insight for a novel role of endogenous GABA signalling as a regulator of LMϕ polarization and inflammatory response. Specifically, tonic GABA signalling provides feedback inhibition of pro-inflammatory cytokine release. IFNγ and LPS decrease GABA signalling,

leading to the release of pro-inflammatory cytokines. Conversely GABA signalling feeds forward to M2a polarization, inducing secretion of IL-4. Primarily, I propose changes in GABA signalling associated with polarization regulates Ca^{2+} signalling and consequently cytokine release and potentially transcriptional changes. This may have therapeutic implications, providing further insight that GABA may be an effective immunomodulatory signalling molecule (Bhat et al., 2010; Prud'homme et al., 2013).

Differential $GABA_AR$ expression may also be a useful indicator for phenotypic polarization. Currently classification of different macrophage phenotypes is confusing, with different markers sometimes being used to classify the same phenotypes. Currently an effort within the immunology is to define a unified set of markers to distinguish between different macrophage phenotypes (Murray et al., 2014). The standardization of marker usage would benefit experienced researchers as well as those entering the field, by establishing definite associations between markers and phenotypes. Results from my studies demonstrate distinct $GABA_AR$ expression patterns in different phenotypical macrophages, therefore expression levels of this receptor may aid in the classification of macrophage subtypes.

LMϕs display a plastic nature and play key roles in pulmonary functions and diseases. This study demonstrates that autocrine GABA signalling regulates the plasticity of LMϕs. The challenge remains to apply the knowledge generated from mechanistic studies of LMϕs towards pulmonary physiology and directed therapies for the treatment of pulmonary disease. I propose that pharmacological manipulation of GABA signalling within the lung may be a potential treatment for lung inflammation, in particular the M2/Th2 inflammation associated with pulmonary allergy and asthma. Specifically, this study demonstrates an increase in GABA signalling associated with M2a polarization, it may be

possible that antagonism of this GABA signalling may restrain M2/Th2 inflammation. Nevertheless, LMϕs are not the only immune cells which exhibit GABA signalling. Studies, including some in our lab, have demonstrated that T lymphocytes and type II alveolar epithelial cells possess autocrine GABA signalling mechanisms, which could interact with the GABA signalling system in LMϕs. Therefore, more *in vivo* studies is imperative for establishing the notion of GABA signalling as an immune regulator.

In conclusion, this study has demonstrated that LMϕs possess an autocrine GABA signalling mechanism which has important implications in regulation of inflammatory responses. Specifically, the role of autocrine GABA signalling in LMϕs is to provide feedback inhibition to the M1/M2b phenotype, and feedforward activation to the M2a phenotype.

5.0 REFERENCES

Akira S, Uematsu S, Takeuchi O. 2006. Pathogen recognition and innate immunity. *Cell* **124**: 783–801.

Aktan F. iNOS-mediated nitric oxide production and its regulation. *Life Sci* **75(6)**: 639–653.

Anderson CF, Gerber JS, Mosser DM. 2002. Modulating macrophage function with IgG immune complex. *J Endotoxin Res* **8(6)**: 477–481.

Arancibia-Cárcamo IL, Fairfax BP, Moss SJ, Kittler JT. 2006. Studying the localization, surface stability and endocytosis of neurotransmitter receptors by antibody labeling and biotinylation approaches. In: Kittler JT, Moss SJ, editors. *The Dynamic Synapse: Molecular Methods in Ionotropic Receptor Biology*. Boca Raton (FL): CRC Press/Taylor & Francis; Chapter 6. Available from: http://www.ncbi.nlm.nih.gov/books/NBK2552/

Atlas D. 2013. The voltage-gated calcium channel functions as the molecular switch of synaptic transmission. *Annu Rev Biochem* **82**: 607–635.

Auffray C, Fogg D, Garfa M, Elain G, Join-Lambert O, Kayal S, Sarnacki S, Cumano A, Lauvau G, Geissmann F. 2007. Monitoring of blood vessels and tissues by a population of monocytes with patrolling behavior. *Science* **317**: 666–670.

Aziz A, Soucie E, Sarrazin S, Sieweke MH. 2009. MafB/c-Maf deficiency enables self-renewal of differentiated functional macrophages. *Science* **326(5954)**: 867–871.

Bach EA, Aguet M, Schreiber RD. 1997. The IFN gamma receptor: a paradigm for cytokine receptor signalling. *Annu Rev Immunol* **15**: 563–591.

Bach EA, Szabo SJ, Dighe AS, Ashkenazi A, Aguet M, Murphy KM, Schreiber RD. 1995. Ligand-induced autoregulation of IFN-gamma receptor beta chain expression in T helper cell subsets. *Science* **270**: 1215–1218.

Barbado M, Fablet K, Ronjat M, De Waard M. 2009. Gene regulation by voltage-dependent calcium channels. *Biochim Biophys Acta* **1793(6)**: 1096–1104.

Barnard EA, Skolnick P, Olsen RW, Mohler H, Sieghart W, Biggio G, Braestrup C, Bateson AN, Langer SZ. 1998. International Union of Pharmacology. XV. Subtypes of gamma-aminobutyric acidA receptors: classification on the basis of subunit structure and receptor function. *Pharmacol Rev* **50(2)**: 291–313.

Barnes EM Jr. 1996. Use-dependent regulation of GABAA receptors. *Int Rev Neurobiol* **39**: 53–76.

Barnes PJ. 2004. Alveolar macrophages as orchestrators of COPD. *COPD* **1**: 59–70.

Bedoret D, Wallemacq H, Marichal T, Desmet C, Quesada Calvo F, Henry E, Closset R, Dewals B, Thielen C, Gustin P, de Leval L, Van Rooijen N, Le Moine A, Vanderplasschen A, Cataldo D, Drion PV, Moser M, Lekeux P, Bureau F. 2009. Lung interstitial macrophages alter dendritic cell functions to prevent airway allergy in mice. *J Clin Invest* **119(12)**: 3723–3738.

Ben-Ari Y. 2002. Excitatory actions of GABA during development: the nature of the nurture. *Nat Rev Neurosci* **3**: 728–739.

Ben-Ari Y, Gaiarsa JL, Tyzio R, Khazipov R. 2007. GABA: a pioneer transmitter that excites immature neurons and generates primitive oscillations. *Physiol Rev* **87(4)**: 1215–1284.

Benarroch EE. 2007. GABAA receptor heterogeneity, function, and implications for epilepsy. *Neurology* **68(8)**: 612–614.

Benoit M, Desnues B, Mege JL. 2008. Macrophage polarization in bacterial infections. *J Immunol* **181**: 3733–3739.

Bernabei P, Coccia EM, Rigamonti L, Bosticardo M, Forni G, Pestka S, Krause CD, Battistini A, Novelli F. 2001. Interferon-gamma receptor 2 expression as the deciding factor in human T, B, and myeloid cell proliferation or death. *J Leukoc Biol* **70**: 950–960.

Bers DM. 2008. Calcium cycling and signalling in cardiac myocytes. *Annu Rev Physiol* **70**: 23–49.

Beutler, B.A. 2009. TLRs and innate immunity. *Blood* **113(1)**: 399–407.

Bhat R, Axtell R, Mitra A, Miranda M, Lock C, Tsien RW, Steinman L. 2010. Inhibitory role for GABA in autoimmune inflammation. *Proc Natl Acad Sci U S A* **107(6)**: 2580–2585.

Boehm U, Klamp T, Groot M, Howard JC. 1997. Cellular responses to interferon-gamma. *Annu Rev Immunol* **15**: 749–795.

Bonder CS, Finlay-Jones JJ, Hart PH. 1999. Interleukin-4 regulation of human monocyte and macrophage interleukin-10 and interleukin-12 production. Role of a functional interleukin-2 receptor gamma-chain. *Immunology* **96(4)**: 529–536.

Bønnelykke K, Sparks R, Waage J, Milner JD. 2015. Genetics of allergy and allergic sensitization: common variants, rare mutations. *Curr Opin Immunol* **36**: 115–126.

Bormann J, Feigenspan A. 1995. GABAC receptors. *Trends Neurosci* **18(12)**: 515–519.

Byrne AJ, Mathie SA, Gregory LG, Lloyd CM. 2015. Pulmonary macrophages: key players in the innate defence of the airways. *Thorax* **70**: 1189–1196.

Caraiscos VB, Elliott EM, You-Ten KE, Cheng VY, Belelli D, Newell JG, Jackson MF, Lambert JJ, Rosahl TW, Wafford KA, MacDonald JF, Orser BA. 2004. Tonic inhibition in mouse hippocampal CA1 pyramidal neurons is mediated by alpha5 subunit-containing gamma-aminobutyric acid type A receptors. *Proc Natl Acad Sci U S A* **101(10)**: 3662–3667.

Chanteux H, Guisset AC, Pilette C, Sibille Y. 2007. LPS induces IL-10 production by human alveolar macrophages via MAPKinases- and Sp1-dependent mechanisms. *Respir Res* **8(1)**: 71

Chávez-Galán L, Olleros ML, Vesin D, Garcia I. 2015. Much more than M1 and M2 macrophages, there are also CD169(+) and TCR(+) macrophages. *Front Immunol* **6:** 263

Chen GY, Nunez G. 2010. Sterile inflammation: sensing and reacting to damage. *Nature Rev Immunol* **10**: 826–837.

Chen Y, Phillips K, Minton G, Sher E. 2005. GABA(B) receptor modulators potentiate baclofen-induced depression of dopamine neuron activity in the rat ventral tegmental area. *Br J Pharmacol* **144(7)**: 926–932.

Chen Y, Zhou D, Zhou K, Ren Y, Dai W, Xu M, Lu L, Lu Z. 2007. Study on olfactory function in GABAC receptor/channel rho1 subunit knockout mice. *Neurosci Lett* **427(1)**: 10-5.

Choii G, Ko J. 2015. Gephyrin: a central GABAergic synapse organizer. *Exp Mol Med* **47**: e158

Chung KF. 2015. Targeting the interleukin pathway in the treatment of asthma. *Lancet* **386(9998)**: 1086–1096.

Crestani F, Löw K, Keist R, Mandelli M, Möhler H, Rudolph U. 2001. Molecular targets for the myorelaxant action of diazepam. *Mol Pharmacol* **59(3)**: 442–445.

Crestani F, Martin JR, Möhler H, Rudolph U. 2000. Mechanism of action of the hypnotic zolpidem in vivo. *Br J Pharmacol* **131(7)**: 1251–1254.

Cutting GR, Lu L, O'Hara BF, Kasch LM, Montrose-Rafizadeh C, Donovan DM, Shimada S, Antonarakis SE, Guggino WB, Uhl GR. 1991. Cloning of the gamma-aminobutyric acid (GABA) rho 1 cDNA: a GABA receptor subunit highly expressed in the retina. *Proc Natl Acad Sci U S A* **88(7)**: 2673–2677.

Cvetanovic M, Ucker DS. 2004. Innate immune discrimination of apoptotic cells: repression of pro-inflammatory macrophage transcription is coupled directly to specific recognition. *J Immunol* **172**: 880–889.

Dejanovic B, Schwarz G. 2014. Neuronal nitric oxide synthase-dependent S-nitrosylation of gephyrin regulates gephyrin clustering at GABAergic synapses. *J Neurosci* **34(23)**: 7763–7768.

Demaurex N, Nunes P. 2016. The role of STIM and ORAI proteins in phagocytic immune cells. *Am J Physiol Cell Physiol* **310(7)**: C496–508.

Dionisio L, Jose De Rosa M, Bouzat C, Esandi Mdel C. 2011. An intrinsic GABAergic system in human lymphocytes. *Neuropharmacology* **60**: 513–519.

Dong H, Xiang YY, Farchi N, Ju W, Wu Y, Chen L, Wang Y, Hochner B, Yang B, Soreq H, Lu WY. 2004. Excessive expression of acetylcholinesterase impairs glutamatergic synaptogenesis in hippocampal neurons. *J Neurosci* **24(41)**: 8950–8960.

Ea CK, Deng L, Xia ZP, Pineda G, Chen ZJ. 2006. Activation of IKK by TNFalpha requires site-specific ubiquitination of RIP1 and polyubiquitin binding by NEMO. *Mol Cell* **22(2)**: 245–257.

Epelman S, Lavine KJ, Randolph GJ. 2014. Origin and function of tissue macrophages. *Immunity* **41**: 21–35.

Estefanía MM, Ganier O, Hernández P, Schvartzman JB, Mechali M, Krimer DB. 2012. DNA replication fading as proliferating cells advance in their commitment to terminal differentiation. *Sci Rep*. **2**: 279.

Evans JE, Frostholm A, Rotter A. 1996. Embryonic and postnatal expression of four gamma-aminobutyric acid transporter mRNAs in the mouse brain and leptomeninges. *J Comp Neurol* **376(3)**: 431–446.

Evans HG, Gullick NJ, Kelly S, Pitzalis C, Lord GM, Kirkham BW, Taams LS. 2009. In vivo activated monocytes from the site of inflammation in humans specifically promote Th17 responses. *Proc Natl Acad Sci U S A* **106**: 6232–6237.

Fairfax BP, Humburg P, Makino S, Naranbhai V, Wong D, Lau E, Jostins L, Plant K, Andrews R, McGee C, Knight JC. 2014. Innate immune activity conditions the effect of regulatory variants upon monocyte gene expression. *Science* **343**: 1246949.

Fathi M, Johansson A, Lundborg M, Orre L, Sköld CM, Camner P. 2001. Functional and morphological differences between human alveolar and interstitial macrophages. *Exp Mol Pathol* **70(2)**: 77–82.

Faust N, Varas F, Kelly LM, Heck S, Graf T. 2000. Insertion of enhanced green fluorescent protein into the lysozyme gene creates mice with green fluorescent granulocytes and macrophages. *Blood* **96(2)**: 719–726.

Feigenspan A, Bormann J. 1998. GABA-gated Cl^- channels in the rat retina. *Prog Retin Eye Res* **17(1)**: 99–126.

Forrester MT, Foster MW, Benhar M, Stamler JS. 2009. Detection of protein S-nitrosylation with the biotin-switch technique. *Free Radic Biol Med* **46(2)**: 119–126

Fortin A, Cregan SP, MacLaurin JG, Kushwaha N, Hickman ES, Thompson CS, Hakim A, Albert PR, Cecconi F, Helin K, Park DS, Slack RS. 2001. APAF1 is a key transcriptional target for p53 in the regulation of neuronal cell death. *J Cell Biol* **155(2)**: 207–216.

Frame JM, McGrath KE, Palis J. 2013. Erythro-myeloid progenitors: "definitive" hematopoiesis in the conceptus prior to the emergence of hematopoietic stem cells. *Blood Cells Mol Dis* **51(4)**: 220–225.

Franke-Ullmann G1, Pförtner C, Walter P, Steinmüller C, Lohmann-Matthes ML, Kobzik L. 1996. Characterization of murine lung interstitial macrophages in comparison with alveolar macrophages in vitro. *J Immunol* **157(7)**: 3097–3104.

Frucht DM, Fukao T, Bogdan C, Schindler H, O'Shea JJ, Koyasu S. 2001. IFN-gamma production by antigen-presenting cells: mechanisms emerge. *Trends Immunol* **22**: 556–560.

Gadea A, López-Colomé AM. 2001. Glial transporters for glutamate, glycine, and GABA: II. GABA transporters. *J Neurosci Res* **63(6)**: 461–468.

Gao S, Zhou J, Liu N, Wang L, Gao Q, Wu Y, Zhao Q, Liu P, Wang S, Liu Y, Guo N, Shen Y, Wu Y, Yuan Z. 2015. Curcumin induces M2 macrophage polarization by secretion IL-4 and/or IL-13. *J Mol Cell Cardiol* **85**:131–139.

Gautier EL, Shay T, Miller J, Greter M, Jakubzik C, Ivanov S, Helft J, Chow A, Elpek KG, Gordonov S, Mazloom AR, Ma'ayan A, Chua WJ, Hansen TH, Turley SJ, Merad M, Randolph GJ, 2012. Gene-expression profiles and transcriptional regulatory pathways that underlie the identity and diversity of mouse tissue macrophages. *Nat Immunol* **13**: 1118–1128.

Gay NJ, Symmons MF, Gangloff M, Bryant CE. 2014. Assembly and localization of Toll-like receptor signalling complexes. *Nat Rev Immunol* **14(8)**: 546–558.

Geissmann F, Manz MG, Jung S, Sieweke MH, Merad M, Ley K. 2010. Development of monocytes, macrophages, and dendritic cells. *Science* **327**: 656–661.

Gensel JC, Zhang B. 2015. Macrophage activation and its role in repair and pathology after spinal cord injury. *Brain Res* **1619**: 1–11.

Gessani S, Belardelli F. 1998. IFN-gamma expression in macrophages and its possible biological significance. *Cytokine Growth Factor Rev* **9**: 117–123.

Ginhoux F, Greter M, Leboeuf M, Nandi S, See P, Gokhan S, Mehler MF, Conway SJ, Ng LG, Stanley ER, Samokhvalov IM, Merad M. 2010. Fate mapping analysis reveals that adult microglia derive from primitive macrophages. *Science* **330(6005)**: 841–845.

Gioannini TL, Teghanemt A, Zhang D, Coussens NP, Dockstader W, Ramaswamy S, Weiss JP. 2004. Isolation of an endotoxin-MD-2 complex that produces Toll-like receptor 4-dependent cell activation at picomolar concentrations. *Proc Natl Acad Sci USA* **101**: 4186–4191.

Gomez Perdiguero E, Klapproth K, Schulz C, Busch K, Azzoni E, Crozet L, Garner H, Trouillet C, de Bruijn MF, Geissmann F, Rodewald HR. 2015. Tissue-resident macrophages originate from yolk-sac-derived erythro-myeloid progenitors. *Nature* **518(7540)**: 547–551.

Goncalves R, Zhan X, Cohen H, Debrabant A, Mosser DM. 2011. Platelet activation attracts a subpopulation of effector monocytes to sites of Leishmania major infection. *J Exp Med*. **208(1)**: 253–65.

Gordon S. 2003. Alternative activation of macrophages. *Nat Rev Immunol* **3**: 23–35.

Hashimoto D, Chow A, Noizat C, Teo P, Beasley MB, Leboeuf M, Becker CD, See P, Price J, Lucas D, Greter M, Mortha A, Boyer SW, Forsberg EC, Tanaka M, van Rooijen N, García-Sastre A, Stanley ER, Ginhoux F, Frenette PS, Merad M. 2013. Tissue-resident macrophages self-maintain locally throughout adult life with minimal contribution from circulating monocytes. *Immunity* **38**: 792–804.

Heinz S, Romanoski CE, Benner C, Allison KA, Kaikkonen MU, Orozco LD, Glass CK. 2013. Effect of natural genetic variation on enhancer selection and function. *Nature* **503**: 487–492.

Heller NM, Qi X, Gesbert F, Keegan AD. 2012. The extracellular and transmembrane domains of the γC and interleukin (IL)-13 receptor α1 chains, not their cytoplasmic domains, dictate the nature of signalling responses to IL-4 and IL-13. *J Biol Chem* **287(38)**: 31948–31961.

Heller NM, Qi X, Junttila IS, Shirey KA, Vogel SN, Paul WE, Keegan AD. 2008. Type I IL-4Rs selectively activate IRS-2 to induce target gene expression in macrophages. *Sci Signal* **1(51)**: ra17.

Herold S, Tabar TS, Janssen H, Hoegner K, Cabanski M, Lewe-Schlosser P, Albrecht J, Driever F, Vadasz I, Seeger W, Steinmueller M, Lohmeyer J. 2011. Exudate macrophages attenuate lung injury by the release of IL-1 receptor antagonist in gram-negative pneumonia. *Am J Respir Crit Care Med* **183:** 1380–1390.

Hershey GKK. 2003. IL-13 receptors and signalling pathways: an evolving web. *J Allergy Clin Immunol* **111(4)**: 677–690.

Hesse M, Modolell M, La Flamme AC, Schito M, Fuentes JM, Cheever AW, Pearce EJ, Wynn TA. 2001. Differential regulation of nitric oxide synthase-2 and arginase-1 by type 1/type 2 cytokines in vivo: Granulomatous pathology is shaped by the pattern of l-arginine metabolism. *J Immunol* **167:** 6533–6544.

Hoeffel G, Chen J, Lavin Y, Low D, Almeida FF, See P, Beaudin AE, Lum J, Low I, Forsberg EC, Poidinger M, Zolezzi F, Larbi A, Ng LG, Chan JK, Greter M, Becher B, Samokhvalov IM, Merad M, Ginhoux F. 2015. C-Myb(+) erythro-myeloid progenitor-derived fetal monocytes give rise to adult tissue-resident macrophages. *Immunity* **42(4)**: 665–678.

Hu X, Ivashkiv LB. 2009. Cross-regulation of signalling pathways by interferon-gamma: implications for immune responses and autoimmune diseases. *Immunity* **31(4)**: 539–550.

Huang W, McCaig LA, Veldhuizen RAW, Yao L-J, Lewis FJ. 2005. Mechanisms responsible for surfactant changes in sepsis-induced lung injury. *Eur Respir J* **26**: 1074–1079.

Hume DA, Freeman TC. 2014. Trancriptomic analysis of mononuclear phagocyte differentiation and activation. *Immunol Rev* **262**: 74–84.

Hume DA. 2015. The many faces of macrophage activation. *Front Immunol* **6**: 370.

Hussell T, Bell TJ. 2014. Alveolar macrophages: plasticity in a tissue-specific context. *Nat Rev Immunol* **14**: 81–93.

Ignarro LJ. 1990. Nitric oxide. A novel signal transduction mechanism for transcellular communication. *Hypertension* **16(5)**: 477–483.

Italiani P, Boraschi D. 2014. Monocytes to M1/M2 macrophages: phenotypical vs. functional differentiation. *Front Immunol* **5**: 514.

Jablonski KA, Amici SA, Webb LM, Ruiz-Rosado Jde D, Popovich PG, Partida-Sanchez S, Guerau-de-Arellano M. 2015. Novel markers to delineate murine M1 and M2 macrophages. *PLoS One* **10(12)**: e0145342.

Jakubzick C, Gautier EL, Gibbings SL, Sojka DK, Schlitzer A, Johnson TE, Ivanov S, Duan Q, Bala S, Condon T, van Rooijen N, Grainger JR, Belkaid Y, Ma'ayan A, Riches DW, Yokoyama WM, Ginhoux F, Henson PM, Randolph GJ. 2013. Minimal differentiation of classical monocytes as they survey steady-state tissues and transport antigen to lymph nodes. *Immunity* **39**: 599–610.

Janssen WJ, Barthel L, Muldrow A, Oberley-Deegan RE, Kearns MT, Jakubzick C, Henson PM. 2011. Fas determines differential fates of resident and recruited macrophages during resolution of acute lung injury. *Am J Respir Crit Care Med* **184(5)**: 547–560.

Jenkins SJ, Hume DA. 2014. Homeostasis in the mononuclear phagocyte system. *Trends Immunol* **35(8)**: 358–367.

Jenkins SJ, Ruckerl D, Cook PC, Jones LH, Finkelman FD, van Rooijen N, MacDonald AS, Allen JE. 2011. Local macrophage proliferation, rather than recruitment from the blood, is a signature of TH2 inflammation. *Science* **332**: 1284–1288.

Johnson CM, Hill CS, Chawla S, Treisman R, Bading H. 1997. Calcium controls gene expression via three distinct pathways that can function independently of the Ras/mitogen-activated protein kinases (ERKs) signalling cascade. *J Neurosci* **17(16)**: 6189–6202.

Kanaani J, Kolibachuk J, Martinez H, Baekkeskov S. 2010. Two distinct mechanisms target GAD67 to vesicular pathways and presynaptic clusters. *J Cell Biol* **190(5)**: 911–925.

Kang K, Reilly SM, Karabacak V, Gangl MR, Fitzgerald K, Hatano B, Lee CH. 2008. Adipocyte-derived Th2 cytokines and myeloid PPAR δ regulate macrophage polarization and insulin sensitivity. *Cell Metab* **7**:485–495.

Kawai T, Akira S. 2010. The role of pattern-recognition receptors in innate immunity: update on Toll-like receptors. *Nat Immunol* **11**: 373–384.

Kawai T, Akira S. 2011. Toll-like receptors and their crosstalk with other innate receptors in infection and immunity. *Immunity* **34**: 637–650.

Kelley SL, Lukk T, Nair SK, Tapping RI. 2013. The crystal structure of human soluble CD14 reveals a bent solenoid with a hydrophobic amino-terminal pocket. *J Immunol* **190**: 1304–1311.

Kelly-Welch AE, Hanson EM, Boothby MR, Keegan AD. 2003. Interleukin-4 and interleukin-13 signalling connections maps. *Science* **300**: 1527–1528.

Kim JI, Lee CJ, Jun MS, Lee CH, Paik SG, Lee H, Lee JO. 2005. Crystal structure of CD14 and its implications for lipopolysaccharide signalling. *J Biol Chem* **280**: 11347–11351.

Kolaczkowska E, Kubes P. 2013. Neutrophil recruitment and function in health and inflammation. *Nat Rev Immunol* **13(3)**: 159–175.

Kuwana S, Okada Y, Sugawara Y, Tsunekawa N, Obata K. 2003. Disturbance of neural respiratory control in neonatal mice lacking GABA synthesizing enzyme 67-kDa isoform of glutamic acid decarboxylase. *Neuroscience* **120(3)**: 861–870.

La Flamme AC, Kharkrang M, Stone S, Mirmoeini S, Chuluundorj D, Kyle R. 2012. Type II-activated murine macrophages produce IL-4. *PLoS One* **7(10)**: e46989.

Lech M, Anders HJ. 2013. Macrophages and fibrosis: how resident and infiltrating mononuclear phagocytes orchestrate all phases of tissue injury and repair. *Biochim Biophys Acta* **1832:** 989–997.

Liao X, Sharma N, Kapadia F, Zhou G, Lu Y, Hong H, Paruchuri K, Mahabeleshwar GH, Dalmas E, Venteclef N, Flask CA, Kim J, Doreian BW, Lu KQ, Kaestner KH, Hamik A, Clément K, Jain MK. 2011. Krüppel-like factor 4 regulates macrophage polarization. *J Clin Investig* **121**: 2736–2749.

Lin HH, Stacey M, Stein-Streilein J, Gordon S. 2010. F4/80: the macrophage-specific adhesion-GPCR and its role in immunoregulation. *Adv Exp Med Biol* **706**: 149–156.

Lin SC, Lo YC, Wu H. 2010. Helical assembly in the MyD88-IRAK4-IRAK2 complex in TLR/IL-1R signalling. *Nature* **465**: 885–890.

Lisi L, Stigliano E, Lauriola L, Navarra P, Dello Russo C. 2014. Proinflammatory-activated glioma cells induce a switch in microglial polarization and activation status, from a predominant M2b phenotype to a mixture of M1 and M2a/B polarized cells. *ASN Neuro* **6(3)**: 171–183.

Liu W, Peterson PE, Carter RJ, Zhou X, Langston JA, Fisher AJ, Toney MD. 2004. Crystal structures of unbound and aminooxyacetate-bound Escherichia coli gamma-aminobutyrate aminotransferase. *Biochemistry* **43(34)**: 10896–10905.

LoTurco JJ, Owens DF, Heath MJS, Davis MBE, Kriegstein AR. 1995. GABA and glutamate depolarize cortical progenitor cells and inhibit DNA synthesis. *Neuron* **15(6)**: 1287–1298.

Lu YC, Yeh WC, Ohashi PS. 2008. LPS/TLR4 signal transduction pathway. *Cytokine* **42(2)**: 145–151.

Luján R. 2007. Subcellular regulation of metabotropic GABA receptors in the developing cerebellum. *Cerebellum* **6(2)**: 123–129.

Lupardus PJ, Birnbaum ME, Garcia KC. 2010. Molecular basis for shared cytokine recognition revealed in the structure of an unusually high affinity complex between IL-13 and IL-13R α 2. *Structure* **18**: 332–342.

MacDermott AB, Role LW, Siegelbaum SA. 1999. Presynaptic ionotropic receptors and the control of transmitter release. *Annu Rev Neurosci* **22**: 443–485.

Macdonald RL, Olsen RW. 1994. GABAA receptor channels. *Annu Rev Neurosci* **17**: 569–602.

MacMicking J, Xie QW, Nathan C. 1997. Nitric oxide and macrophage function. *Annu Rev Immunol* **15**: 323–350.

Madala SK, Dolan MA, Sharma D, Ramalingam TR, Wilson MS, Mentink-Kane MM, Masison DC, Wynn TA. 2011. Mapping mouse IL-13 binding regions using structure modeling, molecular docking, and high-density peptide microarray analysis. *Proteins* **79**: 282–293.

Mammen AL, Huganir RL, O'Brien RJ. 1997. Redistribution and stabilization of cell surface glutamate receptors during synapse formation. *J Neurosci* **17(19)**: 7351–7358.

Mantovani A, Sica A, Sozzani S, Allavena P, Vecchi A, Locati M. 2004. The chemokine system in diverse forms of macrophage activation and polarization. *Trends Immunol* **25:** 677–686.

Martinez FO, Sica A, Mantovani A, Locati M. 2008. Macrophage activation and polarization. *Front Biosci* **13**: 453–461.

Maus UA, Koay MA, Delbeck T, Mack M, Ermert M, Ermert L, Blackwell TS, Christman JW, Schlöndorff D, Seeger W, Lohmeyer J. 2002. Role of resident alveolar macrophages in leukocyte traffic into the alveolar air space of intact mice. *Am J Physiol Lung Cell Mol Physiol* **282**: L1245–1252.

McGrath KE, Frame JM, Fegan KH, Bowen JR, Conway SJ, Catherman SC, Kingsley PD, Koniski AD, Palis J. 2015. Distinct sources of hematopoietic progenitors emerge before HSCs and provide functional blood cells in the mammalian embryo. *Cell Rep* **11(12)**: 1892–1904.

McIntire SL, Reimer RJ, Schuske K, Edwards RH, Jorgensen EM. 1997. Identification and characterization of the vesicular GABA transporter. *Nature* **389(6653)**: 870–876.

Meylan E, Burns K, Hofmann K, Blancheteau V, Martinon F, Kelliher M, Tschopp J. 2004. RIP1 is an essential mediator of Toll-like receptor 3-induced NF-kappa B activation. *Nat Immunol* **5:** 503–507.

Mijatovic T1, Kruys V, Caput D, Defrance P, Huez G. 1997. Interleukin-4 and -13 inhibit tumor necrosis factor-alpha mRNA translational activation in lipopolysaccharide-induced mouse macrophages. *J Biol Chem* **272(22)**: 14394–14398.

Miller SI, Ernst RK, Bader MW. 2005. LPS, TLR4 and infectious disease diversity. *Nat Rev Microbiol* **3**: 36–46.

Mills CD. 2012. M1 and M2 macrophages: oracles of health and disease. *Crit Rev Immunol* **32(6)**: 463–488.

Minelli A, Alonso-Nanclares L, Edwards RH, DeFelipe J, Conti F. 2003. Postnatal development of the vesicular GABA transporter in rat cerebral cortex. *Neuroscience* **117(2)**: 337–346.

Möhler H. 2006. GABA(A) receptor diversity and pharmacology. *Cell Tissue Res* **326(2)**: 505–516.

Morris SM. 2007. Arginine metabolism: boundaries of our knowledge. *J Nutr* **137(1)**: 1602–1609.

Mosser DM, Edwards JP. 2008. Exploring the full spectrum of macrophage activation. *Nat Rev Immunol* **8**: 958–969

Motshwene PG, Moncrieffe MC, Grossmann JG, Kao C, Ayaluru M, Sandercock AM, Carol V, Robinson C, Latz E, Gay NJ. 2009. An oligomeric signalling platform formed by the Toll-like receptor signal transducers MyD88 and IRAK-4. *J Biol Chem* **284**: 25404–25411.

Müller U, Stenzel W, Köhler G, Werner C, Polte T, Hansen G, Schütze N, Straubinger RK, Blessing M, McKenzie AN, Brombacher F, Alber G. 2007. IL-13 induces disease-promoting type 2 cytokines, alternatively activated macrophages and allergic inflammation during pulmonary infection of mice with Cryptococcus neoformans. *J Immunol* **179(8)**: 5367–5377.

Munitz A, Brandt EB, Mingler M, Finkelman FD, Rothenberg ME. 2008. Distinct roles for IL-13 and IL-4 via IL-13 receptor α1 and the type II IL-4 receptor in asthma pathogenesis. *Proc Natl Acad Sci U S A* **105(20)**: 7240–7245.

Murray PJ, Allen JE, Biswas SK, Fisher EA, Gilroy DW, Goerdt S, Gordon S, Hamilton JA, Ivashkiv LB, Lawrence T, Locati M, Mantovani A, Martinez FO, Mege JL, Mosser DM, Natoli G, Saeij JP, Schultze JL, Shirey KA, Sica A, Suttles J, Udalova I, van Ginderachter

JA, Vogel SN, Wynn TA. 2014. Macrophage activation and polarization: nomenclature and experimental guidelines. *Immunity* **41(1)**: 14–20.

Murray PJ, Wynn TA. 2011. Protective and pathogenic functions of macrophage subsets. *Nat Rev Immunol* **11**: 723–37.

Murugan V, Peck MJ. 2009. Signal transduction pathways linking the activation of alveolar macrophages with the recruitment of neutrophils to lungs in chronic obstructive pulmonary disease. *Exp Lung Res* **35(6)**: 439–485.

Nachtomy O, Shavit A, Yakhini Z. 2007. Gene expression and the concept of the phenotype. *Stud Hist Phil Biol Biomed Sci* **38**: 238–254.

Nagai Y, Akashi S, Nagafuku M, Ogata M, Iwakura Y, Akira S, Kitamura T, Kosugi A, Kimoto M, Miyake K. 2002. Essential role of MD-2 in LPS responsiveness and TLR distribution. *Nat Immunol* **3**: 667–672.

Nasreen Z, Jameel T, Hasan A, Parveen N, Sadasivudu B. 2011. Glutamate decarboxylase and GABA aminotransferase levels in different regions of rat brain on the onset of leptazol induced convulsions. *Neurochem Res* **37(1)**: 202–204.

Novak ML, Koh TJ. 2013. Phenotypic transitions of macrophages orchestrate tissue repair. *Am J Pathol* **183**: 1352–1363.

Odegaard JI, Ricardo-Gonzalez RR, Goforth MH, Morel CR, Subramanian V, Mukundan L, Red Eagle A, Vats D, Brombacher F, Ferrante AW, Chawla A. 2007. Macrophage-specific PPARgamma controls alternative activation and improves insulin resistance. *Nature* **447(7148)**: 1116–1120.

Odegaard JI, Ricardo-Gonzalez RR, Red Eagle A, Vats D, Morel CR, Goforth MH, Subramanian V, Mukundan L, Ferrante AW, Chawla A. 2008. Alternative M2 activation of Kupffer cells by PPAR δ ameliorates obesity-induced insulin resistance. *Cell Metab* **7**: 496–507.

Oganesyan G, Saha SK, Guo B, He JQ, Shahangian A, Zarnegar B, Perry A, Cheng G. 2006. Critical role of TRAF3 in the Toll-like receptor-dependent and -independent antiviral response. *Nature* **439**: 208–211.

O'Neill LA, Bowie AG. 2007. The family of five: TIR-domain-containing adaptors in Toll-like receptor signalling. *Nat Rev Immunol* **7**: 353–364.

Owens DF, Boyce LH, Davis MB, Kriegstein AR. 1996. Excitatory GABA responses in embryonic and neonatal cortical slices demonstrated by gramicidin perforated-patch recordings and calcium imaging. *J Neurosci* **16(20)**: 6414–6423.

Owens DF, Kriegstein AR. 2002. Is there more to GABA than synaptic inhibition? *Nat Rev Neurosci* **3**: 715–727.

Park BS, Song DH, Kim HM, Choi BS, Lee H, Lee JO. 2009. The structural basis of lipopolysaccharide recognition by the TLR4-MD-2 complex. *Nature* **458**: 1191–1195.

Paul AM, Branton WG, Walsh JG, Polyak MJ, Lu JQ, Baker GB, Power C. 2014. GABA transport and neuroinflammation are coupled in multiple sclerosis: regulation of the GABA transporter-2 by ganaxolone. *Neuroscience* **273**: 24–38.

Pello OM, De Pizzol M, Mirolo M, Soucek L, Zammataro L, Amabile A, Doni A, Nebuloni M, Swigart LB, Evan GI, Mantovani A, Locati M. 2012. Role of c-MYC in alternative activation of human macrophages and tumor-associated macrophage biology. *Blood* **119**: 411–421.

Peroval MY, Boyd AC, Young JR, Smith AL. 2013. A critical role for MAPK signalling pathways in the transcriptional regulation of toll like receptors. Gay N, ed. *PLoS ONE* **8(2)**: e51243.

Płóciennikowska A1, Hromada-Judycka A, Borzęcka K, Kwiatkowska K. 2015. Co-operation of TLR4 and raft proteins in LPS-induced pro-inflammatory signalling. *Cell Mol Life Sci* **72(3)**: 557–581.

Prokhorova S, Lavnikova N, Laskin DL. 1994. Functional characterization of interstitial macrophages and subpopulations of alveolar macrophages from rat lung. *J Leukoc Biol* **55(2)**: 141–146.

Prud'homme GJ, Glinka Y, Wang Q. 2013. GABA exerts anti-inflammatory and immunosuppressive effects. *J Immunol* **190(1)**: 68–15.

Prud'homme GJ, Glinka Y, Wang Q. 2015. Immunological GABAergic interactions and therapeutic applications in autoimmune diseases. *Autoimmun Rev* **14**: 1048–1056.

Putney JW Jr, Broad LM, Braun FJ, Lievremont JP, Bird GS. 2001. Mechanisms of capacitative calcium entry. *J Cell Sci* **114(12)**: 2223–2229.

Raetz CR, Whitfield C. 2002. Lipopolysaccharide endotoxins. *Annu Rev Biochem* **71**: 635–700.

Randriamampita C, Trautmann A. 1987. Ionic channels in murine macrophages. *J Cell Bio* **105**: 761–769.

Rath M, Müller I, Kropf P, Closs EI, Munder M. 2014. Metabolism via arginase or nitric oxide synthase: two competing arginine pathways in macrophages. *Front Immunol* **5:** 532.

Rauert-Wunderlich H, Siegmund D, Maier E, Giner T, Bargou RC, Wajant H, Stühmer T. 2013. The IKK inhibitor Bay 11-7082 induces cell death independent from inhibition of activation of NFκB transcription factors. *PLoS One* **8(3)**: e59292.

Raza S, Barnett MW, Barnett-Itzhaki Z, Amit I, Hume DA, Freeman TC. 2014. Analysis of the transcriptional networks underpinning the activation of murine macrophages by inflammatory mediators. *J Leukoc Biol* **96(2)**: 167–183.

Reyes-García MG, Hernandez-Hernandez F, Hernandez-Tellez B, Garcia-Tamayo F. 2007. GABA (A) receptor subunits RNA expression in mice peritoneal macrophages modulate their IL-6/IL-12 production. *J Neuroimmunol* **188(1-2)**: 64–68.

Robbe P, Draijer C, Borg TR, Luinge M, Timens W, Wouters IM, Melgert BN, Hylkema MN. 2015. Distinct macrophage phenotypes in allergic and nonallergic lung inflammation. *Am J Physiol Lung Cell Mol Physiol* **308**: L358–L367.

Romo N, Magri G, Muntasell A, Heredia G, Baia D, Angulo A, Guma M, Lopez-Botet M. 2011. Natural killer cell-mediated response to human cytomegalovirus-infected macrophages is modulated by their functional polarization. *J Leuk Biol* **90**: 717–726.

Rőszer T. 2015. Understanding the Mysterious M2 Macrophage through Activation Markers and Effector Mechanisms. *Mediators Inflamm* **2015**: 816460.

Rutschman R, Lang R, Hesse M, Inhle JN, Wynn TA, Murray PJ. 2001. Cutting edge: Stat6-dependent substrate depletion regulates nitric oxide production. *J Immunol* **166(4)**: 2173–2177.

Saclier M, Yacoub-Youssef H, Mackey AL, Arnold L, Ardjoune H, Magnan M, Sailhan F, Chelly J, Pavlath GK, Mounier R, Kjaer M, Chazaud B. 2013. Differentially activated macrophages orchestrate myogenic precursor cell fate during human skeletal muscle regeneration. *Stem Cells* **31(2)**: 384–396.

Salazar P, Velasco-Velázquez MA, Velasco I. 2008. GABA effects during neuronal differentiation of stem cells. *Neurochem Res* **33(8)**: 1546–1557.

Sanders RD, Grover V, Goulding J, Godlee A, Gurney S, Snelgrove R, Ma D, Singh S, Maze M, Hussell T. 2015. Immune cell expression of GABAA receptors and the effects of diazepam on influenza infection. *J Neuroimmunol* **282**: 97–103.

Sato S, Sanjo H, Takeda K, Ninomiya-Tsuji J, Yamamoto M, Kawai T, Matsumoto K, Takeuchi O, Akira S. 2005. Essential function for the kinase TAK1 in innate and adaptive immune responses *Nat Immunol* **6:** 1087–1095.

Schiedlmeier B, Kühlcke K, Eckert HG, Baum C, Zeller WJ, Fruehauf S. 2000. Quantitative assessment of retroviral transfer of the human multidrug resistance 1 gene to human mobilized peripheral blood progenitor cells engrafted in nonobese diabetic/severe combined immunodeficient mice. *Blood* **95(4)**: 1237–1248.

Schilling E, El Chartouni C, Rehli M. 2009. Allele-specific DNA methylation in mouse strains is mainly determined by cis-acting sequences. *Genome Res* **19**: 2028–2035.

Schousboe A, Sarup A, Larsson OM, White HS. 2004. GABA transporters as drug targets for modulation of GABAergic activity. *Biochem Pharmacol* **68(8)**: 1557–1563.

Schroder K, Hertzog PJ, Ravasi T, Hume DA. 2004. Interferon-gamma: an overview of signals, mechanisms and functions. *J Leukoc Biol* **75(2)**: 163–189.

Schulz C, Gomez Perdiguero E, Chorro L, Szabo-Rogers H, Cagnard N, Kierdorf K, Prinz M, Wu B, Jacobsen SE, Pollard JW, Frampton J, Liu KJ, Geissmann F. 2012. A lineage of myeloid cells independent of Myb and hematopoietic stem cells. *Science* **336**: 86–90.

Serbina NV, Jia T, Hohl TM, Pamer EG. 2008. Monocyte-mediated defence against microbial pathogens. *Annu Rev Immunol* **26**: 421–452.

Sheldon KE, Shandilya H, Kepka-Lenhart D, Poljakovic M, Ghosh A, Morris SM Jr. 2013. Shaping the murine macrophage phenotype: IL-4 and cyclic AMP synergistically activate the arginase I promoter. *J Immunol* **191(5)**: 2290–2298.

Shi C, Pamer EG. 2011. Monocyte recruitment during infection and inflammation. *Nat Rev Immunol*. **11**:762–74.

Sieghart W. 2006. Structure, pharmacology, and function of GABAA receptor subtypes. *Adv Pharmacol* **54**: 231–263.

Sieweke MH, Allen JE. 2013. Beyond stem cells: self-renewal of differentiated macrophages. *Science* **342(6161)**: 1242974.

Sigel E, Steinmann ME. 2012. Structure, function, and modulation of GABA(A) receptors. *J Biol Chem* **287(48)**: 40224–40231.

Simmons DL, Tan S, Tenen DG, Nicholson-Weller A, Seed B. 1989. Monocyte antigen CD14 is a phospholipid anchored membrane protein. *Blood* **73**: 284–289.

Singh A, Holvoet S, Mercenier A. 2011. Dietary polyphenols in the prevention and treatment of allergic diseases. *Clin Exp Allergy* **41(10)**: 1346–1359.

Simon J, Wakimoto H, Fujita N, Lalande M, Barnard EA. 2004. Analysis of the set of GABAA receptor genes in the human genome. *J Biol Chem* **279**: 41422–41435.

Soghomonian JJ, Martin DL. 1998. Two isoforms of glutamate decarboxylase: why? *Trends Pharmacol Sci* **19(12)**: 500–505.

Spellberg B, Edwards JE Jr. 2001. Type 1/Type 2 immunity in infectious diseases. *Clin Infect Dis* **32(1)**: 76–102.

Staitieh BS, Egea EE, Fan X, Azih N, Neveu W, Guidot DM. 2015. Activation of alveolar macrophages with interferon-γ promotes antioxidant defenses via the Nrf2-ARE pathway. *J Clin Cell Immunol* **6(5)**: 365.

Stark GR. 2007. How cells respond to interferons revisited: from early history to current complexity. *Cytokine Growth Factor Rev* **18(5-6)**: 419–423.

Stempelj M, Kedinger M, Augenlicht L, Klampfer L. 2007. Essential role of the JAK/STAT1 signalling pathway in the expression of inducible nitric-oxide synthase in intestinal epithelial cells and its regulation by butyrate. *J Biol Chem* **282(13)**: 9797–9804.

Stout RD, Jiang C, Matta B, Tietzel I, Watkins SK, Suttles J. 2005. Macrophages sequentially change their functional phenotype in response to changes in microenvironmental influences. *J Immunol* **175(1)**: 342–349.

Stout RD, Watkins SK, Suttles J. 2009. Functional plasticity of macrophages: in situ reprogramming of tumor-associated macrophages. *J Leukoc Bol* **86(1)**: 105–109.

Takehara A, Hosokawa M, Eguchi H, Ohigashi H, Ishikawa O, Nakamura Y, Nakagawa H. 2007. Gamma aminobutyric acid (GABA) stimulates pancreatic cancer growth through overexpressing GABAA receptor pi subunit. *Cancer Res* **67**: 9704–9712.

Tamayama T, Maemura K Kanbara K, Hayasaki H, Yabumoto Y, Yuasa M, Watanabe M. 2005. Expression of GABA(A) and GABA(B) receptors in rat growth plate chondrocytes: activation of the GABA receptors promotes proliferation of mouse chondrogenic ATDC5 cells. *Mol Cell Biochem* **273**: 117–126.

Taneera J, Jin Z, Jin Y, Muhammed SJ, Zhang E, Lang S, Salehi A, Korsgren O, Renström E, Groop L, Birnir B. 2012. γ-Aminobutyric acid (GABA) signalling in human pancreatic islets is altered in type 2 diabetes. *Diabetologia* **55(7)**: 1985–1994.

Tavian M, Péault B. 2005. Embryonic development of the human hematopoietic system. *Int J Dev Biol* **49(2-3)**: 243–250.

te Velde AA, Huijbens RJ, Heije K, de Vries JE, Figdor CG. 1990. Interleukin-4 (IL-4) inhibits secretion of IL-1 beta, tumor necrosis factor alpha, and IL-6 by human monocytes. *Blood* **76(7)**: 1392–1397.

Tian J, Lu Y, Zhang H, Chau CH, Dang HN, Kaufman DL. 2004. Gamma-aminobutyric acid inhibits T cell autoimmunity and the development of inflammatory responses in a mouse type 1 diabetes model. *J Immunol* **173**: 5298–5304.

Tozuka Y, Fukuda S, Namba T, Seki T, Hisatsune T. 2005. GABAergic excitation promotes neuronal differentiation in adult hippocampal progenitor cells. *Neuron* **47**: 803–815.

Trinchieri G. 2003. Interleukin-12 and the regulation of innate resistance and adaptive immunity. *Nature Rev Immunol* **3**: 133–146.

Trzaskowski B, Latek D, Yuan S, Ghoshdastider U, Debinski A, Filipek S. 2012. Action of molecular switches in GPCRs--theoretical and experimental studies. *Curr Med Chem* **19(8)**: 1090–109.

Van den Bosch MWM, Palsson-Mcdermott E, Johnson DS, O'Neill LAJ. 2014. LPS induces the degradation of programmed Cell Death Protein 4 (PDCD4) to release Twist2, activating c-Maf transcription to promote interleukin-10 production. *J Biol Chem* **289(33)**: 22980–22990.

Van Dyken SJ, Locksley RM. 2013. Interleukin-4 and interleukin-13-mediated alternatively activated macrophages: roles in homeostasis and disease. *Annu Rev Immunol* **31**: 317–343.

Van Furth R, Cohn ZA. 1968. The origin and kinetics of mononuclear phagocytes. *J Exp Med* **128**: 415–435.

Van Haasteren G, Li S, Muda M, Susini S, Schlegel W. 1999. Calcium signalling and gene expression. *J Recept Signal Transduct Res* **19(1-4)**: 481–492.

Vila-del Sol V, Punzón C, Fresno M. IFN-gamma-induced TNF-alpha expression is regulated by interferon regulatory factors 1 and 8 in mouse macrophages. *J Immunol* **181(7)**: 4461–4470.

Wells CA, Ravasi T, Faulker GJ, Carninci P, Okazaki Y, Hayashizaki Y, Sweet M, Wainwright BJ, Hume DA. 2003. Genetic control of the innate immune response. *BMC Immunol* **4**: 5

West AP, Koblansky AA, Ghosh S. 2006. Recognition and signalling by toll-like receptors. *Annu Rev Cell Dev Biol* **22**: 409–437.

Wright SD, Tobias PS, Ulevitch RJ, Ramos RA. 1989. Lipopolysaccharide (LPS) binding protein opsonizes LPS-bearing particles for recognition by a novel receptor on macrophages. *J Exp Med* **170:** 1231–1241.

Yamaguchi T, Takizawa F, Fischer U, Dijkstra JM. 2015. Along the axis between Type 1 and Type 2 Immunity; principles conserved in evolution from fish to mammals. *Biology (Basel)* **4(4)**: 814–59.

Yona S, Kim KW, Wolf Y, Mildner A, Varol D, Breker M, Strauss-Ayali D, Viukov S, Guilliams M, Misharin A, Hume DA, Perlman H, Malissen B, Zelzer E, Jung S. 2013. Fate mapping reveals origins and dynamics of monocytes and tissue macrophages under homeostasis. *Immunity* **38**: 79–91.

Young HA. 1996. Regulation of interferon-gamma gene expression. *J Interferon Cytokine Res* **16(8)**: 563–568.

Xiang YY, Chen X, Li J, Wang S, Faclier G, Macdonald JF, Hogg JC, Orser BA, Lu WY. 2013. Isoflurane regulates atypical type-A γ-aminobutyric acid receptors in alveolar type II epithelial cells. *Anesthesiology* **118(5)**: 1065–1075.

Xue J, Schmidt SV, Sander J, Draffehn A, Krebs W, Quester I, DeNardo D, Gohel TD, Emde M, Schmidleithner L, Ganesan H, Nino-Castro A, Mallmann MR, Labzin L, Theis H, Kraut M, Beyer M, Latz E, Freeman TC, Ulas T, Schultze JL. 2014. Transcriptome-based network analysis reveals a spectrum model of human macrophage activation. *Immunity* **40**: 274–288.

Zhao X, Dai J, Xiao X, Wu L, Zeng J, Sheng J, Su J, Chen X, Wang G, Li K. 2014. PI3K/Akt signalling pathway modulates influenza virus induced mouse alveolar macrophage polarization to M1/M2b. *PLoS One* **9(8):** e104506.

JACOB WILSON POIRIER

EDUCATION

- Bachelor of Medical Sciences – Pharmacology
  Western University, 2015
- Master of Science – Physiology and Pharmacology
  Western University, 2016

SCHOLARSHIPS AND AWARDS

- Ontario Graduate Scholarship (OGS), 2015-2016
- Dean's Honor List, 2014-2015
- Dean's Honor List, 2013-2014

TEACHING EXPERIENCE

- Teaching Assistant – Physiology 3130Z (September 2015-April 2016)

SEMINARS

- Robarts Molecular Medicine Data Club – "Role of autocrine GABA signalling in alveolar macrophage polarization" (April 2015)
- Robarts Molecular Medicine Data Club – "Role of autocrine GABA signalling in lung macrophage immune response" (April 2016)

POSTER PRESENTATIONS

- Undergraduate thesis presentation – Summer 2014
- Dept. of Physiology & Pharmacology Research Day, Western University – November 2014
- London Health Research Day – April 2015
- Robarts Research Retreat – June 2015
- London Health Research Day – March 2016
- Robarts Research Retreat – June 2016

CONFERENCES

- London-Toronto Lung Research Symposium (September 2015)